Atmospheric Degradation Mechanisms of Organic Sulphur Compounds

Dissertation submitted to the Faculty of Chemistry

The Bergische Universität - Gesamthochschule Wuppertal

for the Degree of Doctor of Natural Science

(Dr. rer. nat.)

by

Cecilia Arsene

October 2001

The work described in this thesis was carried out in the Department of Physical Chemistry, the Bergische Universität - Gesamthochschule Wuppertal, under the scientific supervision of Prof. Dr. K.H. Becker, during the period of March, 1998 - October, 2001.

Referee: Prof. Dr. K.H. Becker
Co-referee: Prof. Dr. E.H. Fink

Familiei mele

I would like to express my sincere gratitude to Prof. Dr. Karl H. Becker for the opportunity of doing this Ph.D. in his research group and for the supervision of this work.

I would like to sincere acknowledge Prof. Dr. Ewald H. Fink for agreeing to co-referee the thesis.

My sincere gratitude also to Dr. Ian Barnes. His vision, guidance and experience helped me to learn a lot. I especially appreciate the fruitful discussions during these years which let me to understand at least a part of the vast domain of the atmospheric chemistry.

My distinguished thanks to Prof. Dr. Raluca Delia Mocanu for trusting me and giving the possibility to open a window to the world.

I would like to express my warmest thanks to Dr. Nadya Boutkovskaya for fruitful discussion in the last two years and for giving me encouragement at all times when it was hard.

My sincere thanks to Romeo Olariu for contradictory, but constructive discussions during all these years.

For Dr. Fabrizia Cavalli many thanks for supporting friendship relations.

I especially appreciate the excellent atmosphere created by Dr. Klaus Brockmann during discussion with the Romanian group and also for his intention of understanding a little bit about us. Thanks also to Dr. Jörg Kleffmann for appreciating part of my scientifically activity during our Tuesday seminars. To Markus Spittler thanks for his formal or informal comments which provided a reality check for many things.

I wish to thank also other colleagues for the atmosphere during these years. My special thanks to Techn. Ang. Ronald Giese, Dipl. Ing. Willi Nelsen and Dipl. Ing. Volker Kriesche for their help in solving technical problems.

I am grateful to my parents which have been behind me from the very beginning. From both of them I learnt the most important lesson for the life - to be humane.

Last but not least, I am grateful to my husband for his love, support and patience during these years.

Abstract

In the present work a detailed product study has been performed on the ·OH radical initiated oxidation of dimethyl sulphide and dimethyl sulphoxide, under different conditions of temperature, partial pressure of oxygen and NO_x concentration, in order to better define the degradation mechanism of the above compounds under conditions which prevail in the atmosphere.

The products of the ·OH radical initiated oxidation of dimethyl sulphide have been investigated under NO_x free conditions at temperatures of 284, 295 and 306 ± 2 K and the oxygen partial pressures of 20, 200 and 500 mbar. Dimethyl sulphoxide, sulphur dioxide and methane sulphonic acid were the major identified sulphur-containing products and evidence has been found for the formation of methane sulphinic acid in considerable yield. Formation of methane thiol formate and carbonyl sulphide has been also observed. The variation of the formation yield of dimethyl sulphoxide and sulphur dioxide with temperature and oxygen partial pressure has been found to be consistent with a mechanism involving both addition and abstraction channels of the initial reaction. The found formation yields of dimethyl sulphoxide for 284 K (46.3 ± 5.0 %), 295 K (34.8 ± 7.6 %) and 306 K (24.4 ± 2.8 %), at 200 mbar O_2, give evidence for the predominance of the addition pathway at low temperature. These results support that the OH-DMS adduct, formed in the addition channel, mainly reacts with oxygen to form dimethyl sulphoxide. High overall molar formation yields of sulphur dioxide, about 90 % at all temperatures, leads to the conclusion that further oxidation of the products in both the addition and abstraction channels results mainly in sulphur dioxide production under the experimental conditions of this study.

The major sulphur-containing products identified in the presence of NO_x were sulphur dioxide, dimethyl sulphoxide, dimethyl sulphone, methane sulphonic acid, methane sulphonyl peroxy nitrate and carbonyl sulphide. The variation of the product yields with NO_x concentration at different temperatures was also found to be consistent with the occurrence of both addition and abstraction channels. It was found that increasing the initial NO concentration depresses the dimethyl sulphoxide, sulphur dioxide and carbonyl sulphide formation yields and enhances those of dimethyl sulphone, methane sulphonic acid and methane sulphonyl peroxy nitrate. The branching ratio for dimethyl sulphoxide formation was found to decrease with increasing initial NO and to decrease with increase of the temperature. This behaviour is expected for a reaction

sequence involving formation of a thermally unstable peroxy radical adduct and its subsequent reaction with NO with formation of an oxy-alcoxy species which can react with molecular oxygen to form dimethyl sulphone. Such a reaction sequence offers a plausible explanation for the differences in the dimethyl sulphoxide yield found between systems operating with and without NO. The molar formation yield of sulphur dioxide was found to decrease with increasing both the temperature and initial NO_x. On the contrary, the observed yield of methane sulphonic acid was found to increase with increasing initial NO_x concentrations and temperature, which is in agreement with NO and NO_2 promoting the formation of methane sulphonic acid via reactions involving species such as $CH_3S\cdot$, $CH_2S\cdot(O)$, $CH_3S\cdot(O)_2$. Under high concentration of NO_x the formation of methane sulphonic acid is favoured compared with sulphur dioxide.

A study of the gas phase oxidation of dimethyl sulphoxide by ·OH radicals has been performed under conditions similar to those for dimethyl sulphide. Formation of methane sulphinic acid in a very high yield was found. The results show quite definitely that methane sulphinic acid is the major oxidation product of dimethyl sulphoxide and that its measured yield is independent of the reaction conditions. Formation of dimethyl sulphone, sulphur dioxide, methane sulphonic acid and methane sulphonyl peroxy nitrate has been observed. The observed behaviour of these products supports a formation mechanism involving secondary chemistry of methane sulphinic acid initiated either by ·OH radicals or by peroxy radicals.

The present study has resulted in a significant improvement in our understanding of some of the major atmospheric degradation pathways of organic sulphur-containing compounds.

Contents

Chapter 1

Introduction

The Earth's atmosphere is regarded as one of the most important geophysical compartments. The atmosphere is considered to be a very complex mixture of more than a thousand trace chemicals that are permanently reacting and redistributing either in this compartment or between different adjoined compartments such as the biosphere and the hydrosphere. The atmosphere is thus comparable to a giant chemical reactor containing a large variety of different substances. Their sources and sinks can involve chemical interactions with different atmospheric constituents and/or emissions and uptake of the substance at the Earth's surface.

Due to processes, such as material exchange between adjacent geochemical reservoirs (the ocean and the biosphere) and losses of the trace gases either by a return flow to the same (or another) geochemical reservoir or by chemical reactions, the atmosphere is maintained in a dynamic equilibrium. In the atmosphere, air acts as a carrier for the large number of trace gases and usually many of the trace gases are in equilibrium between sources and sinks. Some trace gases control or affect the Earth's climate and habitability. Nitrogen, halogen and sulphur cycles are considered to be involved in important atmospheric changes.

1.1 Sulphur-containing compounds in the atmosphere

Sulphur is recognised as one of the critical elements for which an understanding of its biogeochemical cycle is pivotal to climate change studies (Wuebbles, 1995). The atmospheric sulphur cycle is considered to be a part of the global biogeochemical sulphur cycle and this is due to both biotic and abiotic processes.

The distributions and residence times of the reduced sulphur compounds in the atmosphere are controlled by chemical and physical processes. Since the atmosphere is an oxidising medium, species which contain sulphur in (-II) to (+IV) oxidation states are subject to reactions with atmospheric oxidants such as O_2, ·OH radicals, H_2O_2 and O_3. Compounds which include sulphur in the highest oxidation state (+VI) are relatively stable under atmospheric conditions.

The atmospheric sulphur cycle begins with the emission of sulphur into the atmosphere and ends with sulphur removal by dry or wet deposition to the Earth's surface. The general sulphur cycle in the global environment, as given by Brasseur et al. (1999), is shown in Figure 1.1. As can be seen, there are two independent environments separated by a mixing barrier: an anoxic region where oxygen is absent, and an oxic region where atmospheric oxygen is present. The mixing barrier is both physical and microbial in nature. For this reason very little of the sulphide produced in the anoxic regime escapes directly into the atmosphere by other means.

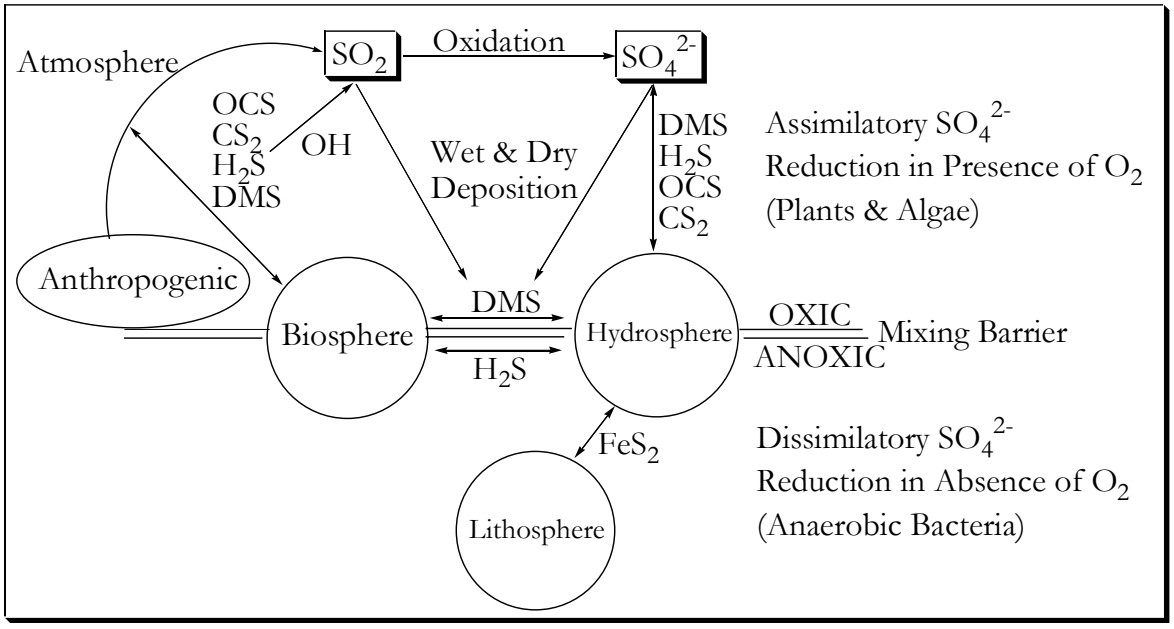

Figure 1.1: The sulphur cycle in the global environment.

Volatile sulphur compounds are emitted into the atmosphere from a large variety of natural (sea spray, biogenic processes, volcanic eruptions, etc.) and anthropogenic (industrial emissions, agriculture, etc.) sources.

Environmental problems due to sulphur pollution range from the local to the global scale and are manifested in phenomena such as health effects, visibility reduction, acid rain and global climate change. Atmospheric compounds containing sulphates can significantly affect humans and the environment. Ambient sulphate typically resides in the sub-micrometer size range of

aerosol particles (Whitby, 1978; Wilson and McMurry, 1981) that can be inhaled, posing health hazards. In addition, aerosols can play a synergistic role in intensifying the toxic effects of gases such as SO_2 and NO_x, in catalysing the oxidation of SO_2 to H_2SO_4 and in reducing visibility (Malm et al., 1994; Waggoner et al., 1981).

An overview of the sulphur containing compounds which have been observed as trace gases in the troposphere (Warneck, 1999 and references therein) is presented in Table 1.1.

Table 1.1: Approximate molar mixing ratios in the air, global distribution, sources and sinks, and residence times for the sulphur containing compounds present as trace gases in the troposphere.

Gas	Mixing ratio	Distribution	Major sources ($Tg\ yr^{-1}$)	Major sinks ($Tg\ yr^{-1}$)	Residence time
OCS	500 pptv	uniform	soils, 0.3 ocean, 0.3 from sulphides, 0.5	uptake by vegetation, 0.4 loss to the stratosphere, 0.1	7 yr
H_2S	5-90 pptv	marine air continental	soils, 0.5 vegetation, 1.2 volcanoes, 1.0	reaction with ·OH	3 d
DMS	5-70 pptv	marine air continental	oceans, 68 soils, 2	reaction with ·OH reaction with NO_3	2 d
SO_2	2-90 pptv	marine air continental	fossil fuel, 160 volcanoes, 14 from sulphides, 70	dry deposition, 100 oxidation to SO_4^{2-}, aerosol and wet deposition, 140	4 d

yr = year; d = day

The most important sulphur-containing compounds in the troposphere are carbonyl sulphide (OCS), hydrogen sulphide (H_2S), dimethyl sulphide (DMS) and sulphur dioxide (SO_2). Compared with anthropogenic sulphur emissions, which are dominated by SO_2, terrestrial biogenic sulphur emissions are dominated by H_2S and DMS (Bates et al., 1992a; Berresheim et al., 1995; Pham et al., 1995).

From all of the reduced sulphur compounds only OCS has a tropospheric residence longer than one year, which is considered to be sufficiently long to ensure long-range transport over wide areas and inter-hemispheric exchange. Due to its low chemical reactivity, OCS is the most abundant sulphur gas in the global background atmosphere. Carbonyl sulphide is also the only sulphur gas which can diffuse into the stratosphere where it can be photolysed at < 288 nm or oxidised to sulphuric acid (H_2SO_4), a process which is considered to be the dominant source of the stratospheric sulphate layer during periods of volcanic quiescence (Crutzen, 1976). Hydrogen sulphide (H_2S), a compound for which the global source strength is difficult to estimate, is oxidised in the atmosphere by ·OH radicals with the formation of SO_2.

Sulphur dioxide (SO_2), one of the most abundant sulphur compounds, is emitted into the atmosphere from anthropogenic activities such as fuel combustion and industrial activities (Li et al., 1999), natural sources including volcanic activity (Thornton et al., 1999) or as a final product of the oxidation of reduced sulphur compounds. Nguyen et al. (1983) have shown that one of the mechanisms of SO_2 formation is the biogenic production of reduced organic sulphur compounds in the ocean. The fate of SO_2 in the atmosphere is mainly dry deposition on the Earth's surface and oxidation to SO_4^{2-}, which then undergoes wet precipitation. Different studies have shown that in some regions wet deposition is more important than dry deposition (Xu and Carmichael, 1999). In other regions the wet deposition of SO_4^{2-} is chemically linked to primary emissions of SO_2 via atmospheric oxidants and, therefore, also to the emissions of nitrogen oxides (NO_x) and hydrocarbons within the region (Stein and Lamb, 2000).

Dimethyl sulphide, an important component of the biogeochemical sulphur cycle and thought to be the second most important source of sulphur in the atmosphere, represents an important biologically produced sulphur compound. It was found that DMS oxidation is a major source of boundary layer SO_2 over the ocean (Shon et al., 2001). The oxidation of DMS produces SO_2 and MSA which are brought back to Earth's surface by wet and dry deposition.

1.2 Dimethyl sulphide in the atmosphere

1.2.1 Sources and sinks of dimethyl sulphide in the atmosphere

Dimethyl sulphide (DMS) plays an important role in the global sulphur cycle and its emissions represent more than 90 % of the biogenic sulphur emissions from oceans (Andreae and Raemdonck, 1983; Dacey et al., 1987). Dimethyl sulphide (DMS) is a product of biological processes involving marine phytoplankton and is estimated to account for approximately 60 % of the total natural sulphur gas released to the atmosphere in both hemispheres (Andreae, 1990; Bates et al., 1992a; Spiro et al., 1992).

The most important pathway responsible for the formation of DMS is through the enzymatic cleavage of dimethylsulphoniopropionate (DMSP) with the formation of DMS and acrylic acid. It occurs usually in saline environments, and, as confirmed by new studies, also through bacterial and chemical degradation of DMSP in the presence of dinoflagellate in freshwater (Ginzburg et al., 1998 and references therein). The concentrations of both DMS and DMSP typically show a maximum a few meters below the ocean surface and a sharp decline at about 100 m depth where the light intensity is reduced to 1 % (Warneck, 1999). The atmospheric

concentration of DMS has been evaluated to be several orders of magnitude below that predicted from the sea water concentration (Georgii and Warneck, 1999). This could be an effect of the bacterial transformation of the DMS (aerobically transformation into CO_2, dimethyl sulphoxide (DMSO) and/or sulphate and anaerobically transformation into CH_4 and H_2S in the sea water) (Hansen et al., 1993) or may be due to the influences of some physical parameters during the transfer process of DMS from the sea surface to the air (Erickson III, 1993).

In samples of surface sea water the concentration of dimethyl sulphide is over-saturated, indicating a net flux from the sea to the air (Bates et al., 1994). The early water-to-air flux of DMS fell into the range 27 - 51 Tg S yr^{-1} (Andreae and Raemdonck, 1983; Barnard et al., 1982), while Bates et al. (1992a) estimated 16 Tg S yr^{-1} in the Northern Hemisphere and Staubes and Georgii (1993) reported 27 Tg S yr^{-1}. In 1994 Andreae et al. reported a flux of 35 Tg S yr^{-1}. Two new investigations (Keetle and Andreae, 2000; Keetle et al., 2001) reported a DMS flux from the oceans in the range from 13 to 17 Tg S yr^{-1} which confirms that DMS represents the greatest flux of reduced sulphur compounds over most regions of the oceans.

The continental sources of DMS are minor compared with the oceanic sources and are estimated to be about 0.6 Tg S yr^{-1} from soil and marshes and between 0.2 - 4.0 Tg S yr^{-1} from vegetation (Andreae and Jaeschke, 1992). The contributions of estuarine DMS emissions to the sulphur budget were found to be clearly insignificant (Cerqueira and Pio, 1999). The DMS concentrations at inland sites have been found to be generally 10 - 15 % lower compared with the values determined at coastal sites (Putaud et al., 1999). In the Canadian boreal region emissions from lakes were found to be an important component of the terrestrial emissions of biogenic sulphur released as DMS to the atmosphere (Sharma et al., 1999).

The atmospheric loss and biological consumption were found to be important removal pathways for DMS in the photic zone of the equatorial Pacific Ocean. The relative importance of each process has been found to be a function of the depth interval considered, sampling location and meteorological conditions (Kieber et al., 1996). The seasonal variation in DMS roughly follows the primary productivity cycle in the oceans (Andreae et al., 1995; Bates et al., 1987; Bates et al., 1992a; Erickson III et al., 1991; Nguyen et al., 1990; Putaud and Nguyen, 1996; Spiro et al., 1992). The major sink of atmospheric DMS is oxidation by ·OH radicals during the daytime and the reaction with NO_3 radicals during the night-time, a process which becomes important only in polluted areas (Winer et al., 1984). The ·OH concentration in marine environments is relatively constant, while the NO_3 concentration depends on the degree of pollution of the atmosphere (Barnes, 1993 and references therein) thus in remote marine environments, where the concentration of NO_x is low, the removal of DMS by NO_3 radicals is generally unimportant.

1.2.2 Chemical transformation of dimethyl sulphide: State of art

Dimethyl sulphide (DMS), emitted from the ocean, is a potential climate-modulating species. The general mechanism involves the oxidation of the sulphur atom in DMS to the +VI oxidation state followed by heteromolecular nucleation, which leads to the formation of new cloud condensation nuclei (CCN). In spite of intensive efforts, determination of the quantitative contribution of DMS-derived non-sea-salt sulphate (nss-SO_4^{2-}) to CCN formation in the marine boundary layer is still highly uncertain. Further progress in the elucidation of the DMS oxidation mechanism requires advances in field studies and detailed kinetic/product studies combined with modelling of the field data.

Field studies aimed at clarifying the oxidation mechanism of atmospheric DMS are focused on the influence of temperature on the relative distributions of measurable stable products and assessments of the diurnal trends in DMS and its associated products in the marine boundary layer (Bandy et al., 1996; Berresheim et al., 1993; Chen et al., 2000; Davison et al., 1996). Modelling of the field data usually shows that the modelled concentrations are in the right range and fit the observed concentrations fairly well (Barth et al., 2000; Hertel et al., 1994; Restad et al., 1998; Saltelli and Hjorth, 1995).

Oxidation of DMS in the atmosphere is a complex process, however, it is well established that the primary step is the reaction with ·OH radicals during the daytime and with NO_3 radicals during the night-time. It is known that the reaction of ·OH radicals with DMS proceeds through two independent channels: H-atom abstraction from the methyl group and ·OH radical addition to the S atom (Hatakeyama and Akimoto, 1983; Hynes et al., 1986; Hynes et al., 1993). Reaction with NO_3 appears to proceed exclusively by hydrogen abstraction as the first step (Atkinson et al., 1984; Butkovskaya and LeBras, 1994; Jensen et al., 1991; Jensen et al., 1992). Several reviews give a detailed account of the presence status of laboratory investigations of these reactions (Barone et al., 1995; Berresheim et al., 1995; Campologno et al., 1999; Ravishankara et al., 1997; Turnipseed and Ravishankara, 1993; Tyndall and Ravishankara, 1991; Yin et al., 1990a, b).

Based on some measurements of reactive halogen species (X_2, XO) and also on the behaviour of non methane hydrocarbons (NMHC), it has been speculated that Cl atoms, ClO and BrO radicals, in particular, might also play a role in the chemistry of the marine boundary layer and, consequently, in the chemistry of DMS oxidation (Barnes et al., 1991; Barnes et al., 1993; Ingham et al., 1999; Maurer et al., 1999; Urbanski and Wine, 1999).

Figure 1.2 shows the initiation reaction steps involving both addition and abstraction channels in the ·OH radical initiated photo-oxidation of DMS. Attack of ·OH radicals at the CH_3

group produces water and the methylthiomethyl radical ($CH_3SCH_2\cdot$), while addition of the ·OH radical to the S atom produces the dimethylhydroxysulphuranyl radical ($CH_3S\cdot(OH)CH_3$: DMS-OH) - an adduct, which can either dissociate back to reactants or react further to form products.

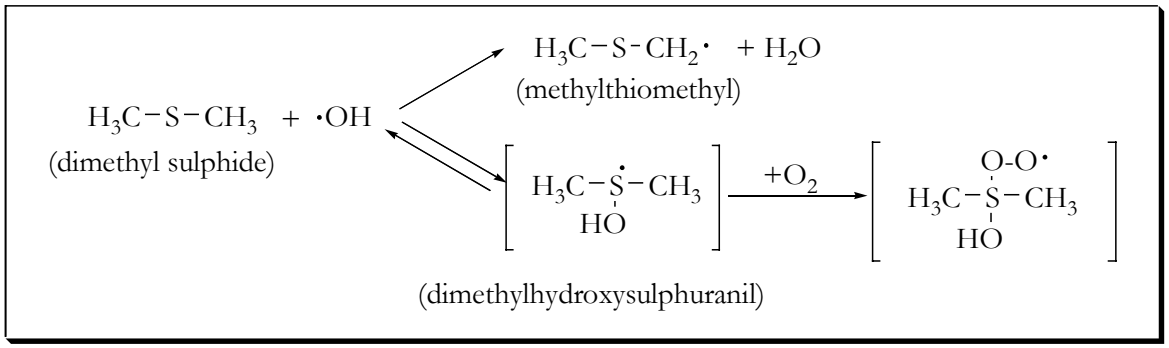

Figure 1.2: The initiation reaction steps in the ·OH radical initiated oxidation of dimethyl sulphide (DMS).

Ab initio calculations indicate that the most favoured pathway for the reaction of DMS with ·OH radicals is hydrogen abstraction with methylthiomethyl radical formation (Sekušak et al., 2000; Tureček, 1994) and that addition of ·OH radical to DMS leads to the formation of a stable DMS-OH complex (McKee, 1993a). However, the abstraction channel dominates in the absence of O_2. The addition channel involves oxidation of the adduct with O_2 in competition with adduct decomposition back into DMS and ·OH. At atmospheric concentrations of O_2 the addition and abstraction channels have equal rates at approximately 285 K. At higher temperatures H atom abstraction dominates (Berresheim et al., 1995 and references therein).

Due to the temperature dependent channels involved in the complex mechanism of DMS photo-oxidation, the product distribution for a given set of environmental conditions, as well as the diurnal trends in DMS, might be expected to have a significant and a very complex dependence on both temperature and the level of photochemical activity. In general, temperature changes should influence the DMS product distribution since it will determine the branching ratio between addition and abstraction. The rate coefficients for the initiation reactions and the overall reaction of DMS with ·OH radicals are fairly well established. In the literature one can find recommended values of the rate constant and equations which describe the dependence of the overall rate constant for the reaction of DMS with ·OH on temperature and O_2 concentration (Atkinson et al., 1997; DeMoore et al., 1997).

In laboratory photoreactor studies at room temperature, sulphur dioxide (SO_2), methane sulphonic acid ($CH_3S(O)_2OH$: MSA), dimethyl sulphoxide ($CH_3S(O)CH_3$: DMSO) and dimethyl sulphone ($CH_3S(O)_2CH_3$: $DMSO_2$) have been observed as products of the ·OH radical initiated

oxidation of dimethyl sulphide (Barnes et al., 1988; Niki et al., 1983; Patroescu et al., 1999; Sørensen et al., 1996). Dimethyl sulphoxide, which has been observed also in the marine boundary layer (Berresheim et al., 1998), appears to be a major product of the addition channel, formed by reaction of the DMS-OH adduct with O_2 (Arsene et al., 1999; Barnes et al., 1996; Sørensen et al., 1996). Dimethyl sulphone, sulphur dioxide and methane sulphonic acid have been observed as products of the further oxidation of DMSO in smog chamber studies (Barnes et al., 1989; Sørensen et al., 1996), however, there are discrepancies concerning their formation yields. Formation of methane sulphinic acid ($CH_3S(O)OH$: MSIA) at a very low yield has been also reported (Sørensen et al., 1996). In DMS oxidation systems free of NO_x, the formation of carbonyl sulphide (OCS) (Barnes et al., 1994; Barnes et al., 1996) and methyl thiolformate (CH_3SCHO: MTF) (Patroescu et al., 1996; Patroescu et al., 1999) were reported.

The presence of NO_x, which represents the sum of the concentrations of nitrogen monoxide and nitrogen dioxide ($NO + NO_2$), in photo-oxidative systems will influence the chemistry of biogenic sulphur compounds by controlling the branching of the reaction products from the photo-oxidation of DMS. Laboratory studies on the oxidation of DMS in the presence of high NO_x concentrations (corresponding to a heavily polluted atmosphere not typical for marine environments) indicate a strong influence of NO_x on the end product distribution, resulting in increasing formation yields of MSA and $DMSO_2$ and low SO_2 production. In the photo-oxidation of DMS initiated by ·OH radicals in the presence of NO_x, the formation of methane sulphonyl peroxynitrate (MSPN: $CH_3S(O)_2OONO_2$) was observed (Patroescu et al., 1999; Van Dingenen et al., 1994).

In studies of the photo-oxidation of DMS, under atmospheric conditions, MSA and H_2SO_4 were detected in sampled aerosols (Hatakeyama et al., 1985). Both species have been measured in field experiments (Mihalopoulos et al., 1992a). In measurement by Eisele and Tanner (1993) their concentrations were found to follow the solar flux. It was found that a decrease in atmospheric temperature causes an increase in the methane sulphonate (MS) to nss-SO_4^{2-} molar ratio in submicrometer aerosol particles (Bates et al., 1992b). In other field measurements in the boundary layer it was found that, at temperatures above 300 K little or no MS and MSA is produced, and the MS/(MS + SO_4^{2-}) ratio distinctly increases with decreasing temperature (Mauldin III et al., 1999). Some investigations (Berresheim et al., 1998; Davis et al., 1998, 1999; Jefferson et al., 1998) indicate that particulate levels of MSA in the boundary layer were higher than could be attributed to condensation of gas phase MSA onto aerosol surface. Photochemical box models were developed to examine the latitudinal and seasonal variations of the MS to non-sea-salt sulphate (nss-SO_4^{2-}) molar ratio in NO_x poor environments of the remote

marine atmosphere. These models gave evidence for the formation of MS through the ·OH radical addition reaction to the sulphur atom from DMS (Koga and Tanaka, 1993; 1999). They observed that if the MS production through the ·OH addition reaction is neglected, the predicted MS to nss-SO_4^{2-} molar ratios were not in agreement with the latitudinal and seasonal variations observed in the atmosphere. It was found that the seasonal variations of MSA in the rain water (Nguyen et al., 1992; Mihalopoulos et al., 1993) and atmosphere (Mukai et al., 1995) are strongly dependent on the primary production activity of the phytoplankton and, hence, on DMS.

1.2.3 Aerosol forming potential of dimethyl sulphide

Chemical processes involving aerosols can affect the Earth's radiative balance and the oxidative state of the troposphere and, thus, the atmospheric lifetimes of important trace gases such as methane, ozone, non methane hydrocarbons (NMHC) and dimethyl sulphide (DMS). It has been postulated that the emission of DMS from the oceans and the subsequent formation of sulphate aerosols can have a significant influence on the Earth's radiation budget and possibly on climate regulation, the so called CLAW hypothesis (Charlson et al., 1987). From the positive correlation between concentrations of dimethyl sulphide (DMS) and cloud condensation nuclei (CCN) in oceanic air mass observed in some studies, it has been concluded that DMS makes a large contribution to the production of nss-sulphate (nss-SO_4^{2-}) and CCN (Nagao et al., 1999).

The major question concerning DMS in the atmosphere is how important is its role in controlling the levels of aerosol in the marine boundary layer (MBL). There are three main sources of aerosol in the remote MBL: sea salt, non-sea-salt (nss) and free tropospheric aerosol. The principal component of nss-aerosol is sulphate derived from the oxidation of gaseous DMS (the SO_2 produced from DMS oxidation is the predominant source of *in situ* nss-sulphate). The relative contributions of the three marine aerosol sources depend upon many factors such as wind speed, frequency of appearance of clouds and precipitation, sea-surface dimethyl sulphide emission rates, oxidation mechanism of DMS to SO_2, MSA and rate of entrainment of free tropospheric aerosol.

Any effect that DMS could have on the climate is considered to be dependent on the production of gas phase H_2SO_4 and new particles. Once formed through chemical reactions, the sulphate particles in the troposphere can cool the climate in two ways: directly, under clear skies, by back reflection of incoming solar radiation or indirectly by increasing the reflectivity of clouds. An important effect of all these phenomena is the changing of the photo-chemistry of some processes, manifested in changes in photolysis rates of important reactions.

1.3 Aims of the present work

The mechanism of the ·OH radical initiated oxidation of dimethyl sulphide is very complex and presently not fully understood. For the reactions of ·OH radicals with both DMS and DMSO, detailed information on the change of the distribution of the reaction products with temperature is not available. The main products from the ·OH initiated photo-oxidation of DMS are known to be sulphur dioxide (SO_2), dimethyl sulphoxide ($CH_3S(O)CH_3$), methane sulphonic acid ($CH_3S(O)_2OH$), formaldehyde (HCHO) and aerosols. The exact yields of the oxidation products, particularly as a function of temperature and different NO_x levels, are not known. To understand the exact mechanism that leads to the final products from dimethyl sulphide oxidation, we need to know in what way parameters such as temperature and the NO_x level can influence the formation of end products.

The general objectives of the present work are as follows:

- determination of the influence of temperature on the product distribution from the ·OH radical initiated oxidation of DMS and DMSO (with emphasis on the SO_2 and DMSO yields);
- determination of the influence of NO_x on the product distribution from the ·OH radical initiated oxidation of DMS and DMSO (with emphasis on the SO_2 and DMSO yields);
- identification of possible intermediate products, *e.g.* methane sulphinic acid ($CH_3S(O)OH$).

The ultimate aim of the work is to provide an extended data base for quantification of the contribution of DMS-derived nss-sulphate (nss-SO_4^{2-}) to cloud condensation nuclei (CCN) in the marine boundary layer (MBL).

Chapter 2

Experimental section

In the main part of the work the experiments were carried out in an 1080 l reaction chamber at a total pressure of 1000 mbar (O_2 + N_2) and temperatures of 284, 295 and 306 ± 2 K. The photolysis of hydrogen peroxide (H_2O_2) and methyl nitrite (CH_3ONO) were used as sources of ·OH radicals. All the commercially available chemicals were used without further purification.

2.1 Description of the reactor

The 1080 l cylindrical reaction chamber made of quartz has a length of 6.2 m and an internal diameter of 0.47 m. It is closed at both ends by aluminium flanges. The reactor consists of two quartz glass cylinders which are connected by a central enamel flange ring and silicon rubber seals. The reactor can be temperature regulated within the range 283 to 308 K with a precision of ± 2 K through a regulation system using three PT-100 thermo-elements.

A magnetic coupled Teflon radial ventilator, which ensures a rapid homogeneity of the reaction mixture in the chamber, is located on the central enamel flange. The pumping system connected to the same enamel flange consists of a turbo molecular pump (Leybold-Heraeus PT 450) backed by a Leybold D65B double stage rotary vacuum pump which provides an end-vacuum of 10^{-3} mbar. In the reactor the temperature and pressure are measured by a special thermo-element and a calibrated capacity vacuumeter (MKS - Baratron), respectively.

One of the aluminium end flanges has ports for the inlet of the reactants and bath gases. The instruments for temperature (T) and pressure (P) monitoring are also connected to this

flange. The opposite aluminium flange has ports for the collection of samples for further analysis using different analytical methods (gas chromatography, ion chromatography and gas chromatography coupled with mass spectrometry). A port for the collection of aerosol samples is located on the central enamel flange.

The experimental set-up of the 1080 l reactor is shown schematically in Figure 2.1.

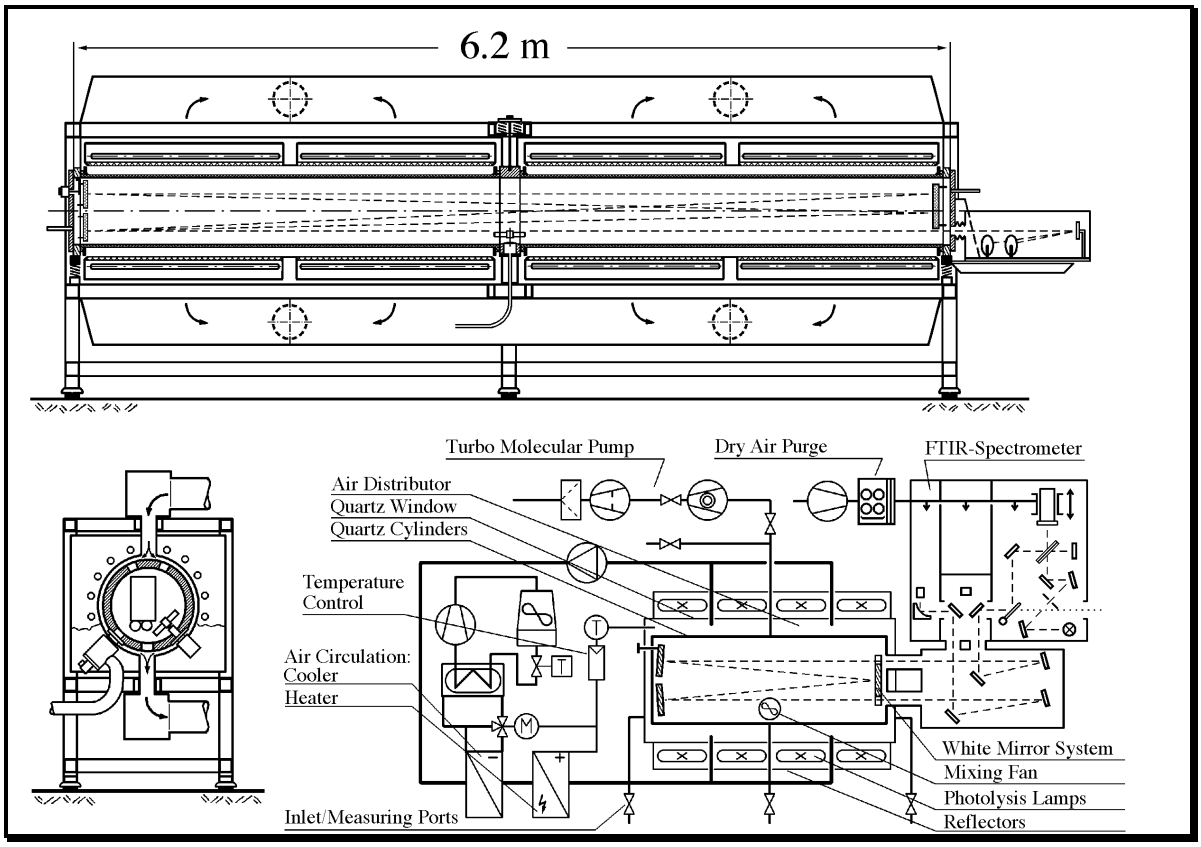

Figure 2.1: Schematic representation of the 1080 l reaction chamber.

The reactor is equipped with 32 super actinic fluorescent lamps (Philips TL 05/40 W: 320 < λ < 480 nm, λ_{max} = 360 nm) and 32 low-pressure mercury lamps (Philips TUV 40 W: λ_{max} = 254 nm) which are equidisposed in four segments around the quartz tubes.

The reaction chamber contains a multiple reflection mirror system mounted on the flanges. The multi-reflection White-type mirror system (5.6 m base length, 492 m total optical path length) is coupled by an external mirror system to a Fourier Transform Infrared (FT-IR) Spectrometer (Bruker IFS 88). The spectrometer is equipped with a KBr beam splitter and HgCdTe detector (MCT - mercury/cadmium/tellurium detector) cooled to 77 K with liquid nitrogen.

This system allows the *in situ* monitoring of reactants and products by long-path infrared (IR) absorption using a resolution of 1 cm^{-1}. A globar is used as IR source for the spectrometer. The spectrometer and the external mirror system, covered by a protective box, are permanently flushed with dry air in order to remove water vapour. The spectrometer is directly controlled by the software provided by Bruker, running on a personal computer where raw data are transferred and stored. The analysis of the spectra is performed by the use of a spectroscopy OPUS software provided by Bruker.

2.2 Measurement procedure

The reaction chamber was evacuated by a vacuum pump able to reduce the pressure inside the chamber below 10^{-3} mbar. Background spectrum was recorded by filling the reaction chamber to a total pressure of 1000 mbar synthetic air.

The investigated compounds were injected into the evacuated chamber by means of calibrated syringes (gas-tight syringes and microlitre syringes) either directly or in a stream of dilution gas. In order to avoid deposition of low vapour pressure reactants to the walls of the inlet system, the inlet port was heated to 70 -100 ^{o}C. The reactants were introduced into the reactor under continuous stirring.

Hydrogen peroxide (H_2O_2) or methyl nitrite (CH_3ONO) were added into the chamber in order to generate ·OH radicals by photolysis.

Photolysis of H_2O_2: The photolysis of hydrogen peroxide is considered a relatively clean ·OH radical source, which allows experiments to be performed in NO_x free systems. The ·OH radicals are generated by the reaction:

$$H_2O_2 + h\nu\ (\lambda_{max} = 254\ nm) \rightarrow 2\ \cdot\mathbf{OH}. \qquad \text{(R 2.1)}$$

Photolysis of methyl nitrite: Photolysis of methyl nitrite produces ·OH radicals in the following sequence of reactions:

$$CH_3ONO + h\nu\ (\lambda_{max} = 360\ nm) \rightarrow CH_3O\cdot + NO \qquad \text{(R 2.2)}$$

$$CH_3O\cdot + O_2 \rightarrow CH_2O + HO_2\cdot \qquad \text{(R 2.3)}$$

$$HO_2\cdot + NO \rightarrow \cdot\mathbf{OH} + NO_2. \qquad \text{(R 2.4)}$$

When photolysis of methyl nitrate in synthetic air was used as the hydroxyl radical source nitric oxide, NO, was added to the reaction mixture to suppress the formation of ozone and hence of nitrate radicals.

The reaction chamber was subsequently filled to 1000 mbar with synthetic air, nitrogen or oxygen in accordance with the type of experiment which was performed. Before starting measurements the reaction mixtures were kept in the dark for approximately 10 minutes in order to allow thermal equilibrium to be established. After acquiring a few spectra of the mixture in the dark, the photo-oxidation was initiated by switching on either the UV or VIS lamps according to the required conditions.

The concentration-time behaviours of the dimethyl sulphide and products were monitored in situ using long path FT-IR spectroscopy (Bruker IFS-88, 492 m path length, HgCdTe detector). Generally infrared spectra were recorded in the 650 - 4000 cm^{-1} wavelength range, with a resolution of 1 cm^{-1}. Usually, about 10 - 15 spectra, derived from 128 co-added interferograms, were collected over irradiation periods of 20 - 30 min. Concentrations of reactant and products were mainly determined by computer-aided spectral abstraction using calibrated reference spectra generated in this laboratory.

The only exceptions were methane sulphinic acid and inorganic sulphate which were determined along with methane sulphonic acid using the Odyssey Ion Chromatography (IC) System. The IC consists of a 526 HPLC pump, an Alltech ERIS 1000 HP autosuppressor, a 550 conductivity detector and a 7725/7725i Rheodyne injection valve. An Allsep hydrophilic anion exchange column filled with methyl acrylate containing quaternary amine functional groups (particle size 7 μm, 100 mm length x 4.6 mm ID) operated at ambient temperature was used for the anion separation. To analyse methane sulphinate, methane sulphonate and sulphate ions, a mobile phase consisting of a mixture of bicarbonate (0.24 mM) and carbonate (0.3 mM) sodium salts solutions was chosen as eluent. During the analysis of the above ions by IC, the flow of the eluent was maintained at rates of 0.5 ml min^{-1} or 1.0 ml min^{-1}.

Calibrations of the methane sulphinate ($CH_3SO_2^-$), methane sulphonate ($CH_3SO_3^-$) and sulphate (SO_4^{2-}) anions were performed using standard solutions of the sodium salts of methane sulphinic and methane sulphonic acids and sulphuric acid. Working standards were prepared by using MSIA and MSA sodium salts provided by Lancaster (97 % purity) and Aldrich (99.5 % purity), respectively, and Milli - Q water (R = 18.5 $M\Omega cm^{-1}$). Calibrations were performed weekly and every day one or two working standards were injected for comparison. Compounds were identified by comparison of the retention time of peaks of the unknown samples with the retention times of peaks in the chromatograms of standard solutions.

It was observed that the heights of the IC peaks corresponding to the $CH_3S(O)O^-$ and $CH_3S(O)_2O^-$ anions were proportional to the concentration of $CH_3S(O)O^-$ and $CH_3S(O)_2O^-$, respectively, and in the range of 0.2 - 12 μg ml^{-1} good correlation coefficients were obtained. Chemical compounds were identified by matching the retention time of peaks of the unknown sample with the retention times of peaks in the chromatograms of the standards.

Methane sulphinic, methane sulphonic and sulphuric acid were cryogenically sampled from the reactor using a system composed of a short Teflon tube attached to 2 empty glass U-tube traps connected in series and immersed in an ethanol/liquid nitrogen slush bath (-112° C), a flow controller and pump (Appendix A).

Due to the low temperature, any methane sulphinate, methane sulphonate or sulphate passing through the trap were condensed on the walls of the tube. The pump rate through the cold trap was adjusted to either 0.5 or 1 l min^{-1} and 5 to 40 l were sampled during different experiments. Due to its high reactivity, MSIA was sampled continuously during the irradiation period rather than after termination of the irradiation.

After the collection, 5 ml reagent grade water was added to the U-tube to dissolve the sampled material which was transferred into a small storage flask. The flasks were then stored at dry ice temperature (-78° C) to reduce oxidation of MSIA to MSA. The samples were analysed as soon as possible after collection by ion chromatography. The samples were analysed for methane sulphinate, methane sulphonate and sulphate anions by injecting a 200 μl aliquot of the collected sample via an injection loop into the IC system.

The detection limits for ion chromatographic analysis were estimated as three times the standard deviation of duplicate analyses of low level samples (below 0.2 μg ml^{-1}) and were about 0.012 μg ml^{-1} for $CH_3S(O)O^-$, 0.014 μg ml^{-1} for $CH_3S(O)O^-$ and 0.011 μg ml^{-1} for SO_4^{2-}.

2.3 Data analysis

Product studies were carried out in the 1080 l reactor described in Paragraph 2.1, Chapter 2 using FT-IR spectroscopy and the IC method.

Products and reactants, first of all, were identified by comparison of the infrared spectra of the reaction mixture with the reference spectra of the pure compounds. Concentrations of reactant and products were determined by computer-aided spectral subtraction using reference spectra. The known concentration of each reference spectra and the subtraction factors allowed the concentration of each compound to be determined.

For most of the identified sulphur-containing products, the plots of their concentration, either versus reaction time or versus the concentration of the consumed reactant, showed a very strong curvature indicating that secondary reactions of the primary products take place during the time of experiment. In order to obtain the formation yields of the products, such as SO_2, DMSO and MTF, their measured concentrations have been corrected for the further reaction with ·OH radicals, the loss on the reactor walls and possible photolysis.

In the case of products such as MSA, MSPN and OCS, secondary formation and removal processes occurring in the system under the conditions employed during the experiments made the procedure for the correction of the measured concentration difficult. Therefore, the molar formation yields of these products was derived from the uncorrected concentration plotted versus the consumption of the reactant in the early stage of reaction, when the secondary processes can largely be neglected.

At atmospheric conditions, *i.e.* 200 mbar partial pressure of O_2, and temperatures of 284, 295 and 306 K, the corrections were performed using the mathematical procedure described by Tuazon et al. (1986). This procedure is based on the reaction sequence:

DMS + ·OH	→ Y (SO_2 or DMSO), k_1	(R 2.5)
(SO_2 or DMSO) + ·OH	→ products, k_2	(R 2.6)
(SO_2 or DMSO)	→ wall, k_3	(R 2.7)

in the case of SO_2 and DMSO, and on the reaction sequence:

DMS + ·OH	→ Y (MTF), k_1	(R 2.8)
MFT + ·OH	→ products, k_2	(R 2.9)
MTF + $h\nu$	→ products, k_3	(R 2.10)

in the case of MTF. It is known that MTF formed in the reaction system can be photolysed and also further oxidised by reaction with ·OH radicals, while the walls loss of MTF is negligible (Patroescu, 1996).

In the reaction schemes presented above, Y is the formation yield of SO_2, DMSO or MTF formed from the ·OH radical initiated oxidation of DMS and k_1, k_2 and k_3 are the rate coefficients for the respective reactions.

Assuming that the ·OH radical concentrations are constant over the small irradiation periods, it can be written:

$$[DMS]_{t_2} = [DMS]_{t_1} \cdot e^{-(k_1[OH])(t_2 - t_1)} \quad \text{(E 2.1)}$$

and

$$[Y]_{t_2} = [Y]_{t_1} \cdot \left[e^{-(k_2[OH]+k_3)(t_2-t_1)} \right] + \frac{Y_{t_1-t_2} \cdot [DMS]_{t_1} \cdot k_1[OH]}{((k_2-k_1)\cdot[OH]+k_3)} \cdot \left[e^{-k_1[OH](t_2-t_1)} - e^{-(k_2[OH]+k_3)(t_2-t_1)} \right] \quad \text{(E 2.2)}$$

where $[DMS]_{t1}$, $[DMS]_{t2}$, $[Y]_{t1}$ and $[Y]_{t2}$ are the concentrations of dimethyl sulphide and the sulphur-containing products observed at times t_1 and t_2, respectively, and $[Y]_{t1\text{-}t2}$ is the formation yield of the individual products over the time period (t_1-t_2).

The ·OH radical concentration was calculated from the decay of the reactant, according to the following equation:

$$[OH] = \frac{\ln\left([DMS]_{t_2} / [DMS]_{t_1}\right)}{k_1 \times (t_2 - t_1)}, \quad \text{(E 2.3)}$$

where k_1 is the rate coefficient of the reaction of DMS with ·OH radicals (overall reaction including abstraction and addition).

The values of k_1 were calculated for different temperatures using the recommended literature expression from Hynes et al. (1986):

$$k_1 = \frac{\left[T \cdot \exp((-234)/T) + 8.46\times10^{-10} \cdot \exp(7230/T) + 2.68\times10^{-10} \cdot \exp(7810/T)\right]}{\left[1.04\times10^{11} \cdot T + 88.1 \cdot \exp(7460/T)\right]} \quad \text{(E 2.4)}$$

$$k_{ab} = 9.6\times10^{-12} \exp\left[-(234/T)\right] \quad \text{(E 2.5)}$$

$$k_{ad} = k_1 - 9.6\times10^{-12} \exp\left[-(234/T)\right] \quad \text{(E 2.6)}$$

where k_{ab} is the rate constant of the abstraction channel and k_{ad} is the rate constant of the addition channel. Both k_{ab} and k_{ad} expressions were used the calculate the contribution of the fraction of the reaction occurring via the addition and abstraction pathways.

For the reaction of ·OH radical with SO_2, the k_2 values were calculated from the Arrhenius expression

$$k_2(OH + SO_2) = 5.07 \times 10^{-13} \exp\left(231/T\right) \quad \text{cm}^3 \text{ molecule}^{-1} \text{ s}^{-1} \qquad \text{(E 2.7)}$$

used in modelling studies (Yin et al., 1990a; Hertel et al., 1994). Dark experiments showed that the walls loss of SO_2 over the time period of the measurements was within the detection error limits. This allows a value of smaller than 1 x 10^{-6} s^{-1} to be placed on k_3 for SO_2.

The rate coefficient for the reaction of ·OH radicals with DMSO is associated with a high degree of uncertainty (Hynes and Wine, 1996; Urbanski et al., 1998). For the purposes of the yield correction, the Arrhenius expression

$$k_2(OH + DMSO) = 10^{-11.2 \pm 0.7} \exp\left(\left(800 \pm 540\right)/T\right) \quad \text{cm}^3 \text{ molecule}^{-1} \text{ s}^{-1} \qquad \text{(E 2.8)}$$

from Hynes and Wine (1996) was used to calculate the rate coefficients for the individual temperatures. Walls loss of dymethyl sulphoxide was found to be quite significant. First order loss rates, k_3 = 7 x 10^{-5} s^{-1} for 284 K and k_3 = 1 x 10^{-4} s^{-1} for 295 and 306 K, obtained in dark experiments, were used in the yield correction calculations. Due to extensive pumping and purging of the reactor between experiments, the variation of the loss rates between the different experiments was negligible, indicating that conditioning of the chamber walls, which could affect the loss rates, was not a problem.

The rate coefficient for the reaction of MTF with ·OH radicals, k_2(MTF) is known only for room temperature. Therefore, a formation yield correction was performed only on the data for 295 K in 1000 mbar of synthetic air. A value of $k_{2(\cdot OH + MTF)}$ = 1.11 x 10^{-11} cm^3 $molecule^{-1}$ s^{-1} taken from Patroescu et al. (1996) was used for the correction. The photolysis frequency for MTF under the conditions of the experiments was k_3 = 5 x 10^{-3} s^{-1}, as determined in earlier study on MTF kinetics in the same reactor.

Using the rate constants k_1, k_2, and k_3 described above together with $[Y]_{t1\text{-}t2}$, sulphur-containing products concentrations corrected for reaction with ·OH radicals, photolysis and/or wall loss are given by

$$[Y]_{t_2}^{corr} = [Y]_{t_1}^{corr} + Y_{t_1 - t_2} \cdot \left([DMS]_{t_2} - [DMS]_{t_1}\right) \qquad \text{(E 2.9)}$$

where $[Y]_{t_1}^{corr}$ and $[Y]_{t_2}^{corr}$ are the corrected product concentrations at times t_1 and t_2, respectively.

The corrected product concentrations were then plotted versus the amount of the reactant consumed. Least square analysis of the slopes of such plots gives the molar formation yield of the individual product. The indicated error of the product formation yields is twice the standard deviation of the linear regression combined with overall uncertainties in the concentration of the reference spectra and in the subtraction factors. Uncertainties in the rate coefficients used for the correction are not included.

Chapter 3

Product study of the photo-oxidation of dimethyl sulphide in NO_x free systems

In this work, investigations on the atmospheric degradation mechanism of dimethyl sulphide (DMS) in NO_x free systems have been performed. The product studies on the gas-phase oxidation of dimethyl sulphide were carried out in the 1080 l reactor. The products of the ·OH radical initiated oxidation of dimethyl sulphide have been investigated using the photolysis of H_2O_2 as the ·OH radical source and long path FT-IR spectroscopy to monitor reactants and products at 1000 mbar total pressure. The behaviour of the products was investigated as a function of temperature (284, 295 and 306 ± 2 K) and oxygen partial pressure (20, 200 and 500 mbar).

3.1 Results

The sulphur-containing products observed and quantified in the irradiation of DMS/H_2O_2/(N_2+O_2) reaction mixtures included sulphur dioxide (SO_2), dimethyl sulphoxide (DMSO: $CH_3S(O)CH_3$), dimethyl sulphone ($DMSO_2$: $CH_3S(O)_2CH_3$), methane sulphonic acid (MSA: $CH_3S(O)_2(OH)$), carbonyl sulphide (OCS), methane thiol formate (MTF: CH_3SCHO), methane sulphinic acid (MSIA: $CH_3S(O)OH$) and inorganic sulphate (SO_4^{2-}). As non-sulphur-containing products methanol (CH_3OH), formic acid (HCOOH), formaldehyde (HCHO), methyl hydroperoxide (CH_3OOH), CO and CO_2 were detected.

3.1.1 FT-IR analysis of stable products

Dimethyl sulphoxide (DMSO)

Figure 3.1 shows all the measured yield-time profiles for DMSO for different temperatures (284, 295 and 306 K) and O_2 partial pressures (20, 200 and 500 mbar). In order to better highlight the observed trends, an example of the yield-time profiles of DMSO as a function of temperature for one O_2 partial pressure (200 mbar) is shown separately in Figure 3.2.

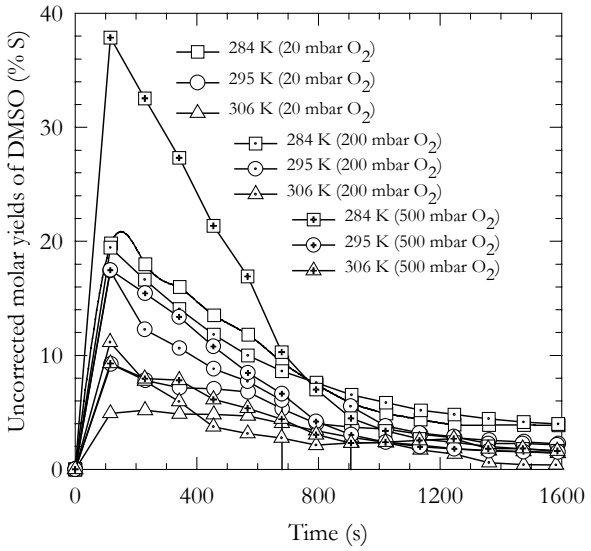

Figure 3.1: Plots of the uncorrected molar yields of DMSO as a function of O_2 partial pressure (20, 200 and 500 mbar) and temperature (284, 295 and 306 K) versus reaction time.

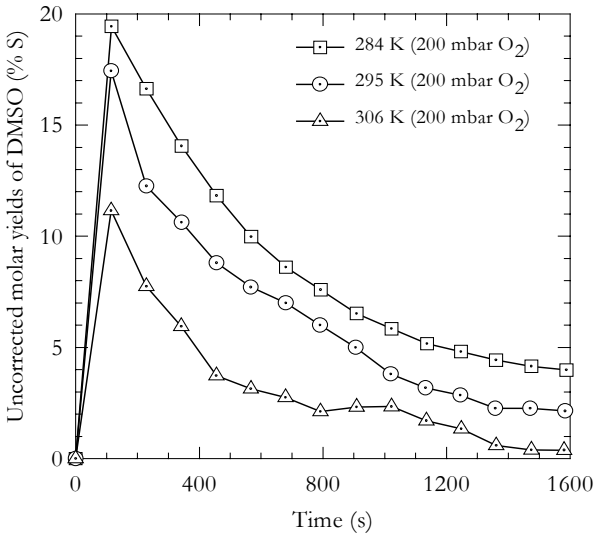

Figure 3.2: Plots of the yields of DMSO as a function of temperature (284, 295 and 306 K) versus reaction time determined with an O_2 partial pressure of 200 mbar, *i.e.* atmospheric conditions.

Figures 3.1 and 3.2 show that the observed yield of DMSO (i) decreases with increasing temperature at constant O_2 partial pressure and (ii) increases with increasing O_2 partial pressure at constant temperature. The shapes of the curves for DMSO in Figure 3.1 are determined by production of DMSO from DMS oxidation, loss to the reactor walls and further oxidation of DMSO by ·OH radicals. To derive the formation yields of DMSO its measured concentration had to be corrected for further reaction with ·OH radicals and wall loss. Corrections were performed using the mathematical procedure described in Chapter 2, Paragraph 2.3. Plots of the DMSO corrected concentrations versus the amount of DMS consumed for an O_2 partial pressure of 200 mbar (atmospheric conditions) and temperatures of 284, 295 and 306 K are shown in Figure 3.3. The slopes of the lines give the formation yield of the compound at the respective temperature. In all cases straight lines are obtained which supports the validity of the corrections.

The corrected formation yields for DMSO obtained by the least-squares analysis of these plots are collected in Table 3.1. The errors quoted in Table 3.1 are the 2σ random scatter in the data plots (Figure 3.3) and reflect the measurement errors in DMSO and DMS concentrations using long path FT-IR spectroscopy (the quantification of DMSO, especially at the end of the experiments, was mostly affected by the formation of formic acid, a compound which overlaps the characteristic spectral features of DMSO in the wave number range of 1150 - 1100 cm^{-1}).

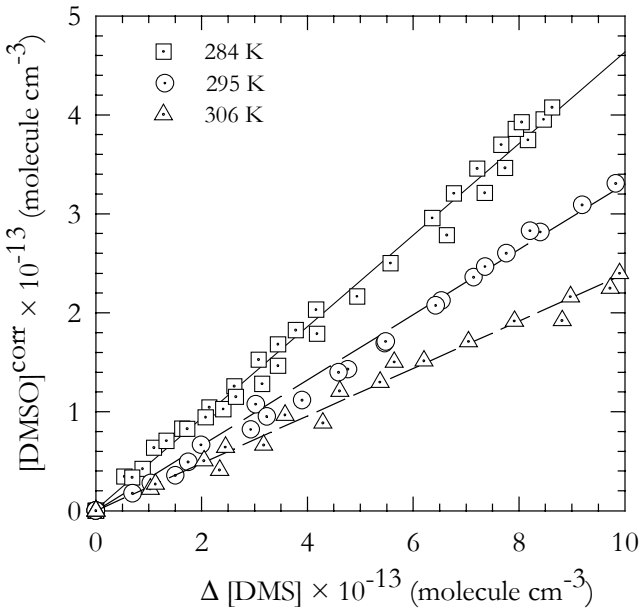

Figure 3.3: Plots of the DMSO corrected concentrations versus the consumption of DMS for an O_2 partial pressure of 200 mbar and temperatures of 284, 295 and 306 K.

Table 3.1: Corrected yields for the formation of DMSO in the reaction of DMS with ·OH radicals in 1000 mbar of synthetic air as a function of temperature.

Temperature (K)	Corrected DMSO yields (% molar yield, ± 2 σ)*	Contribution of addition pathway** (%)
284	46.3 ± 5.0	52
295	34.8 ± 7.6	33
306	24.4 ± 2.8	17

* See Paragraph 2.3, Chapter 2 for details of the correction calculations.

** The yields are compared to the fraction of the reaction occurring *via* the addition pathway calculated using the results of Hynes et al. (1986) for the specific reaction conditions.

Dimethyl sulphone ($DMSO_2$)

The measured yield-time profiles for $DMSO_2$ as a function of the different temperatures and O_2 partial pressures are shown in Figure 3.4. For better clarity of the observed trends, the yield time profiles of $DMSO_2$ as a function of temperature for an O_2 partial pressure of 200 mbar are

shown separately in Figure 3.5. From Figures 3.4 and 3.5 it is evident, that the observed yield of $DMSO_2$ (i) increases with increasing temperature at constant O_2 partial pressure and (ii) increases with increasing O_2 partial pressure at constant temperature.

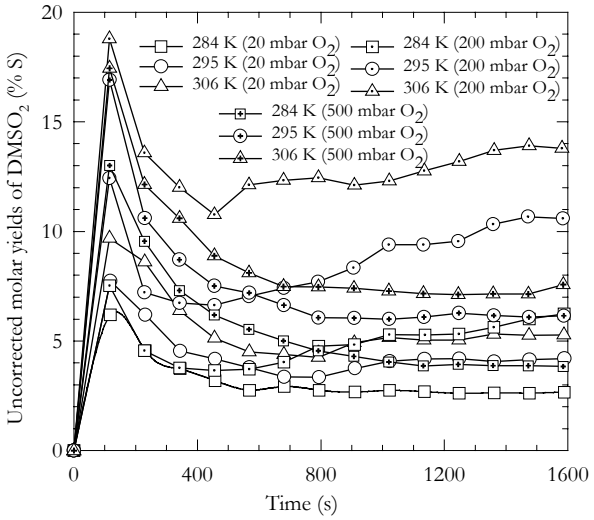

Figure 3.4: Plots of the uncorrected molar yields of $DMSO_2$ as a function of O_2 partial pressure (20, 200 and 500 mbar) and temperature (284, 295 and 306 K) versus reaction time.

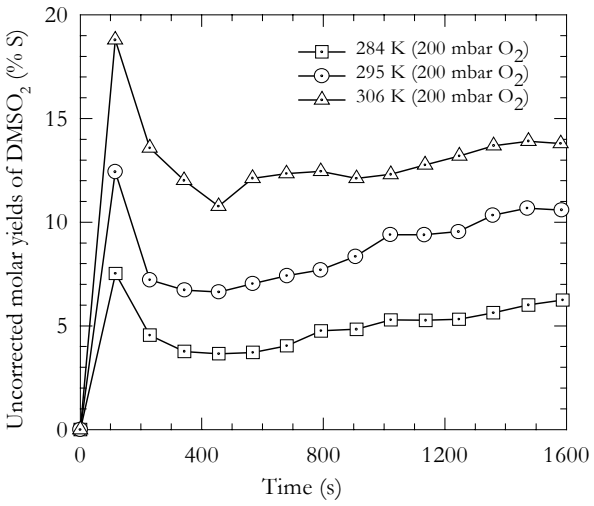

Figure 3.5: Plots of the yields of $DMSO_2$ as a function of temperature (284, 295 and 306 K) versus reaction time at an O_2 partial pressure of 200 mbar, *i.e.* atmospheric conditions.

The shape of the curves for $DMSO_2$, is determined by production of $DMSO_2$ from the oxidation of DMS and loss on the reactor walls. The reaction between $DMSO_2$ and ·OH radicals is slow, a rate constant $k_{(DMSO2+\cdot OH)} = (1.0 + 0.5) \times 10^{-13}$ cm^3 molec^{-1} s^{-1} has been reported (Falbe-Hansen et al., 2000), therefore this reaction will not be important in the system. Accordingly, the $DMSO_2$ yields were corrected only for wall loss ($k_{wall} < 2 \times 10^{-5}$ s^{-1}).

Plots of the $DMSO_2$ concentrations corrected for wall loss versus the consumed amount of DMS (Δ [DMS]) for an O_2 partial pressure of 200 mbar, *i.e.*, atmospheric conditions, and temperatures of 284, 295 and 306 K are shown in Figure 3.6. The slopes of the lines give the formation yield of the compound at the respective temperatures. Linear dependencies were obtained for the experiments with 200 mbar of O_2 (Figure 3.6) and also for the experiments with 20 and 500 mbar O_2 (not shown).

The formation yields for $DMSO_2$ obtained by least-squares analysis of these plots are collected in Table 3.2. From Table 3.2 it is clear that under atmospheric conditions the observed yields of $DMSO_2$ are highly variable, but represent no more than 8 % S. However, the yields tend to be higher at the higher temperatures.

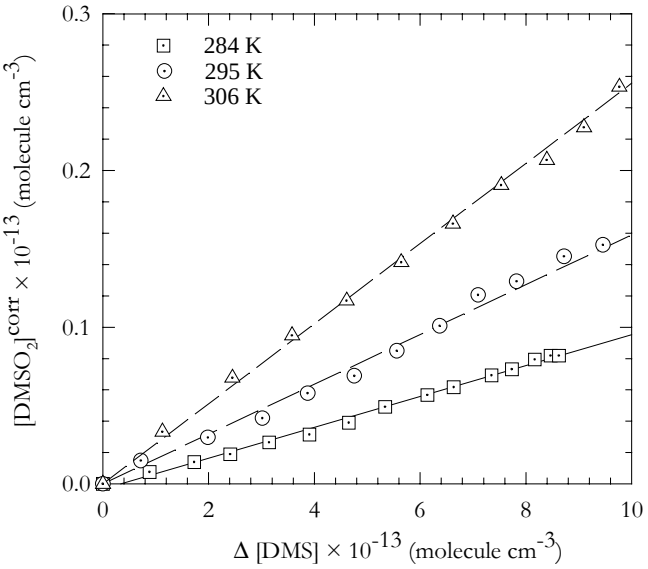

Figure 3.6: Plots of the $DMSO_2$ concentrations versus the consumption of DMS for an O_2 partial pressure of 200 mbar and temperatures of 284, 295 and 306 K.

Table 3.2: Formation yields of $DMSO_2$ in the reaction of DMS with ·OH radicals at different O_2 partial pressures (20, 200 and 500 mbar O_2) as a function of temperature (284, 295, 306 K).

Temperature (K)	$DMSO_2$ yields (% molar yield, $\pm 2\sigma$)		
	20 mbar O_2	200 mbar O_2	500 mbar O_2
284	2.73 ± 0.42	3.89 ± 0.67	4.92 ± 0.79
295	3.15 ± 0.49	4.32 ± 0.64	6.13 ± 0.84
306	5.34 ± 0.73	6.71 ± 1.08	7.56 ± 0.73

Sulphur dioxide (SO_2)

For SO_2 the uncorrected yield-time profiles as a function of the different temperatures and O_2 partial pressures investigated are presented in Figure 3.7. In order to better highlight the observed trends with temperature and O_2 partial pressure, the yield-time profiles of SO_2 as a function of temperature for a constant O_2 partial pressure of 200 mbar are shown separately in Figure 3.8.

The plots of the SO_2 concentrations corrected for reaction with ·OH radicals and wall loss versus the amount of DMS consumed (Δ [DMS]) for an O_2 partial pressure of 200 mbar (atmospheric conditions) and temperatures of 284, 295 and 306 K are shown in Figure 3.9.

The corrected formation yields for SO_2 obtained by the least-squares analysis of the plots presented in Figure 3.9 are collected in Table 3.3. However, compared with DMSO, the accuracy of the SO_2 formation yields is considered to be much superior to those for DMSO, since the rate coefficient $k_{2(\cdot OH + SO2)}$ is much better established than the rate coefficient $k_{2(\cdot OH + DMSO)}$.

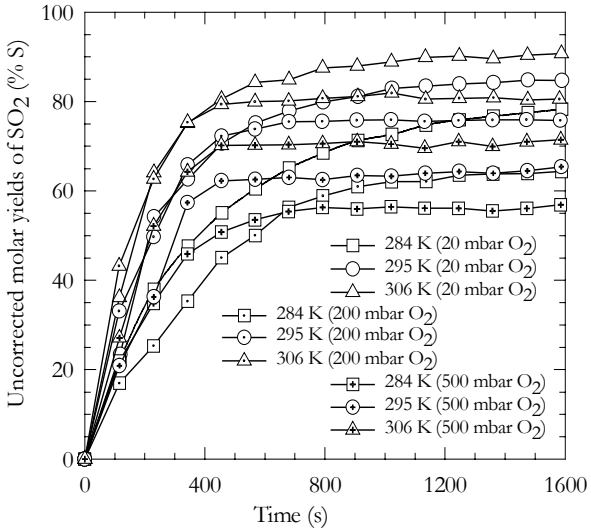

Figure 3.7: Plots of the uncorrected molar yields of SO_2 as a function of O_2 partial pressure (20, 200 and 500 mbar) and temperature (284, 295 and 306 K) versus reaction time.

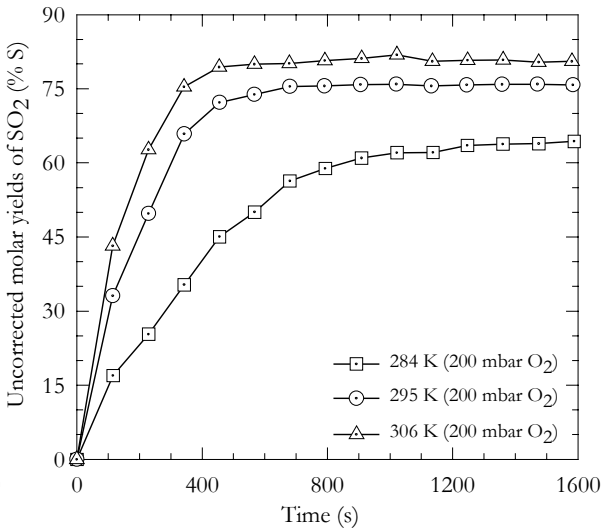

Figure 3.8: Plots of the yields of SO_2 as a function of temperature (284, 295 and 306 K) versus reaction time for a constant O_2 partial pressure of 200 mbar, *i.e.* atmospheric conditions.

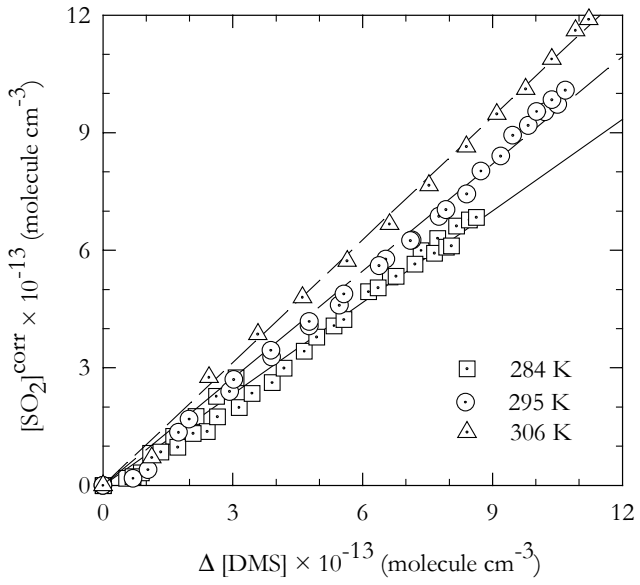

Figure 3.9: Plots of the SO_2 corrected concentrations versus the consumption of DMS for an O_2 partial pressure of 200 mbar and temperatures of 284, 295 and 306 K.

Table 3.3: Corrected yields for the formation of SO_2 in the reaction of DMS with ·OH radicals in 1000 mbar of synthetic air as a function of temperature.

Temperature (K)	Corrected SO_2 yields* (% molar yield, ± 2 σ)	Contribution of addition pathway** (%)	Contribution of abstraction pathway** (%)
284	84.3 ± 6.5	52	48
295	95.0 ± 3.8	33	67
306	99.0 ± 6.5	17	83

* See Paragraph 2.3, Chapter 2 for details of the correction calculations.

** The yields are compared to the addition and abstraction fractions of the reaction calculated using the results of Hynes et al. (1986).

Methane sulphonic acid (MSA)

Methane sulphonic acid (MSA) is a compound with very low vapour pressure. Nevertheless, the infrared spectrum for gaseous MSA is known (Mihalopoulos et al., 1992b) and, hence, the identification and quantification of this compound in the gas phase was possible.

In Figure 3.10 the measured yield-time profiles for gaseous MSA are shown as a function of the different temperatures and O_2 partial pressures. The yield-time profiles of MSA as a function of temperature for a constant O_2 partial pressure of 200 mbar are shown again separately in Figure 3.11. In both figures the yields of MSA have not been corrected for possible secondary processes.

Information on the formation of MSA in both the gas and aerosol phase from the photo-oxidation of DMS in the NO_x free system was obtained by using ion chromatography, as will be described in Chapter 3, Paragraph 3.1.2. The yields of MSA observed using this analytical method were found to be higher than the quantities measured in the gas phase by FT-IR spectroscopy, especially at low temperature.

The levels of gas phase MSA measured by FT-IR spectroscopy are not very high and vary between approximately 1 to 6 % S. In general, the highest values were obtained at the highest temperature and highest O_2 partial pressure and the lowest at the lowest temperature and lowest O_2 partial pressure. The differences between the results at 295 and 284 K are, however, very marginal.

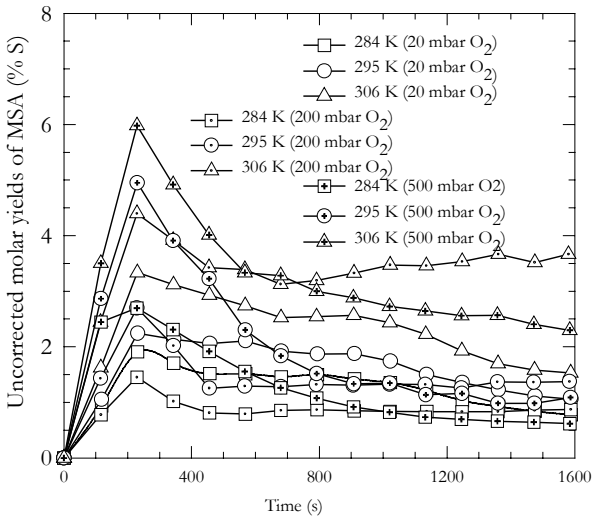

Figure 3.10: Plots of the uncorrected molar yields of MSA as a function of O_2 partial pressure (20, 200 and 500 mbar) and temperature (284, 295 and 306 K) versus reaction time.

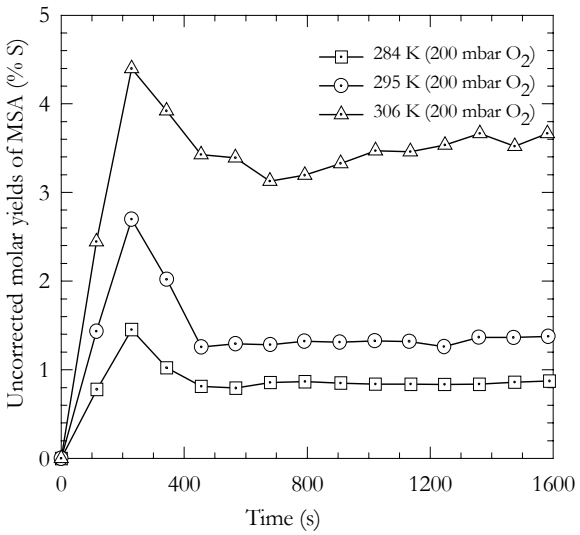

Figure 3.11: Plots of the yields of MSA as a function of temperature (284, 295 and 306 K) versus reaction time for a constant O_2 partial pressure of 200 mbar, *i.e.* atmospheric conditions.

Methane thiol formate (MTF)

For methane thiol formate (MTF) all the measured yield-time profiles at different temperatures and O_2 partial pressures are shown in Figure 3.12. In order to better highlight the observed changes with temperature and O_2 partial pressure, the yield-time profiles of MTF as a function of temperature for a constant O_2 partial pressure of 200 mbar are shown separately in Figure 3.13.

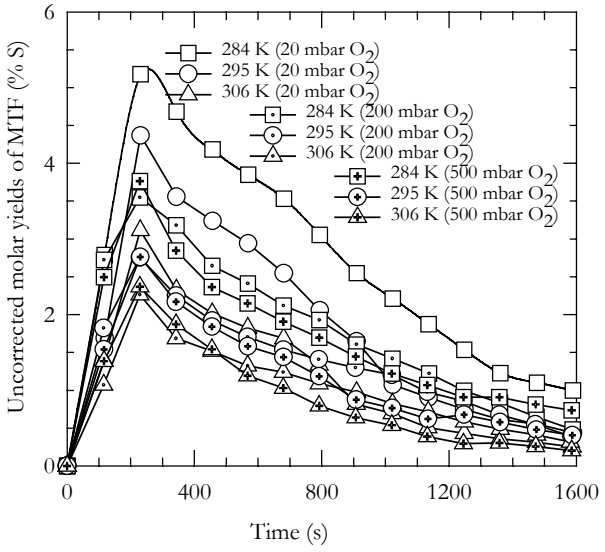

Figure 3.12: Plots of the uncorrected molar yields of MTF as a function of O_2 partial pressure (20, 200 and 500 mbar) and temperature (284, 295 and 306 K) versus reaction time.

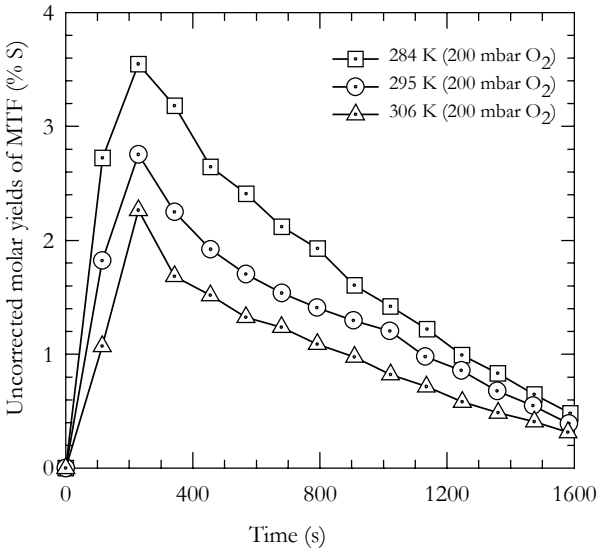

Figure 3.13: Plots of the yields of MTF as a function of temperature (284, 295 and 306 K) versus reaction time at a constant O_2 partial pressure of 200 mbar, *i.e.* atmospheric conditions.

Figures 3.12 and 3.13 demonstrate that the observed yield of MTF (i) increases with decreasing temperature at constant O_2 partial pressure and (ii) increases with decreasing O_2 partial pressure at constant temperature. The shapes of the curves in both figures are determined by competition between production of MTF from DMS oxidation, further oxidation of MTF by ·OH radicals and photolysis of this compound due to the light of mercury lamps. The yields presented in both figures have not been corrected for photolysis or further reaction with ·OH radicals or other oxidants in the system. For the O_2 partial pressure of 200 mbar, *i.e.* atmospheric conditions, and 295 K the MTF concentrations was corrected for reaction with ·OH radicals and photolysis. Plots of the MTF concentration, uncorrected and corrected for secondary processes, versus the consumed amount of DMS (Δ[DMS]) are shown in Figure 3.14. From the slope of the straight line, corresponding to the corrected concentration, a MTF formation yield of 7.2 ± 1.4 % was obtained at 295 K and 200 mbar O_2. This result indicates formation of this compound in considerable yield.

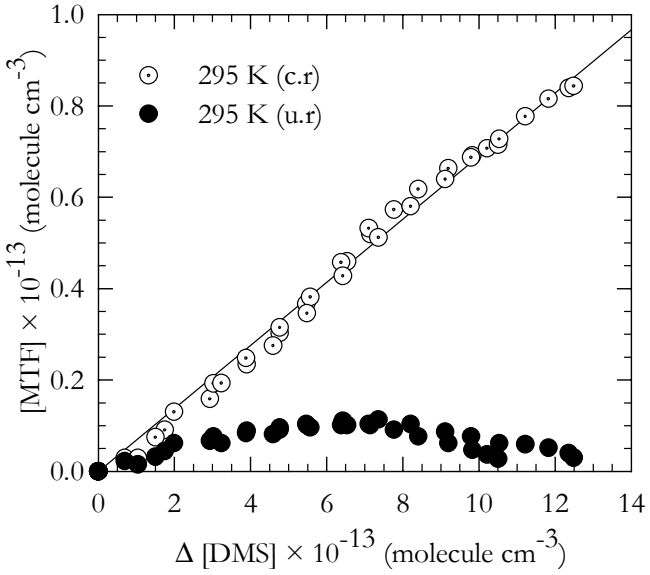

Figure 3.14: Plots of the MTF yield (uncorrected and corrected for reaction with ·OH radicals and photolysis) versus the consumption of DMS (c.r - corrected results; u.r. - uncorrected results).

Carbonyl sulphide (OCS)

The yield-time profiles of OCS measured at different temperatures and O_2 partial pressures are shown in Figure 3.15. Figure 3.16 shows separately the observed OCS curves as a function of temperature for a constant O_2 partial pressure of 200 mbar. Figures 3.15 and 3.16 indicate that the observed yield of OCS (i) increases with increasing temperature at a constant O_2 partial pressure and (ii) increases with increasing O_2 partial pressure at a constant temperature.

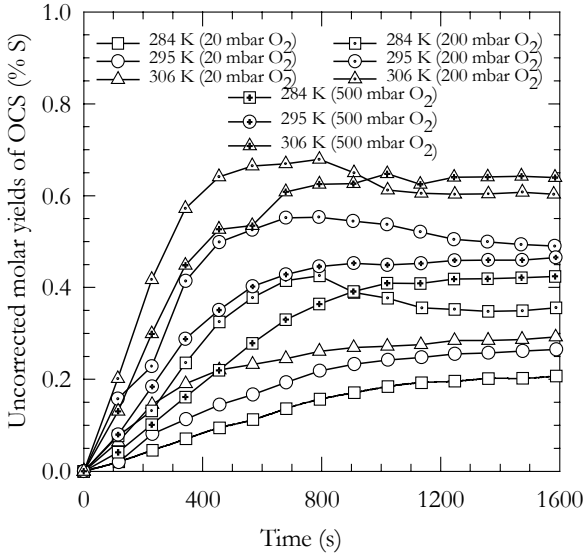

Figure 3.15: Plots of the uncorrected molar yields of OCS as a function of O_2 partial pressure (20, 200 and 500 mbar) and temperature (284, 295 and 306 K) versus reaction time.

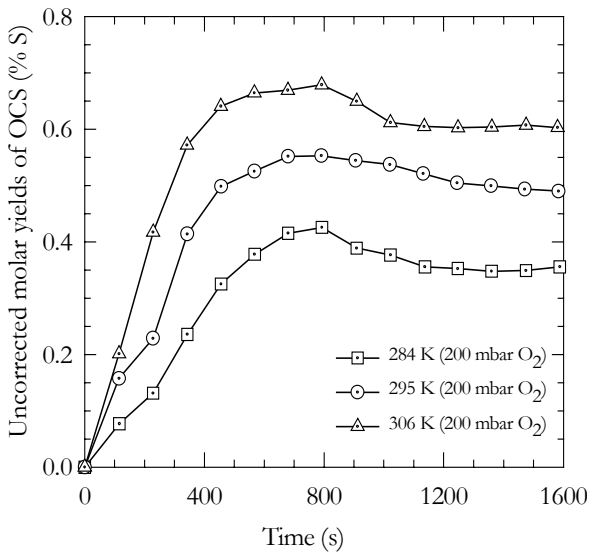

Figure 3.16: Plots of the yields of OCS as a function of temperature (284, 295 and 306 K) versus reaction time for a constant O_2 partial pressure of 200 mbar, *i.e.* atmospheric conditions.

The formation yields for OCS obtained by the least-squares analysis of plots where the uncorrected concentration of OCS was plotted *versus* the consumed amount of DMS (Δ [DMS]) are presented in Table 3.4. The errors quoted in the table are the 2σ random scatter in the data plots, where σ is the mean square deviation, and reflect the errors in the measurement of OCS and DMS concentrations using long path FT-IR spectroscopy. From the results presented in Table 3.4 it is clear that there is little difference between the results for 200 and 500 mbar of O_2, whereas the yields for 20 mbar of O_2 are significantly lower.

Table 3.4: Formation yields of OCS in the reaction of DMS with ·OH radicals at different O_2 partial pressure (20, 200 and 500 mbar O_2) as a function of temperature (284, 295, 306 K).

Temperature (K)	OCS yields (% molar yield, ± 2 σ)		
	20 mbar O_2	200 mbar O_2	500 mbar O_2
284	0.23 ± 0.05	0.37 ± 0.04	0.38 ± 0.06
295	0.29 ± 0.04	0.53 ± 0.06	0.44 ± 0.05
306	0.31 ± 0.06	0.63 ± 0.06	0.71 ± 0.07

3.1.2 Identification of methane sulphinic acid (MSIA), methane sulphonic acid (MSA) and sulphuric acid (H_2SO_4) by ion chromatography (IC)

In contrast to methane sulphonic acid (MSA), the infrared spectrum of methane sulphinic acid (MSIA) is not known, therefore, it is not currently possible to establish the formation of this compound in the gas phase using FT-IR spectroscopy. Some preliminary results concerning the possible identification of MSIA in the gas phase using long path FT-IR spectroscopy will be presented in Appendix B. The results have been obtained in a reactor which can be temperature regulated in the range of 223 to 296 K. Similarly, inorganic sulphate (mainly H_2SO_4) can only be determined by IC. Therefore, ion chromatography was the analytical tool used to prove the presence of MSIA and inorganic sulphate in the DMS oxidation system. This analytical technique was also used to get additional information on the formation of MSA (gas + aerosol) in the oxidation system.

The results presented here were acquired at 284 and 295 K and 1000 mbar synthetic air. Figure 3.17 shows a chromatogram demonstrating the detection of the $CH_3SO_2^-$, $CH_3SO_3^-$ and SO_4^{2-} anions from MSIA, MSA and H_2SO_4, respectively, in samples collected from the irradiation

of DMS/H_2O_2/synthetic air mixtures in the photo-reactor. The shown example is from a measurement performed at 295 K in synthetic air, *i.e.* 200 mbar partial pressure of O_2.

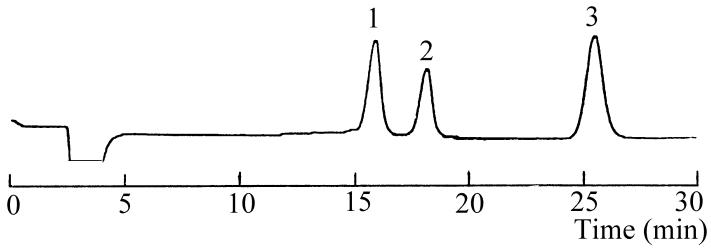

Figure 3.17: Example of chromatogram demonstrating the detection of (1) MSIA, (2) MSA and (3) sulphate ions. The peaks of MSIA and MSA are totally resolved.

The yields of the $CH_3SO_2^-$, $CH_3SO_3^-$ and SO_4^{2-} anions for the measurements performed at 284 and 295 K are collected in Table 3.5. Since the reaction system was probed continuously, these values are the integral yields for the time period of the experiment and represent composite values of production and loss processes. The results from Table 3.5 do not represent the formation yields of the species, however, in the case of MSIA they represent a lower limit of the formation yield.

Table 3.5: Ion chromatographic analysis of methane sulphinate ($CH_3SO_2^-$), methane sulphonate ($CH_3SO_3^-$) and sulphate (SO_4^{2-}) ions from the samples collected from the oxidation of DMS in 1000 mbar synthetic air at 284 and 295 K.

Temperature (K)	Expt. No.	Volume (L)	$CH_3S(O)O^-$		$CH_3S(O)_2O^-$		SO_4^{2-}	
			ppm	% S	ppm	% S	ppm	% S
284	1	11.8	0.37	19.24	0.33	17.41	0.81	42.06
	2	10.9	0.39	17.35	0.32	14.3	0.46	20.83
	3	11.9	0.32	18.62	0.39	23.22	0.57	33.24
295	4	28.7	0.184	4.26	0.45	10.44	0.62	14.42
	5	41.0	0.135	2.53	0.33	6.13	0.81	15.19
	6	42.4	0.218	4.62	0.24	4.98	0.81	17.32
	7	13.1	0.182	6.07	0.24	7.88	(a)	(a)
	8	11.3	0.146	4.88	0.25	8.16	(a)	(a)
	9	29.4	0.423	10.26	0.24	5.89	(a)	(a)

a Not calibrated at the time of experiment.

Relatively high and variable yields of sulphate ion (SO_4^{2-}) formation were observed by IC. One route to H_2SO_4 formation in the ·OH radical initiated oxidation of DMS is SO_2 + ·OH reaction. The contribution of the fraction of SO_2 oxidised by ·OH radicals to gas phase H_2SO_4 at 1000 mbar of synthetic air at different temperatures was estimated from the least-squares analysis of the plots of the uncorrected and corrected values of the SO_2 concentration. The plots are presented in Figure 3.18 and the values obtained are given in Table 3.6.

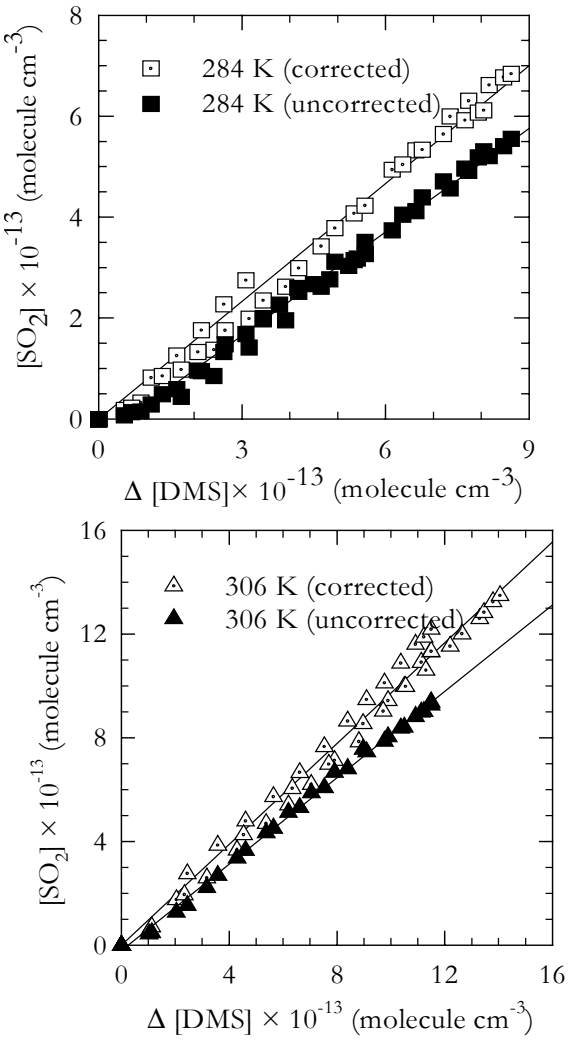

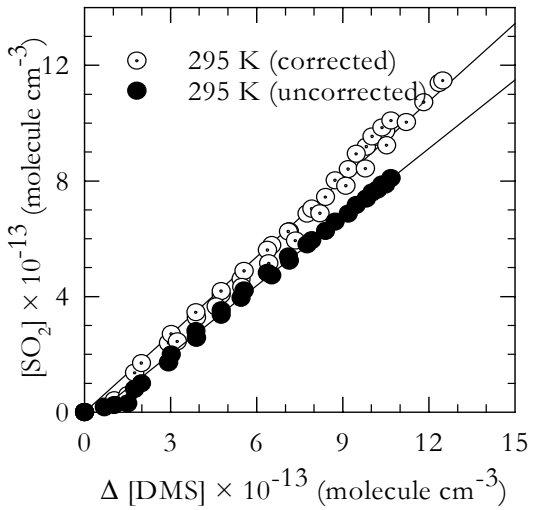

Figure 3.18: Plots of the SO_2 yields (uncorrected and corrected for wall loss and reaction with ·OH radicals) versus the consumption of DMS for conditions corresponding to 1000 mbar synthetic air and different temperatures.

Table 3.6: Contribution of the fraction of SO_2 oxidised by ·OH radicals to gas phase H_2SO_4 in the reaction of DMS with ·OH radicals in 1000 mbar of synthetic air as a function of temperature.

Temperature (K)	Uncorrected SO_2 yields (% molar yield)	Corrected SO_2 yields (% molar yield)	Contribution of the fraction of SO_2 oxidised to H_2SO_4 (g) (%)
284	71.4 ± 4.2	84.3 ± 6.5	13 ± 2.7
295	79.1 ± 4.0	94.3 ± 3.8	15 ± 2.4
306	84.1 ± 4.5	99.0 ± 6.5	15 ± 2.9

Sulphate ion (SO_4^{2-}) formation was observed with values of approximately 14 - 17 % S at 295 K and 20 - 40 % S at 284 K. The observed yields at 284 K are high and very variable. The fraction of SO_2 oxidised by ·OH to gas phase H_2SO_4 is estimated to be of the order of 15 % at 295 K and 13 % at 284 K. From Tables 3.5 and 3.6 it is evident that, whereas the SO_4^{2-} formation yields at 295 K are of the order expected from ·OH induced oxidation of gas phase SO_2, those at 284 K are considerably higher.

3.2 Discussion

3.2.1 Dimethyl sulphoxide (DMSO) formation

The observed behaviour of the yields of DMSO with variation in temperature and O_2 partial pressure (Paragraph 3.1.1, Chapter 3) is generally in line with what would be expected from the current mechanistic models, the initial steps of which can be represented by the following simplified reaction scheme:

$CH_3SCH_3 + \cdot OH \rightarrow CH_3SCH_2\cdot + H_2O$ (abstraction pathway) (R 3.1)

$CH_3SCH_3 + \cdot OH \rightarrow CH_3S\cdot(OH)CH_3$ (addition pathway) (R 3.2)

$CH_3S\cdot(OH)CH_3 + M \rightarrow CH_3SCH_3 + \cdot OH + M$ (R 3.3)

$CH_3S\cdot(OH)CH_3 + O_2 \rightarrow$ products (including DMSO). (R 3.4)

High temperatures and low O_2 partial pressure will favour the abstraction pathway, whereas the contrary will favour the addition channel and, hence, DMSO formation. Although the observed trends of DMSO are in agreement with the above simplified mechanism, the model in its present state ignores the possible formation of SO_2 from the further oxidation of DMSO which has been observed in laboratory product studies (Barnes et al., 1989; Sørensen et al., 1996).

Formation of the DMS-OH adduct was first proposed by Hynes et al. (1986) in order to explain the observation that the loss rate of ·OH in the presence of DMS increased significantly upon the addition of oxygen. In their study the enhancement in the ·OH loss rate in the presence of O_2 was explained by the occurrence of a reaction between the OH-DMS adduct and oxygen (such as R 3.4).

An electronic *ab-initio* structure calculation of McKee (1993a) yielded a bound geometry for the OH-DMS adduct with a bond strength of 6.0 kcal mol^{-1}. Contrary to these results, theoretical calculations by Turecek (1994) suggested that OH-DMS is not a stable intermediate but a transition state in the reaction of ·OH radicals with DMS.

The most probable fate of the DMS-OH adduct is either thermal decomposition back to reactants or its reaction with O_2 ($k_{O2+DMS\text{-}OH} = (1.00 + 0.33) \times 10^{-12}$ cm^3 $molecule^{-1}$ s^{-1}; Barone et al., 1996) by the reactions R. 3.3 and R. 3.4, respectively. The latter is considered to be the most important pathway leading to DMSO formation (Barnes et al., 1987a; Barone et al., 1995; Turnipseed et al., 1996; Yin et al., 1990a,b).

Possible mechanisms responsible for DMSO formation are:

$CH_3S\cdot(OH)CH_3 + O_2 \rightarrow CH_3S(O)CH_3 + HO_2\cdot$ (R 3.5)

$CH_3S\cdot(OH)CH_3 + O_2 + M \rightarrow CH_3S(OH)(OO\cdot)CH_3 + M$ (R 3.6)

$CH_3S(OH)(OO\cdot)CH_3 + M \rightarrow CH_3S(O)CH_3 + HO_2\cdot + M.$ (R 3.7)

The formation of DMSO *via* reactions with peroxy radicals

$CH_3SCH_3 + HO_2\cdot + M \rightarrow CH_3S(O)CH_3 + \cdot OH + M$ (R 3.8)

$CH_3SCH_3 + RO_2\cdot + M \rightarrow CH_3S(O)CH_3 + RO\cdot + M$ (R 3.9)

is probably negligible in systems without NO_x. The reaction between DMS and $HO_2\cdot$ is known to be very slow ($k_{298} < 5 \times 10^{-15}$ cm^3 molecule^{-1} s^{-1}, Mellouki and Ravishankara, 1994) and reaction with $CH_3OO\cdot$ radicals, which can also be formed in the system, is also expected to be negligible.

In Table 3.1 presented in Paragraph 3.1.1, Chapter 3, the formation yields of DMSO are compared with the fraction of the ·OH + DMS reaction occurring *via* the addition pathway calculated from the data of Hynes et al. (1986). The DMSO yield values for 284 and 295 K are approximately equal to the corresponding addition fractions, while the yield value for 306 K is somewhat higher. The numbers, as they stand, suggest that, virtually, all of the formed DMS-OH adducts react with O_2 to produce DMSO.

In a pulsed laser photolysis/pulsed laser-induced fluorescence study on the reaction of ·OH with DMS at 234 and 258 K, Turnipseed et al. (1996) have reported a branching ratio of $\Phi = 0.5 \pm 0.15$ for $HO_2\cdot$ production from the $CH_3S\cdot(OH)CH_3 + O_2$ reaction. They assumed that $HO_2\cdot$ was formed *via* abstraction of H atom from the hydroxyl. The co-product was assumed to be DMSO in equivalent yield.

The yield of 50 % from the work of Turnipseed et al. (1996) is considerably lower than the near unity yield suggested by the present study. However, there are a number of important points which must be considered when comparing the yields from this study with those from Turnipseed et al. (1996). The latter work was performed at low temperature and pressure. Though the work of Turnipseed et al. (1996) suggested that the $HO_2\cdot$ yield was temperature independent and a significant pressure dependence for the DMS-OH + O_2 reaction is not expected, extrapolation of the results to the conditions of the present study is not possible.

The formation yields for DMSO which were calculated in the present work were very sensitive to the value of $k_{2(\cdot OH + DMSO)}$ used in the correction procedure. As stated above, the absolute value of $k_{2(\cdot OH + DMSO)}$ is associated with a high degree of uncertainty which has not been incorporated into the formation yield calculation.

It is interesting to note, that if the results of Turnipseed et al. (1996) are correct, this implies a lower value for the rate coefficient of the reaction of ·OH with DMSO than currently recommended. This uncertainty and the different experiment conditions employed complicates a meaningful comparison of the results from both studies.

More precise values of $k_{2(\cdot OH + DMSO)}$ as a function of temperature would greatly help to improve the accuracy of the formation yield data for DMSO obtained in this work for the ·OH + DMS reaction. Until such values become available the exact yield of DMSO from the reaction of O_2 with the DMS-OH adduct in the absence of NO_x will remain an open question. However, both the results from this study and that of Turnipseed et al. (1996) confirm that the branching ratio of the DMSO producing path is quite substantial.

3.2.2 Dimethyl sulphone ($DMSO_2$) formation

The observations concerning $DMSO_2$ formation in the studied system are not easy to interpret. A fraction of the $DMSO_2$ production can certainly be ascribed to H_2O_2/DMS interactions, probably, heterogeneous interaction at the reactor walls.

Formation of $DMSO_2$ has been reported from the reaction of ·OH + DMSO (Barnes et al., 1989; Barnes et al., 1996; Patroescu et al., 1999; Sørensen et al., 1996). However, there is evidence from studies in this laboratory (Arsene et al., 2000; Beyer, 1998) and also from the laboratory studies of Sørensen et al. (1996) that formation of $DMSO_2$ in chamber studies of the reaction of ·OH with DMSO is mainly due to secondary oxidation processes and is dependent on the initial DMSO concentration.

Because of high variability in the heterogeneous production of $DMSO_2$ and also because of uncertainty in its formation pathway from the oxidation of DMSO, it is not possible to establish the extend to which $DMSO_2$ is being formed from the ·OH + DMS reaction. However, if account is taken of the relatively large heterogeneous contribution and the relatively low intermediate DMSO concentrations in the present experimental system, the yield of $DMSO_2$ from ·OH + DMS is not considered to be particularly significant.

Chemical routes which may lead to $DMSO_2$ formation in the oxidation of DMS with ·OH radicals, by the addition channel, include:

$$CH_3S\cdot(OH)CH_3 + O_2 + M \leftrightarrow CH_3S(OH)(OO\cdot)CH_3 + M \quad \text{(R 3.6)}$$

$$CH_3S(OH)(OO\cdot)CH_3 + M \rightarrow CH_3S(O)CH_3 + HO_2\cdot + M \quad \text{(R 3.7)}$$

$CH_3S(OH)(OO\cdot)CH_3 + RO_2\cdot + M \rightarrow CH_3S(OH)(O\cdot)CH_3 + RO\cdot + O_2 + M$ (R 3.10)

$CH_3S(OH)(O\cdot)CH_3 + O_2 + M \rightarrow CH_3S(O)_2CH_3 + HO_2\cdot + M$ (R 3.11)

$CH_3S(O)CH_3 + \cdot OH + M \rightarrow CH_3S\cdot(O)(OH)CH_3 + M$ (R 3.12)

$CH_3S\cdot(O)(OH)CH_3 + O_2 \rightarrow CH_3S(O)(OH)(OO\cdot)CH_3$ (R 3.13)

$CH_3S(O)(OH)(OO\cdot)CH_3 + M \rightarrow CH_3S(O)_2CH_3 + HO_2\cdot + M.$ (R 3.14)

3.2.3 Sulphur dioxide (SO_2) formation

The observed behaviour of the SO_2 yields with variation in temperature and O_2 partial pressure (Paragraph 3.1.1, Chapter 3) are broadly in line with what would be expected from current mechanistic models the initial steps of which can be represented by the following simplified mechanism:

$CH_3SCH_3 + \cdot OH \rightarrow CH_3SCH_2\cdot + H_2O$ (abstraction pathway) (R 3.1)

$CH_3SCH_3 + \cdot OH \rightarrow CH_3S\cdot(OH)CH_3 + H_2O$ (addition pathway) (R 3.2)

$CH_3S\cdot(OH)CH_3 + M \rightarrow CH_3SCH_3 + \cdot OH + M$ (R 3.3)

$CH_3S\cdot(OH)CH_3 + O_2 \rightarrow$ products (R 3.4)

$CH_3SCH_2\cdot + O_2 \rightarrow$ products (including SO_2, MTF, MSA etc.) (R 3.15)

Increasing the temperature or lowering the O_2 partial pressure favours the abstraction pathway and, hence, SO_2 formation, whereas reversing these conditions will favour the addition channel and DMSO formation. From a comparison of the high corrected formation yields for SO_2 in synthetic air at different temperatures, *i.e.* atmospheric conditions, with the fractions of the ·OH + DMS reaction proceeding *via* the addition and abstraction pathways calculated according to Hynes et al. (1986) (see Table 3.3, Paragraph 3.1.1, Chapter 3), it is obvious, that it must be formed in both channels.

The following reaction schemes can explain formation of SO_2 in the addition channel:

$CH_3S\cdot(OH)CH_3 + O_2 + M \rightarrow CH_3S(O)(OO\cdot)CH_3 + M$ (R 3.6)

$CH_3S(OH)(OO\cdot)CH_3 + M \rightarrow CH_3S(O)CH_3 + HO_2\cdot + M$ (R 3.7)

$CH_3S(O)CH_3 + \cdot OH + M \rightarrow CH_3S\cdot(O)(OH)CH_3 + M$ (R 3.12)

$CH_3S{\cdot}(O)(OH)CH_3 + M \rightarrow CH_3S(O)(OH) + CH_3{\cdot} + M$ (R 3.16)

$CH_3S(O)(OH) + {\cdot}OH \rightarrow CH_3S{\cdot}(O)_2 + H_2O$ (R 3.17)

$CH_3S{\cdot}(O)_2 \rightarrow SO_2 + CH_3{\cdot}$ (R 3.18)

and in the abstraction channel:

$CH_3SCH_2{\cdot} + O_2 + M \rightarrow CH_3SCH_2OO{\cdot} + M$ (R 3.19)

$2CH_3SCH_2OO{\cdot} \rightarrow CH_3SCH_2O{\cdot} + CH_3SCH_2O{\cdot} + O_2$ (R 3.20)

$CH_3SCH_2O{\cdot} \rightarrow CH_3S{\cdot} + HCHO$ (R 3.21)

$CH_3S{\cdot} + O_2 + M \leftrightarrow CH_3SOO{\cdot} + M$ (R 3.22)

$CH_3SOO{\cdot} \rightarrow \rightarrow CH_3S{\cdot}(O)_2$ (R 3.23)

$CH_3S{\cdot}(O)_2 \rightarrow SO_2 + CH_3{\cdot}.$ (R 3.18)

The high formation yields of SO_2 determined in the present study under NO_x free conditions also infer that the principal fate of DMSO in the system is oxidation to SO_2. Since the results from the present study also support that MSIA is a major DMSO oxidation product (as will be shown in Chapter 5, Paragraphs 5.1.1 and 5.2.1), this further implies that the predominant fate of MSIA in the reaction system is oxidation *via* reaction with ·OH radicals to form SO_2 (reactions R 3.17 and R 3.18).

The contribution of the abstraction channel to SO_2 production can be explained by formation of the $CH_3S{\cdot}(O)_2$ radicals *via* successive oxidation of the $CH_3S{\cdot}$ radical. In both channels SO_2 is formed in a competition between thermal decomposition step of $CH_3S{\cdot}(O)_2$, with a fairly large activation energy, and its bimolecular reactions with some oxidative species, with a fairly small activation energy (Seinfeld and Pandis, 1998). Higher temperatures favour the decomposition step of the $CH_3S{\cdot}(O)_2$ radical. Theoretical calculations predict that the methylsulphonyl radical ($CH_3S{\cdot}(O)_2$) is a stable species in the gas phase and the dissociation energy for the reaction $CH_3S{\cdot}(O)_2 \rightarrow CH_3{\cdot} + SO_2$ is lower than the barrier for unimolecular isomerisation to the methoxysulphinyl radical (CH_3OSO) (Frank and Tureček, 1999).

The observed behaviour of the molar yields of SO_2 with temperature in the studied system is consistent with occurrence of thermal decomposition of $CH_3S{\cdot}(O)_2$ in the general mechanism of DMS photo-oxidation. However, although the $CH_3S{\cdot}(O)_2$ radical is quite probably the precursor of SO_2 production, the route which leads to its formation still remains to be validated experimentally.

3.2.4 Methane sulphonic acid (MSA) formation in the gas phase

The yield of gas phase MSA measured in the present work was not very high and varied between approximately 1 to 6 % S. The trends in the MSA data are difficult to interpret. Since the gas phase production of MSA was very low at all temperatures it is not possible to extract any meaningful mechanistic information on the origin of MSA. Differences in the MSA formation yields in the studied range of temperatures can be masked by several factors. The walls loss rates of MSA, for example, are probably temperature dependent, which can affect the observed MSA yield. Loss of MSA to the aerosol phase can also be different at the various temperatures, however, it is expected that none of these effects is particularly pronounced over the small temperature range investigated. This is supported by the large observed formation yields of SO_2 at all temperature investigated (Paragraph 3.1.1, Chapter 3). Any large variation in the gas phase formation of MSA would have led to large variations in the SO_2 yield.

In addition, interpretation of the present results was made even more complicated by the recent results from this laboratory which have shown, contrary to the previous notion that MSA is formed not only in the abstraction channel by the following reaction sequence which involve $CH_3S\cdot$ radical:

$$CH_3S\cdot + O_2 + M \leftrightarrow CH_3SOO\cdot + M \quad \text{(R 3.22)}$$

$$CH_3SOO\cdot \rightarrow\rightarrow CH_3S\cdot(O)_2 \quad \text{(R 3.23)}$$

$$CH_3S\cdot(O)_2 + O_2 + M \rightarrow CH_3S(O)_2(OO\cdot) \quad \text{(R 3.24)}$$

$$CH_3S(O)_2(OO\cdot) + CH_3SO_{x(x=0\text{-}2)} \rightarrow CH_3S(O)_2(O\cdot) + CH_3SO_{x(x=1\text{-}3)} \quad \text{(R 3.25)}$$

$$CH_3S(O)_2(O\cdot) + RH \rightarrow CH_3S(O)_2(OH) + R\cdot \quad \text{(R 3.26)}$$

but can also be formed in the addition route, *i.e.* from the further gas phase oxidation of DMSO (as will be shown in Chapter 5, Paragraph 5.1.2) *via* the following reaction sequence:

$$CH_3S(O)CH_3 + \cdot OH + M \rightarrow CH_3S\cdot(O)(OH)CH_3 + M \quad \text{(R 3.12)}$$

$$CH_3S\cdot(O)(OH)CH_3 + M \rightarrow CH_3S(O)(OH) + CH_3\cdot + M \quad \text{(R 3.16)}$$

$$CH_3S(O)(OH) + \cdot OH \rightarrow CH_3S\cdot(O)_2 + H_2O \quad \text{(R 3.17)}$$

$$CH_3S\cdot(O)_2 + O_2 + M \rightarrow CH_3S(O)_2(OO\cdot) \quad \text{(R 3.24)}$$

$$CH_3S(O)_2(OO\cdot) + CH_3SO_{x(x=0\text{-}2)} \rightarrow CH_3S(O)_2(O\cdot) + CH_3SO_{x(x=1\text{-}3)} \quad \text{(R 3.25)}$$

$$CH_3S(O)_2(O\cdot) + RH \rightarrow CH_3S(O)_2(OH) + R\cdot \quad \text{(R 3.26)}$$

The intermediates, which should be responsible for MSA formation, can be formed either in the addition channel (DMS-OH: $CH_3S{\cdot}(OH)CH_3$) or in the abstraction channel ($CH_3SCH_2{\cdot}$) of the ·OH radical initiated oxidation of DMS. The DMS-OH adduct can also decompose to methane sulphenic acid (MSEA: CH_3SOH) or react further with oxygen to produce DMSO or $DMSO_2$. Further oxidation of DMSO is a possible source of MSA formation.

Methane sulphenic acid has not been yet directly observed up to now but there have been suggestion that it is an important intermediate in the oxidation of DMS. It is believed to be formed by the unimolecular decomposition of the $CH_3S{\cdot}(OH)CH_3$ adduct in a speculative mechanism suggested by Yin et al. (1990a). The possible ways of MSA formation *via* multistep process involving oxidation of MSEA at the present state of knowledge can not be recognised.

Studies in the liquid phase have shown that sulphenic and sulphinic acids undergo facile H atom abstraction by ·OH radicals. Based on this, it was proposed that the abstraction of the H atom should be a dominant atmospheric reaction pathway for both CH_3SOH and $CH_3S(O)OH$. Further reactions which involve oxidation of the $CH_3SO{\cdot}$ and $CH_3S(O)O{\cdot}$ radicals will lead to $CH_3S(O)_2O{\cdot}$ radical formation. The $CH_3S(O)_2O{\cdot}$ radical species can form methane sulphonic acid ($CH_3S(O)_2OH$) by reaction with a hydrocarbon (RH) where R = H(O)C-, CH_3SCH_2-, CH_3S-, CH_3SO-, $CH_3S(O)O$-, CH_3O-.

The $CH_3SCH_2{\cdot}$ radicals produced in the abstraction channel of the ·OH + DMS reaction can react with molecular oxygen to form $CH_3SCH_2OO{\cdot}$ radicals which will lead further to $CH_3SCH_2O{\cdot}$ radicals (both radicals have been investigated theoretically by McKee (1994) and Resende and De Almeida (1999)). The major fate of the $CH_3SCH_2O{\cdot}$ radical is thought to be decomposition to the methyl sulphenyl radical ($CH_3S{\cdot}$) and formaldehyde (the yield of H_2CO from $CH_3SCH_2OO{\cdot}$ was found to be near unity, Urbanski et al., 1997).

The reaction of the $CH_3S{\cdot}$ radical with oxygen will lead either to reversible formation of a $CH_3SOO{\cdot}$ peroxy radical (McKee, 1993b; Turnipseed and Ravishankara, 1992; Tyndall and Ravishankara, 1989), or to formation of the $CH_3S{\cdot}(O)$ species:

$$CH_3S{\cdot} + O_2 + M \leftrightarrow CH_3SOO{\cdot} + M \qquad \text{(R 3.22)}$$

$$2CH_3SOO{\cdot} \rightarrow 2CH_3S{\cdot}(O) + O_2. \qquad \text{(R 3.27)}$$

Further reactions of the $CH_3S{\cdot}(O)$ radical lead to production of SO_2 and CH_3SO_3H. According to the low gas phase methane sulphonic acid production obtained in the present study, the fate of the $CH_3S{\cdot}(O)$ radicals in the absence of NO_x is expected to form rather SO_2 than MSA.

3.2.5 Methane thiol formate (MTF) production

The observation of the formation of methane thiol formate (MTF) has been reported several times in the photo-oxidation studies of DMS under conditions of low NO_x (Barnes et al., 1994; Barnes et al., 1996; Patroescu et al., 1996). The ultraviolet spectrum of MTF was measured by Patroescu et al. (1996) and a lifetime with respect to photolysis was inferred assuming a quantum yield of unity. Possible reactions channels leading to formation of MTF under the present experimental conditions include:

$$2CH_3SCH_2OO\cdot \rightarrow CH_3SCH_2O\cdot + CH_3SCH_2O\cdot + O_2 \quad \text{(R 3.20)}$$

$$2CH_3SCH_2OO\cdot \rightarrow CH_3SCHO + CH_3SCH_2OH + O_2 \quad \text{(R 3.28)}$$

$$CH_3SCH_2O\cdot + O_2 \rightarrow CH_3SCHO + HO_2\cdot \quad \text{(R 3.29)}$$

$$CH_3SCH_2OO\cdot + HO_2\cdot \rightarrow CH_3SCH_2OOH + O_2 \quad \text{(R 3.30)}$$

$$CH_3SCH_2OO\cdot + HO_2\cdot \rightarrow CH_3SCHO + O_2 + H_2O. \quad \text{(R 3.31)}$$

In the above reaction sequence both R 3.30 and R 3.31 are plausible. Wallington et al. (1993a) have observed both channels with approximately equal yields for the analogous reaction of the $CH_3OCH_2OO\cdot$ radical with $HO_2\cdot$.

The behaviour of MTF formation with temperature in the present study was found to be opposite to that observed for SO_2, whereas the effect of changing the O_2 partial pressure is similar to that of SO_2 (see Figures 3.7 and 3.12 presented in Paragraph 3.1.1, Chapter 3). It is difficult to predict how the changes in temperature and O_2 partial pressure will affect the direct formation of MTF either in self reaction of $CH_3SCH_2OO\cdot$ radicals or reaction with $HO_2\cdot$ because the chemistry of these reactions is not well studied.

Under the experimental conditions of the present study, the self reaction of $CH_3SCH_2OO\cdot$ is expected to be the dominate fate of this radical, which gives either $CH_3SCH_2O\cdot$ radicals, or CH_3SCHO and CH_3SCH_2OH.

The observed O_2 and temperature effects from the present study do not agree with the supposition that the direct formation of MTF from $CH_3SCH_2OO\cdot$ self reaction is the only source of MTF in the reaction system. The observed temperature effect agrees more with a simple competition between thermal decomposition of the $CH_3SCH_2O\cdot$ radical to $CH_3S\cdot$ and HCHO and reaction with O_2 forming MTF. At low temperatures reaction with O_2 will be favoured over the thermal decomposition.

At first glance the increase in the yield of MTF with decreasing O_2 partial pressure would seem to be in contradiction with the above reaction mechanism, since decreasing the O_2 should increase the probability of the thermal decomposition channel. However, it must be kept in mind that when the O_2 partial pressure is decreased the fraction of the reaction proceeding *via* the abstraction channel is considerably enhanced compared to the addition channel.

The magnitude of this enhancement is probably sufficient to compensate any expected reduction in the MTF yield with reduction in the O_2 partial pressure. Therefore, the observed changes in the MTF yield with variation in temperature and O_2 partial pressure agree with its production, at least in part, *via* the abstraction channel and reaction of the $CH_3SCH_2O\cdot$ radical with O_2. Even if the evidence from previous studies has always been inconclusive (Barnes et al., 1994; Barnes et al., 1996; Patroescu et al., 1996), the observations presented here, although circumstantial, show the possible existence of this reaction pathway.

As outlined above, there are several potential pathways which can be responsible for the formation of MTF, all stemming from the reactions of the $CH_3SCH_2OO\cdot$ radical. All these processes can occur in the present system and, at present, it is not possible to differentiate between the different channels.

However, the observed sensitivity of the MTF to the changes in temperature and O_2 partial pressure suggests that the reaction of $CH_3SCH_2O\cdot$ radicals with O_2 which competes with thermal decomposition, can be a major source of MTF in the present reaction system.

It would be interesting to calculate the yields for lower temperatures, since the importance of the MTF production pathway from $CH_3SCH_2O\cdot + O_2$, if operative, should increase with decreasing temperature. Unfortunately, this can be done only when kinetic data for MTF + ·OH at different temperature become available. Anyhow, in order to properly estimate the importance of the various MTF producing pathways from $CH_3SCH_2OO\cdot$ reactions it is necessary to investigate the various channels individually.

3.2.6 Carbonyl sulphide (OCS) formation

The yield of OCS at 295 K and an oxygen partial pressure of 200 mbar, as determined in the present study, was found to be similar to that previously obtained in studies on the oxidation of DMS performed in this laboratory (Barnes et al., 1994; Barnes et al. 1996; Patroescu et al., 1999). The present results confirm that OCS is a minor but important product of the ·OH radical initiated oxidation of DMS under NO_x-free conditions.

The mechanism producing OCS is at the present time not known. Carbonyl sulphide can be produced during the photolysis of MTF (Patroescu et al., 1996) which is forming $CH_3S{\cdot}CO$ radicals. The thermal decomposition of $CH_3S{\cdot}CO$ radical leads to the formation of OCS and CH_3. Possible reactions channels leading to formation of OCS include:

$$CH_3SCHO + h\nu \rightarrow CH_3S{\cdot}CO + H{\cdot} \quad \text{(R 3.32)}$$

$$CH_3S{\cdot}CO + \Delta \rightarrow CH_3{\cdot} + O{=}C{=}S \quad \text{(R 3.33)}$$

$$CH_3S{\cdot}CO + \Delta \rightarrow CH_3S{\cdot} + CO. \quad \text{(R 3.34)}$$

In the present study it was observed that both the temperature and O_2 partial trends of MTF and OCS production are anti-correlated (see Figures 3.12 and 3.15 presented in Paragraph 3.1.1, Chapter 3). Although the photolysis of MTF contributes to the formation of OCS it is definitely not the only source.

The self-reaction of the $CH_3S{\cdot}$ radicals leads through a minor channel to the formation of methyl mercaptan (CH_3SH) and methyl thioformaldehide (CH_2S) (Barnes et al., 1996):

$$CH_3S{\cdot} + CH_3S{\cdot} \rightarrow CH_3SH + CH_2S. \quad \text{(R 3.35)}$$

Further reactions of CH_2S, such as photolysis or reaction with ·OH radicals, can give OCS as one of the products:

$$CH_2S + {\cdot}OH \rightarrow HC{\cdot}S + H_2O \quad \text{(R 3.36)}$$

$$CH_2S + h\nu \rightarrow HC{\cdot}S + H{\cdot} \quad \text{(R 3.37)}$$

$$HC{\cdot}S + O_2 \rightarrow O{=}C{=}S + {\cdot}OH. \quad \text{(R 3.38)}$$

In the experiments performed with high partial pressures of O_2 the major fate of the $CH_3S{\cdot}$ radical is, most probably, reaction with O_2. The only way which can lead to OCS under these conditions involves the reaction of $CH_3S{\cdot}$ radicals with O_2 to form CH_2S:

$$CH_3S{\cdot} + O_2 \rightarrow CH_2S + HO_2{\cdot}. \quad \text{(R 3.39)}$$

The further oxidation of the CH_2S species may produce OCS *via* sequence of reactions from R 3.36 to R 3.38. Other potential sources could include OCS production from ·OH radical attack at the methyl group of such compounds as CH_3SCHO and CH_3SCH_2OOH.

3.2.7 Discussion of the ion chromatographic data

From the IC analysis for 295 K the integral yield of MSIA, incorporating all production and loss processes of MSIA, is between 4 - 10 % S whereas at 284 K it is much higher at about 20 % S. However, the measured yields of MSIA at 295 K (see Table 3.5, Paragraph 3.1.2, Chapter 3) are much higher than the yield of 1.5 ± 1.1 % S reported by Sørensen et al. (1996) for the study of the oxidation of DMS at 295 ± 3 K. This can, probably, be explained by the method of sampling used by Sørensen et al (1996). In their study the samples were collected at the end of the irradiation period and not during the irradiation as in this study. Since MSIA is subject to further fast oxidation by ·OH radicals (Yin et al., 1990a) and wall loss processes, a low yield of MSIA will be obtained if the measurements are conducted at the end of the irradiation. Besides, in the present study it was employed much lower collection and storage temperatures which, probably, assists in inhibiting the further oxidation of MSIA to MSA by any oxidising material co-collected in the sampling medium.

The yields of MSA observed using IC are higher than the quantities measured in the gas phase, especially at low temperature. This is, probably, due to (i) the method of sampling, *i.e.* continuous collection of the samples during irradiation and (ii) oxidation of MSIA to MSA either in the sampling line or in the liquid sample itself. The measured values of MSA using the IC method cannot, therefore, be compared directly with the gas phase formation yield of MSA. The measured quantities of MSA by IC are the composite values of the gas phase MSA yield plus the contribution from the oxidation of MSIA. Because of the high reactivity of MSIA, it is very difficult to avoid its further oxidation to MSA in analytical probing systems. The higher values of methane sulphonic acid determined by IC compared to the gas phase values of this compound obtained by long path FT-IR spectroscopy are a further indication of the importance of MSIA production in the reaction system.

The formation yields of SO_4^{2-} ion, measured in the present work by IC method, at 295 K are of the order expected from ·OH induced oxidation of gas phase SO_2 while those at 284 K are considerably higher (see Tables 3.5 and 3.6 in Paragraph 3.1.2, Chapter 3). As for MSA, it is suspected, that part of the variability in the H_2SO_2 yields at low temperature is a sampling problem. It is likely that at 284 K there is more condensation of H_2O_2 in the sampling line than at 295 K. This could result in more effective oxidation of SO_2 at 284 K and, hence, erroneously high sulphate yields. Because of the sampling problems the values of the SO_4^{2-} yield should be viewed with caution, particularly at low temperature.

However, the observation of H_2SO_4 by IC in the ·OH radical initiated oxidation of DMS provide a clear evidence for the role of DMS as a potential precursor of particle formation. Preliminary investigations on aerosol formation from DMS photo-oxidation indicate production of particles in the sub-micrometer range. Indirect evidence has also been found that sulphuric acid is the predominant species in the aerosol phase and that methane sulphonic acid contribution to the aerosol phase might be of a minor importance.

Test experiments showed that mixtures of DMS and H_2O_2 do not produce MSIA, MSA or H_2SO_4 in the dark. Thus, the only route to MSIA in the present experiments appears to be gas phase ·OH initiated oxidation of DMS. The results of the IC analysis experiments also show a substantial increase in the measured yield of MSIA on decreasing the temperature from 295 to 284 K. The decrease in temperature increases the importance of the addition pathway and also the formation of DMSO (see Chapter 3, Paragraphs 3.1.1 and 3.2.1). Therefore, the results support the conclusion that the further oxidation of DMSO with ·OH will be the major pathway leading to production of MSIA in the present system by the reaction sequence:

$$CH_3S(O)CH_3 + \cdot OH \longrightarrow CH_3S\cdot(O)(OH)CH_3 \xrightarrow{\text{thermal decomposition}} CH_3S(O)OH + CH_3\cdot \quad \text{(R 3.40)}$$

Although, the measurements do not allow an exact determination of the formation yield of MSIA, a simple consideration based on the magnitude of the measured MSIA yield in combination with the sampling efficiency and the loss processes involved (wall loss, gas phase oxidation, oxidation to MSA in the liquid sample) leads to the conclusion that the fraction of the ·OH + DMSO reaction leading to MSIA formation must be fairly considerable. This would be in agreement with the recent absolute study of Urbanski et al. (1998) who obtained nearly unit yield of CH_3 from the ·OH + DMSO reaction and assumed $CH_3S(O)OH$ to be the co-product.

3.3 Summary of results and conclusions

The ·OH radical initiated oxidation of dimethyl sulphide (DMS) has been investigated as a function of temperature and O_2 partial pressure. Formation of sulphur dioxide (SO_2), dimethyl sulphoxide (DMSO), dimethyl sulphone ($DMSO_2$), methane sulphinic acid (MSIA), methane sulphonic acid (MSA), carbonyl sulphide (OCS), methane thiol formate (MTF) and inorganic sulphate was observed.

The present results imply that the oxidation of DMS under low NO_x conditions such as often encountered in the marine boundary layer will produce mainly SO_2 and DMSO as the main

sulphur containing products. Based on the obtained uncorrected molar yields of the gas phase products using long path FT-IR spectroscopy it is shown (Figure 3.19) once more that SO_2 and DMSO are the major oxidation products of DMS in NO_x free conditions for different oxygen partial pressure and different temperatures.

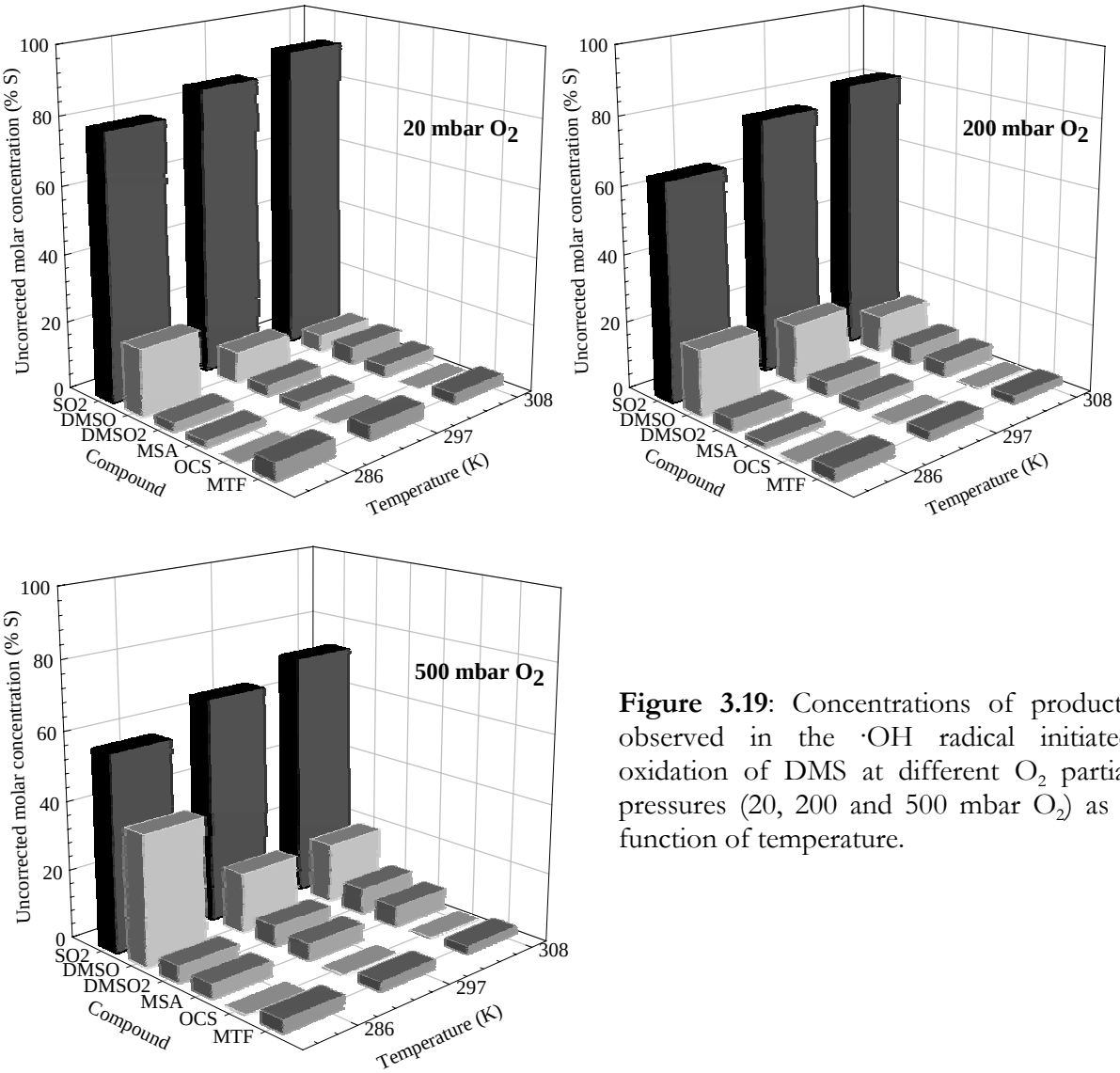

Figure 3.19: Concentrations of products observed in the ·OH radical initiated oxidation of DMS at different O_2 partial pressures (20, 200 and 500 mbar O_2) as a function of temperature.

The experimental product data of the present study have helped to highlight important mechanistic features of the atmospheric degradation mechanism of dimethyl sulphide (DMS). On the basis of the results obtained in the present study in combination with observations from previous studies on DMS oxidation, a general mechanism for the oxidation of DMS in the absence of NO_x has been constructed. Figure 3.20 and Figure 3.21 show the general mechanisms for the addition and abstraction channels, respectively involved in the ·OH radical initiated oxidation of DMS.

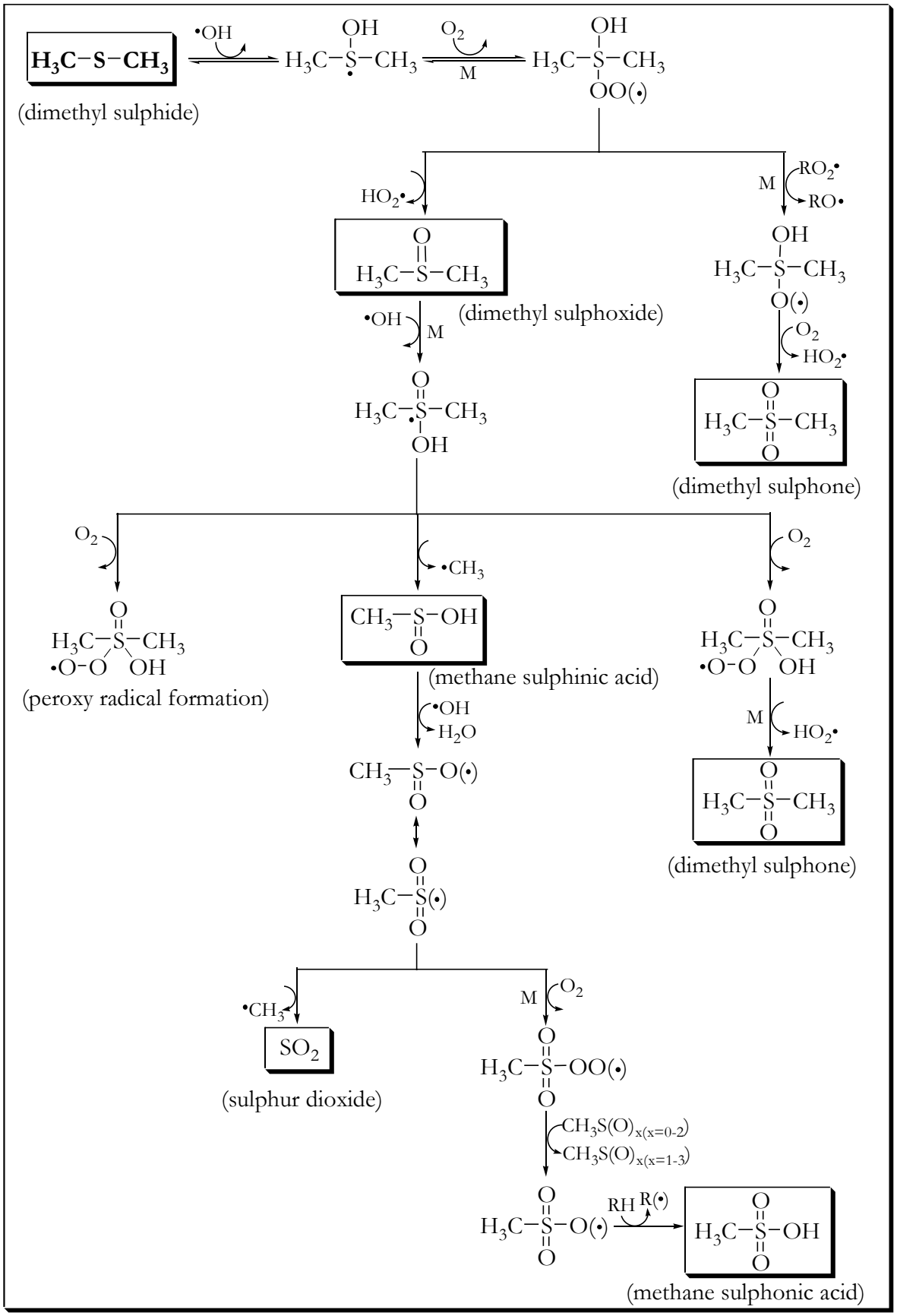

Figure 3.20: Mechanism proposed for the addition channel of the ·OH radical initiated oxidation of DMS in the absence of NO_x. The proposed mechanism is based on the results obtained in the present work in combination with observations from previous studies.

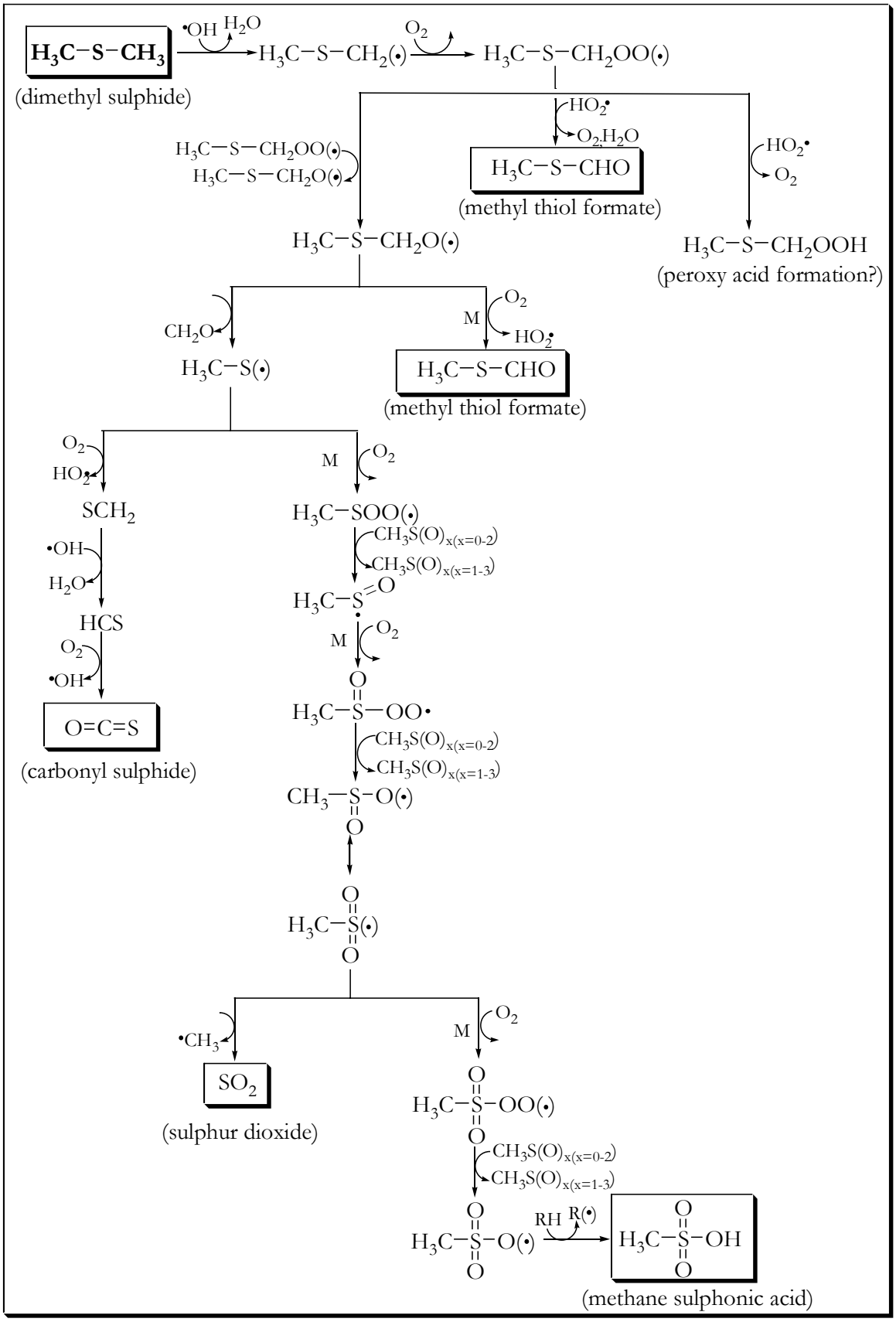

Figure 3.21: Mechanism proposed for the abstraction channel of the ·OH radical initiated oxidation of DMS in the absence of NO_x. The proposed mechanism is based on the results obtained in the present work in combination with observations from previous studies.

Compounds such as DMSO, SO_2 and MSA were the major sulphur-containing products identified in the ·OH radical initiated oxidation of DMS in the absence of NO_x. Also, evidence was found for the formation of MSIA in considerable yield. The observed behaviour of formation of SO_2 and DMSO at various temperatures and O_2 partial pressures is in agreement with current mechanistic models involving addition and abstraction channels of the primary reaction.

The molar formation yields of DMSO, determined in the present study, support that in the absence of NO_x the OH-DMS adduct, formed in the addition channel, mainly reacts with oxygen to form DMSO. However, because of the uncertainty in the rate coefficients used to extract the formation yield of DMSO the possibility of channels leading to products other than DMSO can not be completely excluded.

High overall molar formation yields of SO_2 have been measured in all the experiments. This indicates that the further oxidation of the products in both the addition and abstraction channels results predominantly in SO_2 production under the conditions of the experiments. The contribution of the fraction of SO_2 oxidised by ·OH radicals to gas phase H_2SO_4 was estimated to be considerably high.

The present experiments only prove that MSIA is formed and indicate that the further ·OH radical reaction with DMSO predominantly results in formation of the acid. Since the yield of methane thiol formate (MTF) was determined to be fairly low, this implies that under atmospheric conditions, where the chemistry of $CH_3SCH_2OO·$ is not controlled by reaction with NO, *i.e.* in the remote marine boundary layer (MBL), the production of MTF is also low.

In the present study a large data set of information was generated. Modelling studies of the present results will give more information on production pathways for OCS, MTF and other sulphur-containing products obtained from the ·OH radical initiated oxidation of DMS. The results of the present study also suggest that the importance of the role of the MSIA chemistry in controlling the contribution of DMS to CCN formation in the remote MBL will increase with decreasing temperature, because of the increase of the importance of the DMSO producing channel.

Chapter 4

Product study of the photo-oxidation of dimethyl sulphide in the presence of NO_x

As part of the work on the different factors affecting the photo-oxidation mechanism of DMS, detailed product studies of the ·OH radical initiated oxidation of DMS, as a function of temperature and different initial concentrations of NO_x (NO + NO_2), have been performed.

The experiments were carried out at 1000 mbar total pressure in synthetic air using the photolysis of H_2O_2 as the ·OH radical source and long path FT-IR spectroscopy to monitor reactants and products. The products of the ·OH radical initiated oxidation of DMS were investigated at 284, 295, and 306 K and different initial NO_x concentrations: initial NO was varied between (434 – 2821) ppb and NO_2 between (135 – 739) ppb.

4.1 Results

The major identified sulphur-containing products were sulphur dioxide (SO_2), dimethyl sulphoxide (DMSO: $CH_3S(O)CH_3$), dimethyl sulphone ($DMSO_2$: $CH_3S(O)_2CH_3$), methane sulphonic acid (MSA: $CH_3S(O)_2OH$) and methane sulphonyl peroxy nitrate (MSPN: $CH_3S(O)_2OONO_2$). Formation of carbonyl sulphide (OCS) was observed in the experiments when the NO_x concentration level became low in the system. As non-sulphur-containing products methanol (CH_3OH), formic acid (HCOOH), formaldehyde (HCHO), methyl hydroperoxide (CH_3OOH), CO and CO_2 were detected. Nitric acid (HNO_3) and peroxy nitric acid (HO_2NO_2) were also identified.

Dimethyl sulphoxide (DMSO)

The plots of the measured yield-time profiles for DMSO as a function of the different temperatures and initial NO_x conditions investigated are shown in Figure 4.1. In order to facilitate the discussion on trends in the product behaviour, the yield-time profiles of DMSO for 295 K and 1000 mbar synthetic air as a function of NO_x concentration are shown separately in Figure 4.2.

Figures 4.1 and 4.2 show that the observed yield of DMSO (i) decreases with increasing temperature and (ii) decreases with increasing NO_x concentration. From both figures it is observable that the yield-time behaviour of DMSO varied systematically with changes in temperature and initial NO_x concentration. In both figures the yields of DMSO have not been corrected for possible secondary loss processes such as reaction with ·OH radicals and wall loss.

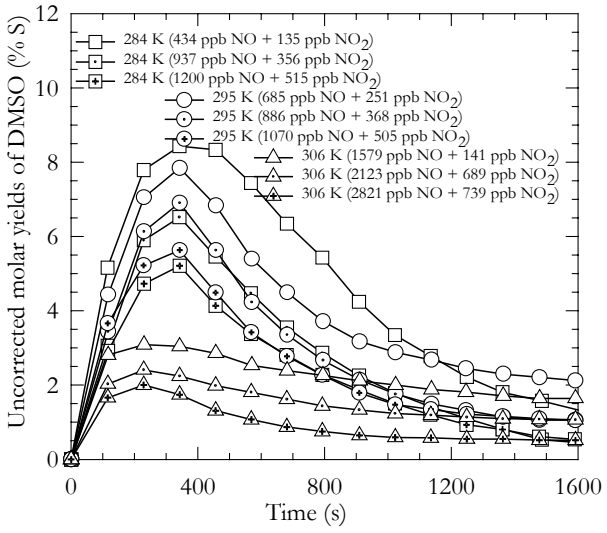

Figure 4.1: Plots of the uncorrected molar yields of DMSO as a function of temperature (284, 295 and 306 K) and initial NO_x concentration versus reaction time.

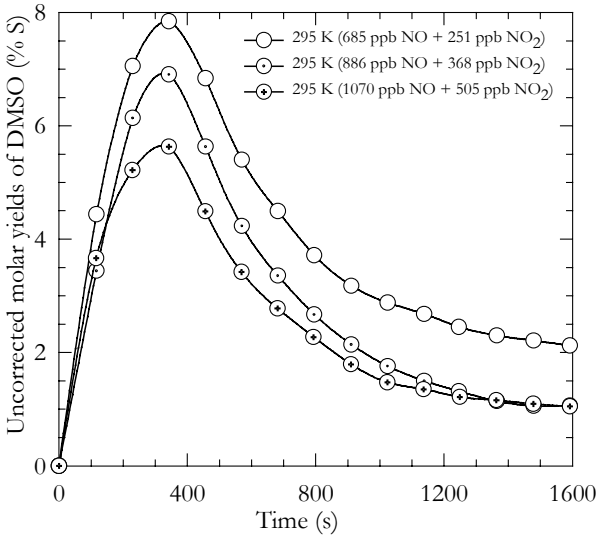

Figure 4.2: Plots of the yields of DMSO for 295 K and 1000 mbar synthetic air as a function of different initial NO_x concentrations versus reaction time.

The shapes of the curves for DMSO are determined by production from DMS oxidation, loss to the reactor walls and further oxidation of DMSO by ·OH radicals. In order to obtain the "exact" formation yields for DMSO, corrections have been performed for its reaction with ·OH radicals and also loss to the reactor walls.

Corrections were made using the mathematical procedure described in Chapter 2, Paragraph 2.3. The rate constants used for the corrections are the same as those given in the previous description. Figures 4.3 shows plots of the DMSO concentrations corrected for wall

loss and reaction with ·OH radicals versus the consumption of DMS. The true formation yields of the compound were determined from the slopes of the lines. The calculated true formation yields for DMSO, obtained by the linear regression analysis of the initial reaction periods are shown in Table 4.1. The errors quoted in Table 4.1 are the 2σ random scatter in the data plots (Figure 4.3) and reflect the errors in the measurement of DMSO and DMS concentration using FT-IR spectroscopy.

Except for the study at 284 K, the plots for DMSO in Figure 4.3 show quite large deviations from linearity. Two distinct linear periods are evident: an initial period with lower formation rate followed by a second period when the DMSO yield increases. The onset of the increase occurs at the point, where the NO concentration approaches the detection limit (about 10 ppb). This behaviour is attributed to a change in the reaction mechanism as will be discussed in Paragraph 4.2.1, Chapter 4.

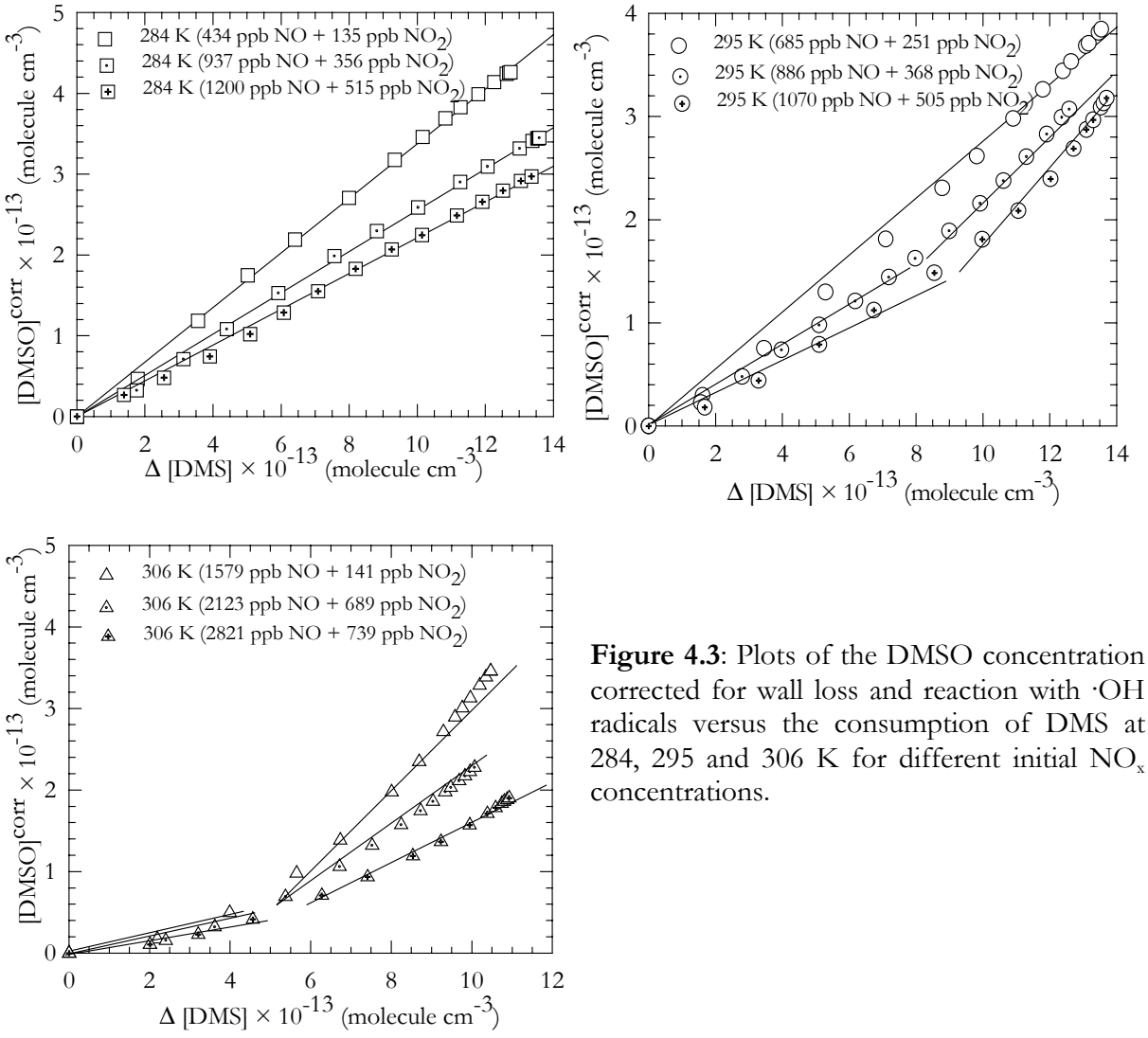

Figure 4.3: Plots of the DMSO concentration corrected for wall loss and reaction with ·OH radicals versus the consumption of DMS at 284, 295 and 306 K for different initial NO_x concentrations.

Table 4.1: Corrected yields for the formation of DMSO in the reaction of ·OH with DMS in 1000 mbar of synthetic air as a function of temperature and NO_x concentration for the initial reaction period.

Temperature (K)	NO (ppb)	NO_2 (ppb)	Corrected DMSO yields* (% molar yield, ± 2 σ)	Contribution of addition pathway** (%)
284	434	135	34.24 ± 5.24	52
	937	356	26.41 ± 4.61	
	1200	515	22.16 ± 4.03	
295	685	251	27.14 ± 4.17	33
	886	368	19.63 ± 3.25	
	1070	505	17.33 ± 3.39	
306	1579	141	14.99 ± 3.56	17
	2123	689	11.01 ± 3.09	
	2821	739	8.99 ± 3.96	

* See Paragraph 2.3, Chapter 2 for details of the correction calculations.

** The yields are compared to the fraction of the reaction occurring *via* the addition pathway calculated using the results of Hynes et al. (1986).

Dimethyl sulphone

The plots of the measured yield-time profiles for $DMSO_2$ as a function of the temperatures and initial NO_x conditions investigated are shown in Figure 4.4. The yield-time profiles of $DMSO_2$ for 295 K and 1000 mbar synthetic air as a function of NO_x concentration are shown separately in Figure 4.5 in order to facilitate the discussion on trends in the product behaviour.

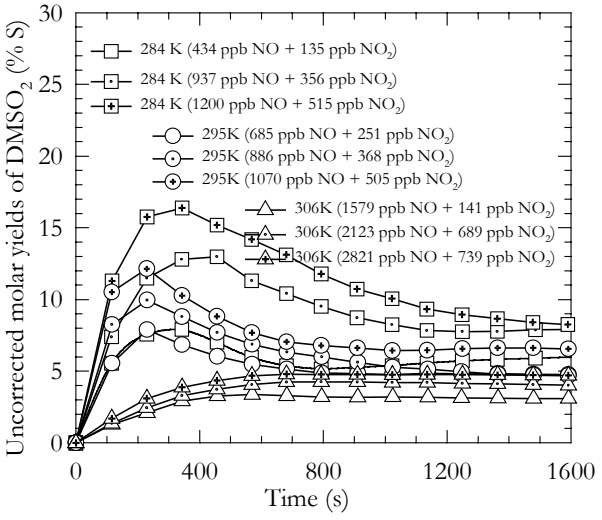

Figure 4.4: Plots of the uncorrected molar yields of $DMSO_2$ as a function of temperature (284, 295 and 306 K) and initial NO_x concentration versus reaction time.

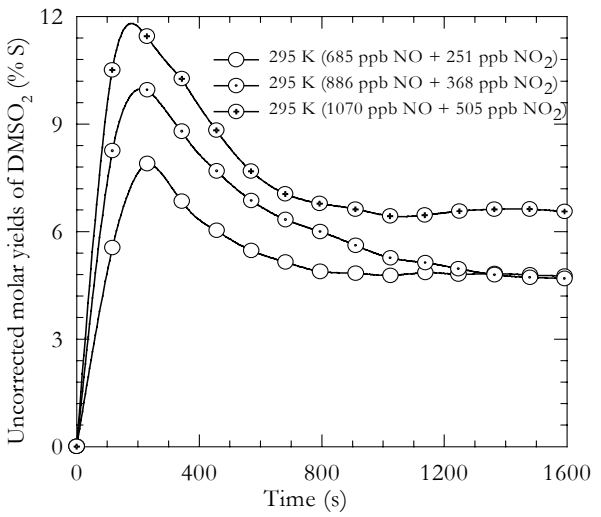

Figure 4.5: Plots of the yields of $DMSO_2$ for 295 K and 1000 mbar synthetic air as a function of different initial NO_x concentrations versus reaction time.

From Figures 4.4 and 4.5 it can be seen, that the observed yield of $DMSO_2$ (i) decreases with increasing temperature and (ii) increases with increasing NO_x concentration. In both figures the yields of $DMSO_2$ were not corrected for possible secondary loss processes.

The formation yields of $DMSO_2$ obtained by the least-squares analysis of the plots of $DMSO_2$ concentrations corrected for wall loss *versu*s the consumed amount of DMS are collected in Table 4.2. The obtained dependencies were straight lines at each temperature and NO_x concentration.

Table 4.2: Formation yields of $DMSO_2$ in the reaction of DMS with ·OH radicals in 1000 mbar of synthetic air as a function of temperature for different concentrations of NO_x.

Temperature (K)	NO (ppb)	NO_2 (ppb)	$DMSO_2$ yields (% molar yield, $\pm 2\sigma$)
284	434	135	8.74 ± 0.94
	937	356	13.56 ± 1.34
	1200	515	17.52 ± 1.36
295	685	251	8.97 ± 0.92
	886	368	10.43 ± 1.49
	1070	505	13.23 ± 1.53
306	1579	141	3.84 ± 0.83
	2123	689	4.71 ± 1.03
	2821	739	5.75 ± 1.06

Sulphur dioxide (SO_2)

The plots of the measured yield-time profiles for SO_2, at different temperatures and initial NO_x conditions are shown in Figure 4.6. In order to facilitate the discussion of the trends in the product behaviour, the yield-time profiles of SO_2 at 295 K and 1000 mbar synthetic air as a function of NO_x concentration are shown separately in Figure 4.7. From both Figure 4.6 and 4.7 it is clear that increasing the concentration of NO_x and increasing the temperature in the DMS oxidation system resulted in a reduction of the SO_2 formation yield.

In Figures 4.6 and 4.7 the yields of SO_2 are not corrected for secondary loss processes such as further reaction with ·OH or wall loss. Figure 4.8 shows the plots of SO_2 concentrations corrected for wall loss and reaction with ·OH radicals versus the amount of DMS consumed. Corrections have been performed using the mathematical procedure described in Chapter 2, Paragraph 2.3. The corrected formation yields of SO_2 obtained by linear regression analysis of the plots in Figure 4.8 are collected in Table 4.3.

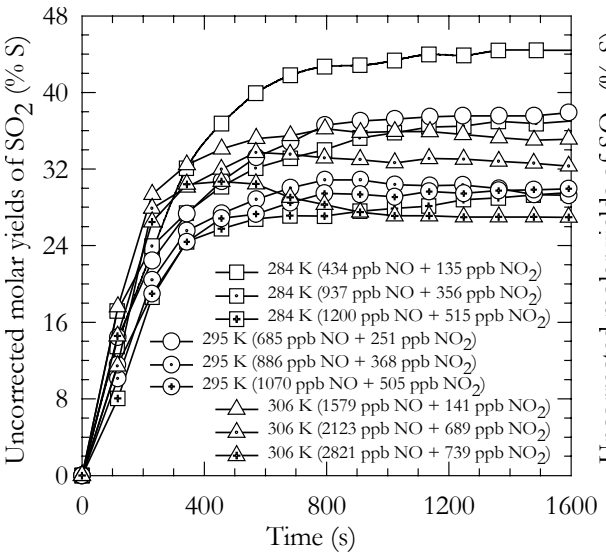

Figure 4.6: Plots of the uncorrected yields of SO_2 as a function of temperature (284, 295 and 306 K) and initial NO_x concentration versus reaction time.

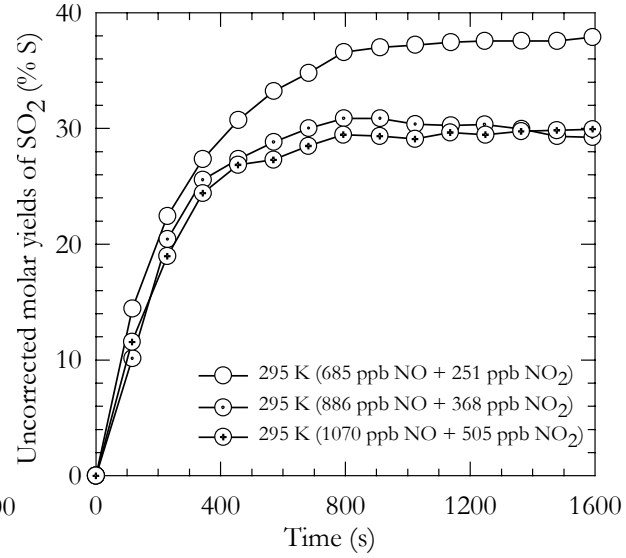

Figure 4.7: Plots of the yields of SO_2 for 295 K and 1000 mbar synthetic air as a function of different initial NO_x concentrations versus reaction time.

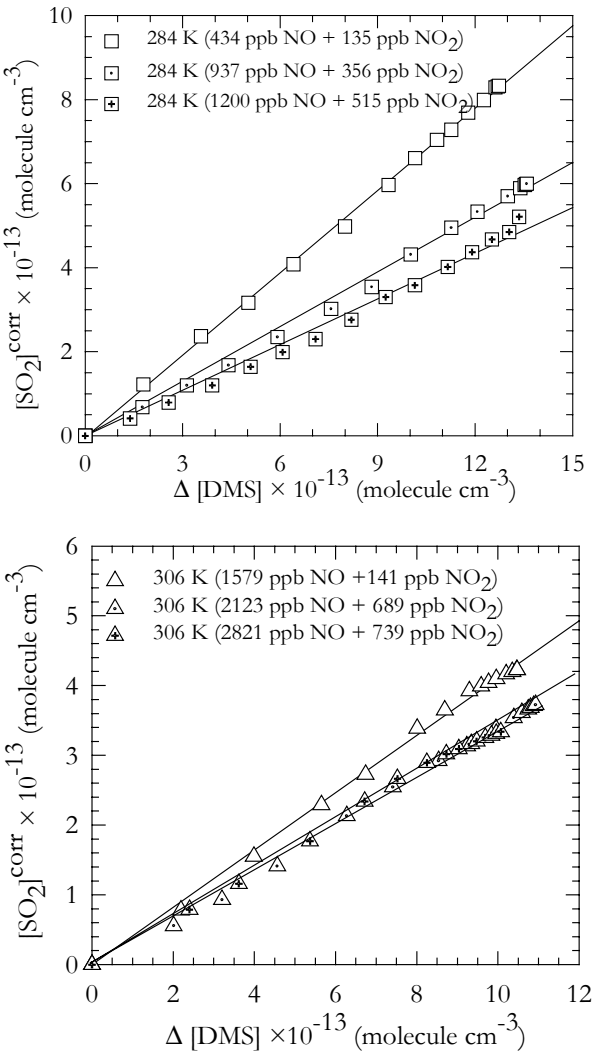

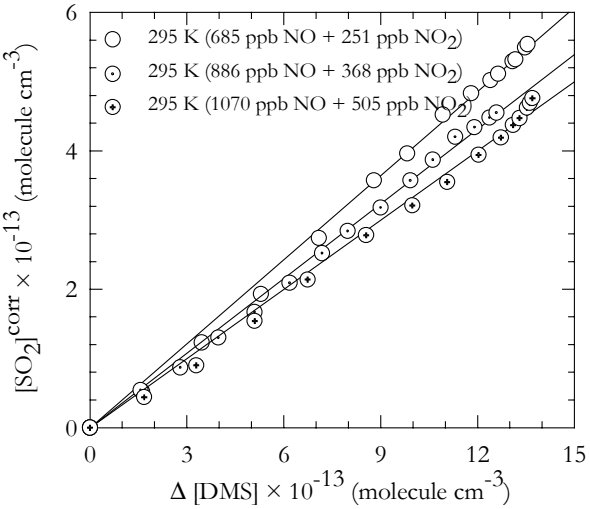

Figure 4.8: Plots of the SO_2 concentration corrected for wall loss and reaction with ·OH radicals versus the consumption of DMS at 284, 295 and 306 K for different initial NO_x concentrations.

Table 4.3: Corrected yields of the formation of SO_2 in the reaction of ·OH with DMS in 1000 mbar of synthetic air as a function of temperature.

Temperature (K)	NO (ppb)	NO_2 (ppb)	Corrected SO_2 yields* (% molar yield, $\pm 2\sigma$)	Contribution of addition pathway** (%)	Contribution of abstraction pathway** (%)
284	434 937 1200	135 356 515	65.34 ± 4.32 42.82 ± 3.58 35.14 ± 3.23	52	48
295	685 886 1070	251 368 505	41.43 ± 3.63 35.85 ± 4.08 33.37 ± 2.24	33	67
306	1579 2123 2821	141 689 739	41.14 ± 3.93 34.46 ± 4.38 33.07 ± 4.97	17	83

* See Paragraph 2.3, Chapter 2 for details of the correction calculations.

** The yields are compared to the fractions of the reaction occurring *via* the addition and abstraction pathways calculated using the results of Hynes et al. (1986).

Methane sulphonic acid (MSA)

The plots of the measured yield-time profiles for MSA measured at different temperatures and initial NO_x conditions are shown in Figure 4.9. In order to facilitate the discussion, the yield-time profiles of MSA for 295 K and 1000 mbar synthetic air as a function of NO_x concentration are shown separately in Figure 4.10.

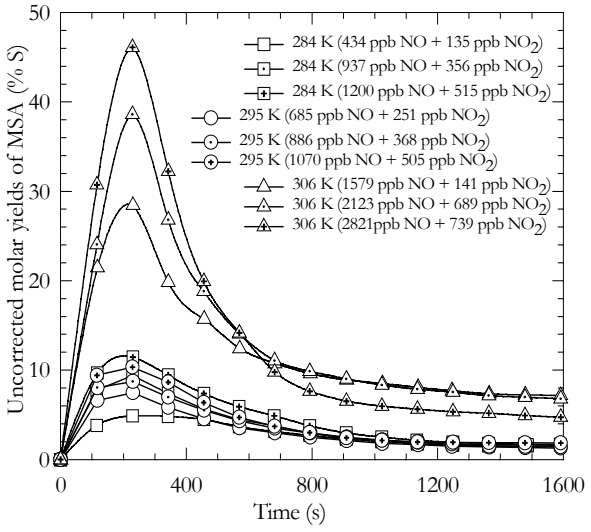

Figure 4.9: Plots of the yields of MSA as a function of temperature (284, 295 and 306 K) and initial NO_x concentration versus reaction time.

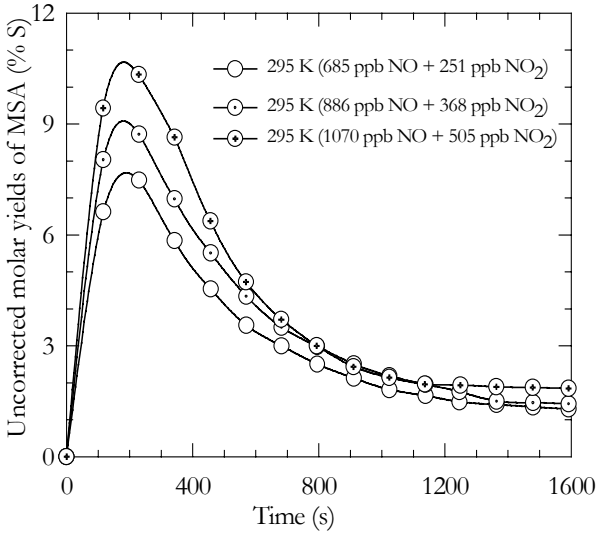

Figure 4.10: Plots of the yields of MSA for 295 K and 1000 mbar synthetic air as a function of different initial NO_x concentrations versus reaction time.

In both Figure 4.9 and Figure 4.10 the yields of MSA were not corrected for secondary loss processes. From both figures it can be observed that all the yield-time contours of MSA pass through a fairly sharp maximum followed by a relatively slower decay caused by loss to the aerosol phase and uptake by the reactor walls. The same trend with respect to NO is observed for all temperatures: the yield maximum increases with increasing initial NO concentration. At 284 and 295 K the maximum yield varies between 5 - 12 molar %. At 306 K, where the initial NO concentrations are much higher, the MSA maximum yields are much higher and vary between 28 - 46 molar %.

Methane sulphonyl peroxy nitrate (MSPN)

The plots of the measured yield-time profiles for MSPN measured at different temperatures and initial NO_x conditions are shown in Figure 4.11. In order to facilitate the discussion, the yield-time profiles of MSPN for 295 K and 1000 mbar synthetic air as a function of NO_x concentration are shown separately in Figure 4.12.

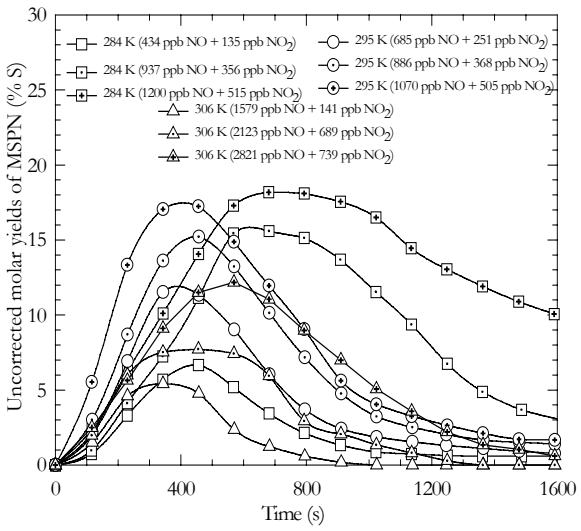

Figure 4.11: Plots of the yields of MSPN as a function of temperature (284, 295 and 306 K) and initial NO_x concentration versus reaction time.

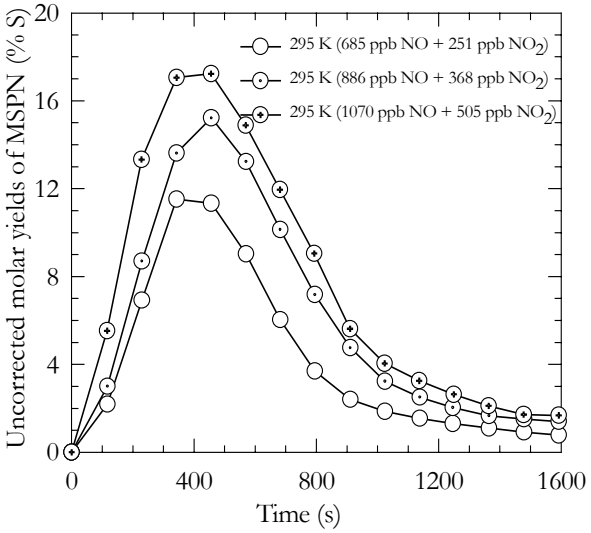

Figure 4.12: Plots of the yields of MSPN for 295 K and 1000 mbar synthetic air as a function of different initial NO_x concentrations versus reaction time.

In both Figure 4.11 and Figure 4.12 the yields of MSPN were not corrected for secondary loss processes. Both Figure 4.11 and Figure 4.12 show that the time-yield contours of MSPN have a maximum followed by a rapid decay and that at all three temperatures the yield maximum increases with increasing initial NO_x concentration.

However, there are several distinct differences compared to the MSA profiles. In contrast to MSA, the molar yield of MSPN increases with decreasing temperature. The position of the MSPN yield maximum compared to MSA is shifted to longer reaction times, especially at low temperature and becomes broader.

Carbonyl sulphide (OCS)

The plots of the yield-time profiles for OCS measured at different temperatures and initial NO_x conditions are shown in Figure 4.13. As seen in Figure 4.13, the formation of OCS was observed only after an initial delay. Analysis of the concentration-time profiles revealed that the onset of OCS formation occurs as the NO concentration approaches zero (Figure 4.14). However, at the high initial NO_x concentrations of the experiments performed at 306 K, formation of OCS was not observed. The absolute yields of OCS calculated from the time-point of formation varied from 0.17 to 0.24 % molar yields (Figure 4.15). The results are presented in Table 4.4.

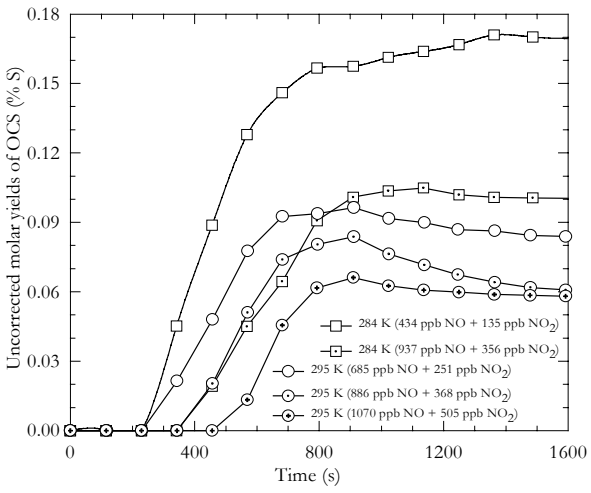

Figure 4.13: Plots of the yields of OCS as a function of temperature (284, 295 and 306 K) and initial NO_x concentration versus reaction time.

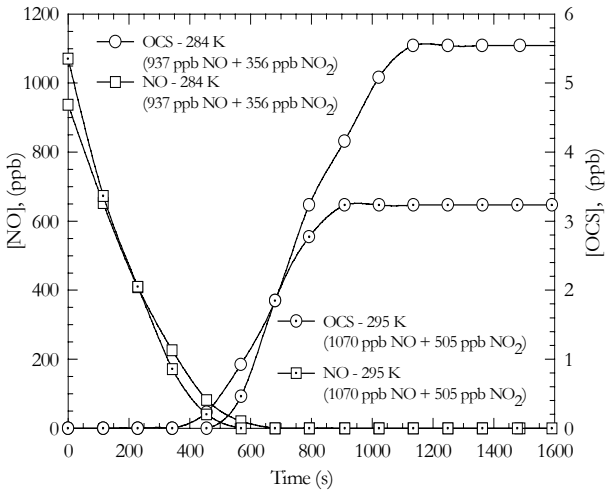

Figure 4.14: Plots of the concentration-time profiles for OCS and NO which show that the onset of OCS formation occurs when the NO concentration approaches zero (examples for 284 and 295 K).

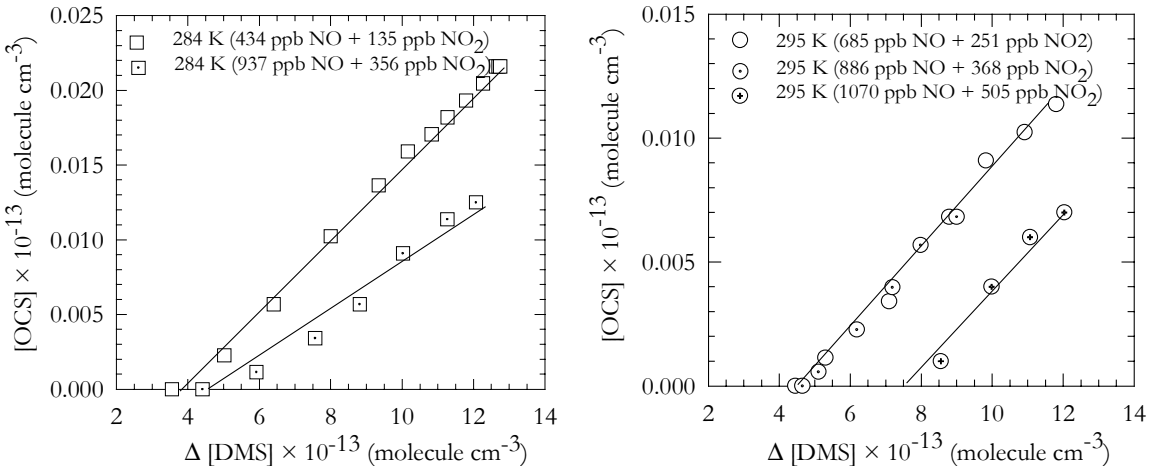

Figure 4.15: Plots of the OCS concentration versus the consumption of DMS at 284 K and 295 K for different initial NO_x concentrations.

Table 4.4: Formation yields of OCS in the reaction of DMS with ·OH radicals in 1000 mbar of synthetic air as a function of temperature for different initial concentration of NO_x.

Temperature (K)	NO (ppb)	NO_2 (ppb)	OCS yields (% molar yield)
284	434	135	0.24 ± 0.05
	937	356	0.16 ± 0.03
	1200	515	-
295	685	251	0.16 ± 0.04
	886	368	0.17 ± 0.05
	1070	505	0.16 ± 0.05
306	1579	141	-
	2123	689	-
	2821	739	-

4.2 Discussion

4.2.1 Dimethyl sulphoxide (DMSO) and dimethyl sulphone ($DMSO_2$) formation

From the results presented in Paragraph 4.1 it is obvious that the yield-time behaviour of DMSO varies systematically with the changes in temperature and initial NO_x concentration. The uncorrected yield-time profiles for DMSO (Figures 4.1 and 4.2) show that at each temperature and initial NO_x concentration the yield initially increases, passes through a maximum and then decreases. The magnitude of the maximum yield increases with decreasing temperature for similar initial NO_x conditions.

The DMSO yield is also strongly dependent on the initial NO concentration: increasing the initial NO concentration depressed the DMSO yield maximum at all temperatures. For the measurements at 306 K, the bell-shaped behaviour observed at 284 and 295 K is not so pronounced. After attainment of the yield maximum there is only a further slow decay of DMSO.

In the experiments at 306 K it was observed that the consumption of DMS also slows down significantly near the point of the DMSO maximum. This behaviour suggests termination of the propagation of the ·OH radical production chain at this point. The probable explanation of the termination is the efficient scavenging of the ·OH radicals *via* the $\cdot OH + NO_2 + M \rightarrow HNO_3 + M$ reaction at the high levels of NO_2, which are generated under the conditions of these experiments. Therefore, the flatness of the DMSO curves at 306 K after the maximum can be attributed to the cessation of its photo-oxidation.

The increase in the DMSO yield with decreasing temperature and the shape of the curves from Figures 4.1 and 4.2 is completely analogous to the behaviour presented in Chapter 3, Paragraph 3.1.1 on the oxidation of DMS under NO_x free conditions. As was already mentioned, the ·OH radical initiated oxidation of DMS is known to proceed by both addition and abstraction channels, the addition channel producing the dimethylhydroxysulphuranyl radical ($CH_3S\cdot(OH)CH_3$). This adduct can either thermally decompose back to reactants or react with molecular oxygen to form products including dimethyl sulphoxide (DMSO):

$CH_3S\cdot(OH)CH_3 + \Delta \rightarrow CH_3SCH_3 + \cdot OH$ (R 4.1)

$CH_3S\cdot(OH)CH_3 + O_2 \rightarrow$ products including DMSO. (R 4.2)

According to the above mechanism, the importance of the addition channel and, hence, DMSO formation will increase with decreasing temperature. This is in broad agreement with the experimental observations reported in Paragraph 4.1. The bell-shape of the yield-time curves is caused by a period of rapid production of DMSO from ·OH + DMS followed by a period of fast removal via ·OH + DMSO as this removal reaction gradually becomes more competitive with the production process. However, this simple mechanism can not explain the significant dependence of the DMSO yield on the initial NO concentration. The simplest explanation of this phenomenon is that the DMS-OH adduct also undergoes a reversible addition of molecular oxygen with formation of a second adduct, which should be in fast equilibrium with DMS and ·OH through the DMS-OH adduct.

$CH_3S\cdot(OH)CH_3 + O_2 + M \leftrightarrow CH_3S(OH)(OO\cdot)CH_3 + M.$ (R 4.3)

Further reaction of the resulting peroxy radical with NO can form an oxy radical which reacts further with O_2 to form dimethyl sulphone ($DMSO_2$) and the hydroperoxy radical. The uncorrected yield-time profiles for $DMSO_2$ show that at 284 and 295 K the yield initially increases, passes through a maximum and then decreases (Figures 4.4 and 4.5). For the measurements at 306 K, the bell-shaped behaviour is not observed.

The bell shape of the $DMSO_2$ yield curves for the 284 and 295 K measurements (Figures 4.4 and 4.5) is what would be expected for a formation mechanism which is active in the initial stages of the reaction and then ceases when one of the reactants is exhausted, *i.e.* in this case NO. At 284 and 295 K, therefore, the behaviour of $DMSO_2$ is generally in qualitative agreement with formation from reaction of a DMS-OH-O_2 alcoxy-peroxy radical with NO being an important pathway in the reaction system. For the $DMSO_2$ profiles obtained at 306 K the $DMSO_2$ yield increases to a plateau rather than going through a maximum. The behaviour of the $DMSO_2$ yield at 306 K is attributable to the considerable slowing in the DMS oxidation just after the DMSO maximum. This halts production of $DMSO_2$ and causes its yield-time plot to approach a plateau.

In general, the overall behaviour of $DMSO_2$ with temperature and NO conditions is not inconsistent with the occurrence of the DMS-OH-O_2 peroxy radical mechanism. These reactions can explain the increased $DMSO_2$ yield observed after NO addition into the system:

$$CH_3S(OH)(OO\cdot)CH_3 + NO \rightarrow CH_3S(OH)(O\cdot)CH_3 + NO_2 \quad \text{(R 4.4)}$$

$$CH_3S(OH)(O\cdot)CH_3 + O_2 \rightarrow CH_3S(O)_2CH_3 + HO_2\cdot. \quad \text{(R 4.5)}$$

Since formation of $DMSO_2$ is also observed in NO_x-free product studies of DMS photo-oxidation (Chapter 3, Paragraphs 3.1.1 and 3.2.2), there are obviously other routes forming $DMSO_2$. Self reaction of the $CH_3S(OH)(OO\cdot)CH_3$ radical or its reactions with other peroxy radicals can also lead to the formation of the $CH_3S(OH)(O\cdot)CH_3$ oxy radical and subsequently dimethyl sulphone ($DMSO_2$), *e.g via* following reactions:

$$2CH_3S(OH)(OO\cdot)CH_3 \rightarrow 2CH_3S(OH)(O\cdot)CH_3 + O_2 \quad \text{(R 4.6)}$$

$$CH_3S(OH)(OO\cdot)CH_3 + CH_3OO\cdot \rightarrow CH_3S(OH)(O\cdot)CH_3 + CH_3O\cdot + O_2. \quad \text{(R 4.7)}$$

It is quite probable that such routes are operative under NO_x-free conditions in smog chambers. As stated previously, the reaction of ·OH with DMSO is also known to produce $DMSO_2$ (Sørensen et al., 1996) possibly *via* the following reactions:

$CH_3S(O)CH_3 + \cdot OH \rightarrow CH_3S\cdot(O)(OH)CH_3$ (R 4.8)

$CH_3S\cdot(O)(OH)CH_3 + O_2 \rightarrow CH_3S(O)_2CH_3 + HO_2\cdot$. (R 4.9)

However, this formation route can not explain the observed behaviour of DMSO in the presence of NO_x. The yield maximum of $DMSO_2$ would be expected to be shifted to longer reaction times compared to that of DMSO which is not the case and no effect on variation of NO would be expected.

Reaction of NO_2 with the OH-DMS adduct, or even the OH-DMSO adduct, are also potential routes of $DMSO_2$:

$CH_3S\cdot(OH)CH_3 + NO_2 \rightarrow CH_3S(OH)(O\cdot)CH_3 + NO$ (R 4.10)

$CH_3S(OH)(O\cdot)CH_3 + O_2 \rightarrow CH_3S(O)_2CH_3 + HO_2\cdot$ (R 4.11)

$CH_3S(O)(OH)CH_3 + NO_2 \rightarrow CH_3S(O)_2CH_3 + HONO$. (R 4.12)

However, these routes are apparently not very important. If they were the major routes of $DMSO_2$ formation, their importance would increase with increasing reaction time because the NO_2 concentration in the system is increasing with time in the initial reaction period.

The formation of $DMSO_2$ *via* reaction of a DMS-OH-O_2 peroxy radical with NO should reduce the yield of DMSO from the addition channel. As can be seen in Table 4.1 from Paragraph 4.1, Chapter 4, the DMSO formation yield in the initial stages of the reaction is systematically depressed with increases in the initial NO concentration. Further, the plots of the corrected DMSO concentration versus the consumption of DMS (see Figure 4.3, Paragraph 4.1, Chapter 4) show that the formation of DMSO increases when the NO concentration falls to low levels. All these facts support that a major mechanism for the formation of $DMSO_2$ is reaction of a DMS-OH-O_2 peroxy radical with NO as described above.

It is of interest at this stage to compare the corrected formation yields of DMSO with the calculated fraction of the ·OH + DMS reaction proceeding *via* the addition pathway. It should be borne in mind, during this comparison, that there are quite substantial uncertainties involved in both the correction of the DMSO yields, particularly at 306 K when the yields are low, and also in the estimates of the addition fraction (Arsene et al., 1999).

It is evident from Table 4.1, that the branching ratios for DMSO formation from $CH_3S\cdot(OH)CH_3 + O_2$ is considerably less than unity under all the conditions. It is only at 306 K that the differences are not quite so pronounced, particularly at the low NO levels. According to the results presented in Table 4.1 the branching ratio decreases with increasing initial NO and the

effectiveness of the depression of the DMSO yield with NO would appear to fall off with increasing temperature. This general type of behaviour is expected for a reaction sequence involving addition of oxygen to an DMS-OH adduct with formation of a thermally unstable DMS-OH-O_2 peroxy radical adduct (Arsene et al., 2001). This behaviour contrasts strongly with the results from Chapter 3, Paragraphs 3.1.1 and 3.2.1, for NO_x-free conditions, where the DMSO yield was close to unity under all the reaction conditions employed.

The branching ratio values for DMSO formation are, however, quite similar to the branching ratio of $\Phi = 0.5 \pm 0.15$ at 234 and 258 K for $HO_2\cdot$ production from $CH_3S\cdot(OH)CH_3 + O_2 \rightarrow HO_2\cdot$ + DMSO reported by Turnipseed et al. (1996) in a pulsed laser photolysis/pulsed laser-induced fluorescence study on the reaction of ·OH with DMS. Turnipseed et al. (1996) measured hydroperoxy radical ($HO_2\cdot$) by converting it to ·OH using NO. In their reaction system NO could also disturb the equilibrium DMS-OH + $O_2 \leftrightarrow$ DMS-OH-O_2 through the reaction DMS-OH-O_2 + NO $\rightarrow$ DMS-OH-O + NO_2. Such a reaction, if it occurred in their system would have resulted in a reduction in the apparent branching ratio for DMSO formation.

The results from the present work showing the existence of the addition of O_2 to the DMS-OH adduct with subsequent reaction with NO offers a plausible explanation for the differences in the DMSO yield found between systems operating with and without NO.

4.2.2 Sulphur dioxide (SO_2) formation

From both Figure 4.6 and 4.7 presented in Paragraph 4.1, Chapter 4, it is clear that increasing the concentration of NO_x and increasing the temperature in the DMS oxidation system resulted in a reduction of the SO_2 formation yield.

The uncorrected yield-time curves of SO_2 show a steep initial rise followed by a much slower increase to a plateau. Since it was difficult to set the initial NO_x conditions to the same level in all the experiments, there is no general pattern with respect to the onset of the approach to the plateau, which is governed mainly by the level of NO_2 in the system. However, at all three temperatures there is a general decrease of the yield with increasing initial NO_x concentration, the effect being most pronounced at the lowest temperature.

From Table 4.3 it can be seen that the yields of SO_2 are much lower than those observed in NO_x free systems (Chapter 3, Paragraphs 3.1.1 and 3.2.3), but are similar to those which have been reported previously for DMS oxidation systems containing NO_x (Patroescu et al., 1999; Sørensen et al., 1996).

In contrast to DMSO, deviations from linearity were generally not observed in the plots of the corrected SO_2 concentration versus consumption of DMS (see Figure 4.8, Paragraph 4.1, Chapter 4). This is not too surprising, since SO_2 is not a direct product from the ·OH radical initiated oxidation of DMS and the pathways leading to SO_2 formation in the presence of NO_x are much more complex than those of DMSO and involve formation of thermally unstable peroxy nitrate intermediates. SO_2 is assumed to react only with ·OH in the reaction system. However, the increasing importance of the $DMSO_2$ formation pathway with the increase of the initial NO should result in a decreases in the SO_2 yield. In the present work it has been observed that the corrected SO_2 yield does indeed decrease with higher initial NO concentration in accordance with the mechanistic expectations.

4.2.3 Methane sulphonic acid (MSA) and methane sulphonyl peroxy nitrate (MSPN) formation

In the ·OH radical initiated oxidation of DMS in the presence of NO_x both MSA and MSPN compounds can be formed in the addition and abstraction channels. For the atmospheric oxidation of the CH_3SCH_2· radical the following reaction sequence has been proposed (Niki et al., 1983):

$$CH_3SCH_2\cdot + O_2 + M \rightarrow CH_3SCH_2OO\cdot + M \quad \text{(R 4.13)}$$

$$CH_3SCH_2OO\cdot + NO \rightarrow CH_3SCH_2O\cdot + NO_2 \quad \text{(R 4.14)}$$

$$CH_3SCH_2O\cdot + M \rightarrow CH_3S\cdot + CH_2O + M. \quad \text{(R 4.15)}$$

The occurrence of these reactions during the DMS photo-oxidation has been confirmed by laboratory investigations (Turnipseed et al., 1996; Wallington et al., 1993b). It was also established that the CH_3SCH_2OO· + NO reaction produces CH_2O and CH_3S· in approximately unit yield probably *via* the decomposition of the unstable CH_3SCH_2O· intermediate (Urbanski et al., 1997).

The CH_3S· radical can react with O_2, and for this reaction the following speculative mechanism was proposed by Yin et al. (1990a):

$$CH_3S\cdot + O_2 + M \leftrightarrow CH_3SOO\cdot + M \quad \text{(R 4.16)}$$

$$CH_3SOO\cdot + CH_3S\cdot \rightarrow CH_3S\cdot(O) + CH_3S\cdot(O) \quad \text{(R 4.17)}$$

$$CH_3SOO\cdot + NO \rightarrow \rightarrow CH_3S\cdot(O) + NO_2. \quad \text{(R 4.18)}$$

Laboratory investigations have established that the $CH_3S\cdot(O)$ radical can react with NO_x and, hence, in analysing the results from ·OH radical initiated oxidation of DMS in the presence of NO_x, possible influences of these reactions on the product distribution have to be considered. Further reactions of the $CH_3S\cdot(O)$ radical produce SO_2, $CH_3S(O)_2OH$ and $CH_3S(O)_2OONO_2$, which have been identified as major products in the photo-oxidation of DMS (Barnes et al., 1988; Grosjean, 1984; Patroescu et al., 1999).

The methyl sulphonyl radical ($CH_3S\cdot(O)_2$) is considered to be a possible key intermediate in the oxidation mechanism of DMS and it can be formed *via* the reactions:

$$CH_3S\cdot(O) + NO_2 \rightarrow CH_3S\cdot(O)_2 + NO \qquad \text{(R 4.19)}$$

and

$$CH_3S(O)CH_3 + \cdot OH + M \rightarrow \rightarrow CH_3S(O)OH + CH_3\cdot + M \qquad \text{(R 4.20)}$$

$$CH_3S(O)OH + \cdot OH \rightarrow CH_3S\cdot(O)_2 + H_2O. \qquad \text{(R 4.21)}$$

Therefore, both abstraction and addition channels in the ·OH radical initiated oxidation of DMS can lead to $CH_3S\cdot(O)_2$ and, hence, further reactions of this radical can influence the SO_2, MSA and MSPN yields.

The stability of the $CH_3S\cdot(O)_2$ radical and its reaction with NO_2 have been investigated by Ray et al. (1996) using the discharge flow laser induced fluorescence/mass spectrometry method. For the conditions employed during their experiments (298 K and 1 Torr pressure) the thermal decomposition of $CH_3S\cdot(O)_2$ has been found to be important with a rate of about 500 s^{-1}. In more recent investigations of $CH_3S\cdot(O)_2$ radical decomposition and on the mechanism of SO_2 and $CH_3\cdot$ formation from reaction of the $CH_3S\cdot(O)$ radical with NO_2, the pressure range was extended to 612 Torr (Kukui et al., 2000). At this pressure and temperature of 300 K the upper limit for the rate of thermal decomposition of $CH_3S\cdot(O)_2$ radical was found to be 100 s^{-1}.

Based on the available kinetic data, decomposition of the $CH_3S\cdot(O)_2$ radical (R 4.22) must be the main pathway for SO_2 formation. This reaction competes with further oxidation of the $CH_3S\cdot(O)_2$ radical to $CH_3S(O)_2O\cdot$ (reactions R 4.23 - R 4.25). In the absence of NO_x, or at very low NO_x concentrations, the unimolecular decomposition of the $CH_3S\cdot(O)_2$ radical with formation of SO_2 dominates the competitive reaction sequence:

$$CH_3S\cdot(O)_2 + M \rightarrow CH_3\cdot + SO_2 + M \qquad \text{(R 4.22)}$$

$$CH_3S\cdot(O)_2 + O_2 \rightarrow CH_3S(O)_2OO\cdot \qquad \text{(R 4.23)}$$

$$CH_3S(O)_2OO\cdot + NO \rightarrow CH_3S(O)_2O\cdot + NO_2 \qquad \text{(R 4.24)}$$

$CH_3S\cdot(O)_2 + NO_2 \rightarrow CH_3S(O)_2O\cdot + NO$ (R 4.25)

$CH_3S(O)_2O\cdot + RH \rightarrow CH_3S(O)_2OH + R\cdot$ (R 4.26)

$CH_3S(O)_2OO\cdot + NO_2 + M \leftrightarrow CH_3S(O)_2OONO_2 + M.$ (R 4.27)

In the case of high NO_x concentrations, the reactions (R 4.23) and (R 4.25) become competitive with $CH_3S\cdot(O)_2$ decomposition.

The $CH_3S(O)_2OO\cdot$ radical reaction with NO_2 leads to $CH_3S(O)_2OONO_2$, a peroxy nitrate which has been identified in other studies (Patroescu et al., 1999). When NO is present in excess, the $CH_3S(O)_2OO\cdot$ radical is converted to $CH_3S(O)_2O\cdot$ which leads to $CH_3S(O)_2OH$ formation (increase in the formation yields of MSA but a decrease in $CH_3S(O)_2OONO_2$ formation). Competition between $CH_3S\cdot(O)_2$ decomposition and further oxidation leads to the decreases in the formation yield of SO_2 and increases in the formation yield of $CH_3S(O)_2OH$ as observed here and also as has been reported by Patroescu et al. (1999).

Barone et al. (1995) showed that NO is responsible for converting $CH_3S(O)_xOO\cdot$ to the $CH_3S(O)_xO\cdot$ radical. They came to conclusion that NO_x plays an important role in determining the $[MSA]/[SO_4^{2-}]$ ratio because in the presence of O_2, the NO + $CH_3S(O)_2OO\cdot$ reaction becomes the rate limiting step in the conversion of $CH_3S\cdot(O)_2$ to $CH_3S(O)_2O\cdot$. Calculations, made by Ray et al. (1996), indicate that the $[MSA]/[SO_4^{2-}]$ ratio would not be sensitive to the NO_2 levels in the remote atmosphere, where the typical levels of NO_2 are 10 pptv and 1 ppbv, but would be strongly dependent on NO_2 in the regions with significant levels of NO_x.

From the general trends in the yields of MSA and MSPN, with changes in temperature and NO_x concentration, obtained in the present study, it is clear that the observed yields of both compounds are temperature dependent and increase with increasing NO_x. The observed behaviour of methane sulphonic acid corresponds to the fact that NO and NO_2 promote the formation of this compound, as proposed in previous studies, *via* the reactions:

$CH_3S(O)OO\cdot + NO \rightarrow CH_3S(O)O\cdot + NO_2$ (R 4.28)

$CH_3S(O)_2OO\cdot + NO \rightarrow CH_3S(O)_2O\cdot + NO_2$ (R 4.24)

$CH_3S\cdot + NO_2 \rightarrow CH_3S\cdot(O) + NO$ (R 4.29)

$CH_3S\cdot(O) + NO_2 \rightarrow CH_3S\cdot(O)_2 + NO$ (R 4.19)

$CH_3S\cdot(O)_2 + NO_2 \rightarrow \rightarrow CH_3S(O)_2O\cdot + NO$ (R 4.25)

followed by

$CH_3S(O)_2O\cdot + RH \rightarrow CH_3S(O)_2OH + R\cdot$. (R 4.26)

The observed behaviour of MSPN is perfectly in agreement with what would be expected for a thermally labile peroxy nitrate compound

$CH_3S(O)_2OONO_2 + M \leftrightarrow CH_3S(O)_2OO\cdot + NO_2 + M$ (R 4.27)

because in such an equilibrium, a decrease in temperature and an increase in the NO_2 concentration obviously will favour formation of the peroxy nitrate.

The ratio of NO to NO_2 is also important since the equilibrium is in competition with reaction

$CH_3S(O)_2OO\cdot + NO \rightarrow CH_3S(O)_2O\cdot + NO_2$, (R 4.24)

which favours formation of MSA. It is worth noting that further reactions of the $CH_3S(O)_2OO\cdot$ and $CH_3S(O)_2O\cdot$ radicals cannot lead to SO_2 formation.

The main effect of the presence of NO/NO_2 in the reaction system appears to be a very efficient conversion of peroxy radicals such as $CH_3S(O)_2OO\cdot$ to $CH_3S(O)_2O\cdot$ radicals (R 4.24). Occurrence of such reactions favours formation of MSA rather than production of SO_2. The variation of the profiles of MSA and MSPN observed in the present work are in accord with the behaviour expected in course of the above reactions.

4.2.4 Formation of carbonyl sulphide (OCS) in the presence of NO_x

The observed behaviour of carbonyl sulphide (OCS) agrees with previous reports on OCS formation from the oxidation of DMS from this laboratory (Barnes et al., 1994; Barnes et al, 1996; Patroescu et al., 1999).

Increasing the temperature increases the branching factor for $CH_3SCH_2\cdot$ formation in the ·OH radical initiated oxidation of DMS. Methylthiomethyl radical is considered to be a precursor of the $CH_3S\cdot$ radical and MTF. Further transformations of MTF, such as ·OH radical initiated oxidation or photolysis of MTF, can give OCS. Methane thiol formate was not observed as a product in the present system which is characterised by high NO_x levels. Formation of MTF has been previously observed from the ·OH radical initiated oxidation of DMS in the presence of

NO_x, (Patroescu et al.,1999), however, formation was observed only when the level of NO fell below 30 ppb.

The thermal decomposition of CH_3SCO radicals produced in the photolysis or ·OH radical initiated oxidation of CH_3SCHO can possibly give OCS *via* the loss of an H atom in reaction with ·OH or photo-detachment followed by unimolecular decomposition:

$$CH_3SCHO + {\cdot}OH/h\nu \rightarrow CH_3SCO + H_2O/H \quad \text{(R 4.30)}$$

$$CH_3SCO + \Delta \rightarrow CH_3{\cdot} + O{=}C{=}S. \quad \text{(R 4.31)}$$

Possible reactions of CH_3S· radicals leading to OCS formation include:

$$CH_3S{\cdot} + CH_3S{\cdot} \rightarrow CH_3SH + H_2C{=}S \quad \text{(R 4.32)}$$

$$CH_3S{\cdot} + O_2 \rightarrow H_2C{=}S + HO_2{\cdot} \quad \text{(R 4.33)}$$

$$H_2C{=}S + OH/h\nu \rightarrow HCS + H_2O/H \quad \text{(R 4.34)}$$

$$HCS + O_2 \rightarrow O{=}C{=}S + {\cdot}OH. \quad \text{(R 4.35)}$$

Addition of NO_2 to the reaction system will reduce the OCS yield due to the effective scavenging of the CH_3S· radicals by the reaction with NO_2 with formation of $CH_3S{\cdot}(O)$ and NO:

$$CH_3S{\cdot} + NO_2 \rightarrow CH_3S{\cdot}(O) + NO. \quad \text{(R 4.29)}$$

The reaction of CH_3S· radicals with NO_2 (k_{298} = 5.6 × 10^{-11} cm^3 $molecule^{-1}$ s^{-1}; Tyndall and Ravishankara, 1989) producing $CH_3S{\cdot}(O)$ and NO (Barnes et al., 1987b; Tyndall and Ravishankara, 1989) is faster than the reaction of CH_3S· radicals with O_2 (k_{298} = 2 × 10^{-18} cm^3 $molecule^{-1}$ s^{-1}; Tyndall and Ravishankara, 1989) and, hence, the competition of both reactions will be NO_2 concentration dependent.

The reaction of the CH_3S· radicals with molecular oxygen, which leads to the formation of methyl thioformaldehide (H_2CS) the further oxidation of which results in the formation of OCS, is probably only of minor importance in the reaction system. The reaction between CH_3S· and NO with CH_3SNO formation and its further oxidation is not a likely source of OCS. In the clean marine troposphere, the reactions of CH_3S· with NO_x species is negligible (Yin et al., 1990a,b). However, in coastal regions, where polluted continental air can be transported over the oceans, NO_x concentrations can reach a magnitude sufficient to increase the importance of the reaction between CH_3S· and NO_2. Over polluted areas, the presence of NO_x will be more favourable to MSA rather than OCS or SO_2 production.

4.3 Summary of results and conclusions

The ·OH radical initiated oxidation of DMS has been investigated as a function of temperature and initial NO_x concentration at 1000 mbar of synthetic air. Formation of dimethyl sulphoxide (DMSO), dimethyl sulphone ($DMSO_2$), sulphur dioxide (SO_2), methane sulphonic acid (MSA), methane sulphonyl peroxy nitrate (MSPN) and carbonyl sulphide (OCS) was observed in the reaction system. Based on the obtained uncorrected molar yields of the gas phase products, using long path FT-IR spectroscopy, it is shown (Figure 4.16) that the level of NO concentration in the reaction system was a crucial factor in determining the yields of the products at different temperatures. On the basis of the results obtained in the present study in combination with observations from previous studies on DMS oxidation, a general mechanism for the oxidation of DMS in the presence of NO_x has been constructed. Figures 4.17 and 4.18 show the mechanism for the addition and abstraction channels, respectively.

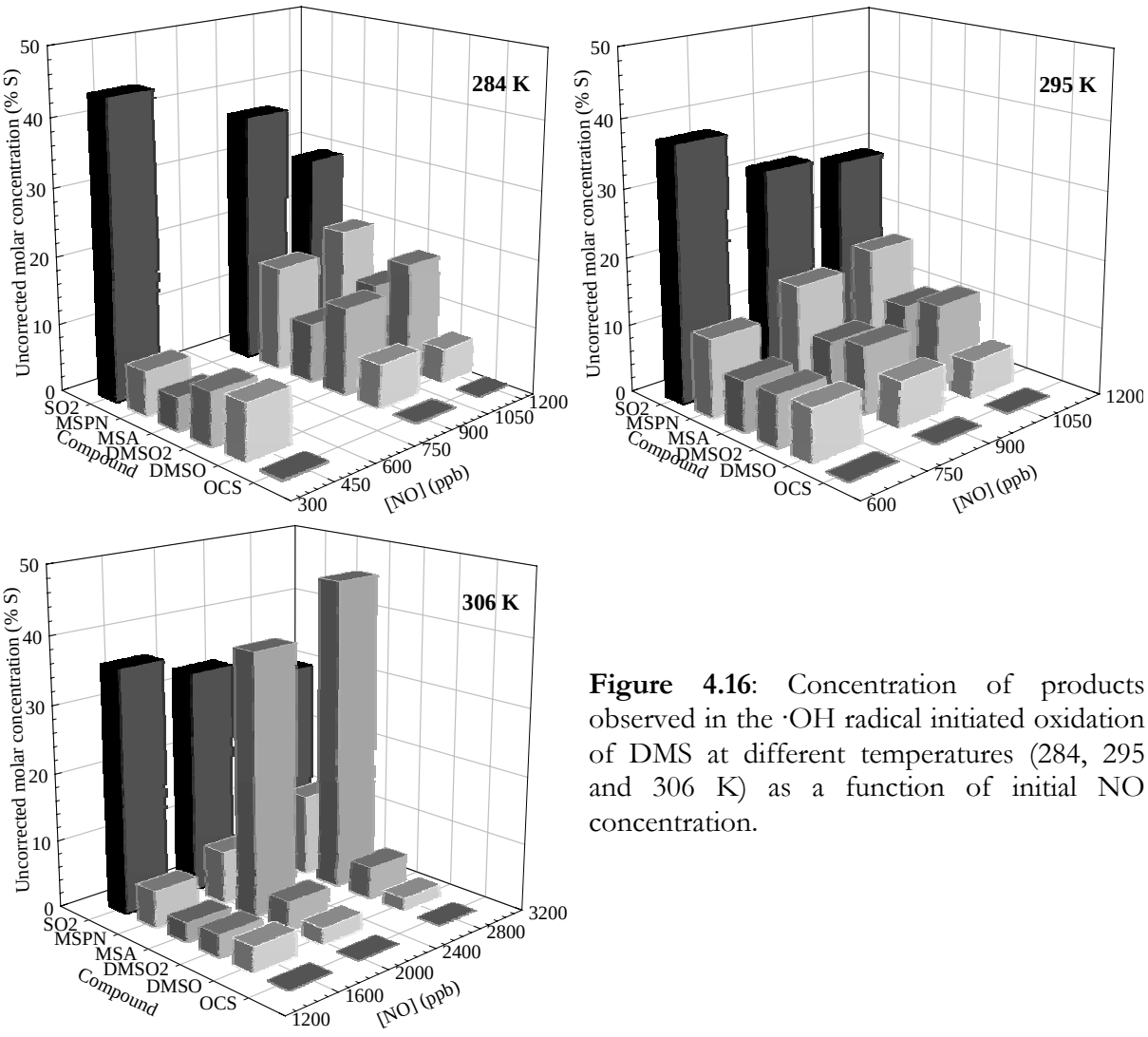

Figure 4.16: Concentration of products observed in the ·OH radical initiated oxidation of DMS at different temperatures (284, 295 and 306 K) as a function of initial NO concentration.

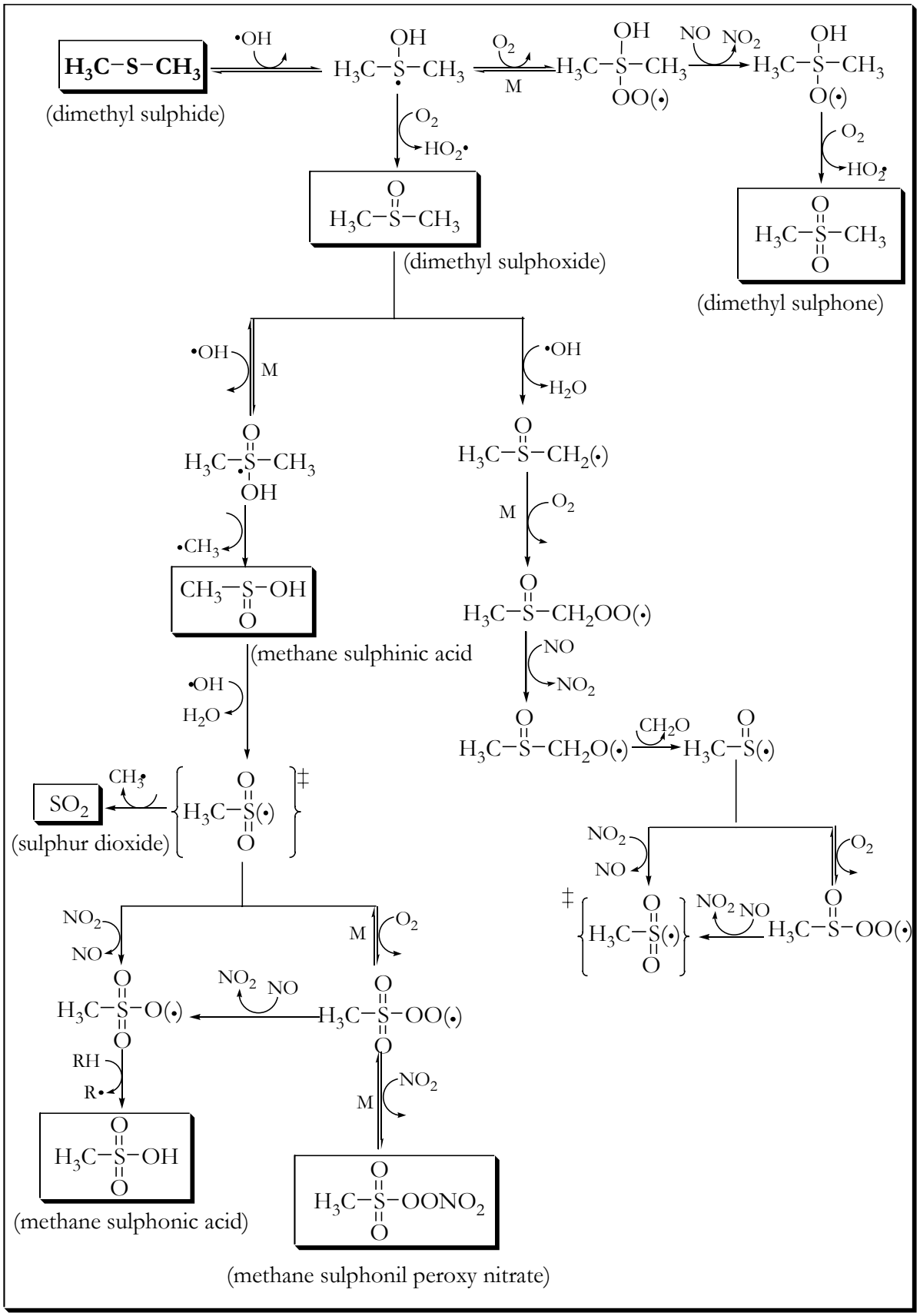

Figure 4.17: Proposed reaction mechanism for the addition channel of the ·OH radical initiated oxidation of DMS in the presence of NO_x.

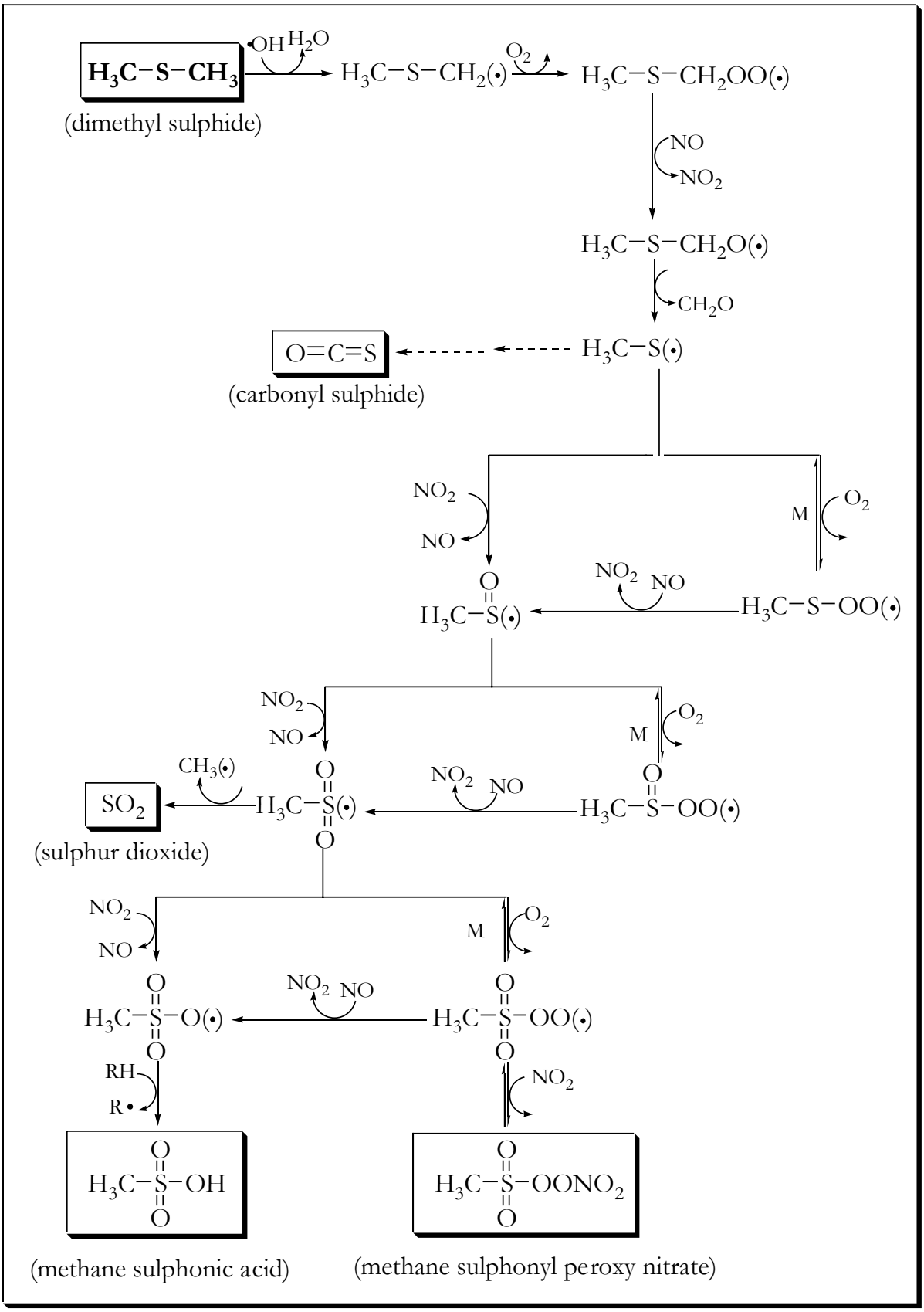

Figure 4.18: Proposed reaction mechanism for the abstraction channel of the ·OH radical initiated oxidation of DMS in the presence of NO_x.

The major sulphur-containing products identified in the ·OH radical initiated oxidation of DMS in the presence of NO_x were SO_2, DMSO, $DMSO_2$, MSA, MSPN and OCS. The variation of the product yields with temperature and NO_x concentration are consistent with the occurrence of both addition and abstraction channels in ·OH radical initiated oxidation of DMS. Distinct trends in the yields of the various products have been observed as a function of temperature, initial NO_x conditions and also reaction time as NO is consumed in the system. Increasing the initial NO concentration was found to depress the DMSO, SO_2 and OCS formation yields and enhance those of $DMSO_2$, MSA and MSPN. In the present study it was found that the level of NO concentration in the reaction system was a crucial factor in determining the yields of DMSO and $DMSO_2$, which were anti-correlated. The observed yield time behaviour of $DMSO_2$ is supportive of a formation mechanism involving reversible addition of O_2 to a $(CH_3)_2S$-OH adduct, formed via the addition channel, followed by sequential reactions with NO and molecular oxygen. The reaction sequence which can explain $DMSO_2$ formation in the ·OH radical initiated oxidation of DMS in the presence of NO_x has been proposed previously in a slightly modified form by Yin et al. (1990a). In their mechanism the reaction of the $(CH_3)_2S$-OH adduct with oxygen was not reversible and a thermal decomposition pathway to DMSO and HO_2 was included. The results from the present work does, however, represent the first study where experimental evidence for such a reaction mechanism has been found.

It is presently difficult to extrapolate the results to typical atmospheric concentrations of NO to obtain meaningful information about the possible significance of the above reaction mechanism in the troposphere. Should the reaction sequence not be significant under tropospheric conditions this, in combination with the results from the NO_x free system, would imply a near unit formation yield of DMSO from the addition channel of the reaction of ·OH with DMS. However, under the low NO_x conditions which often prevail in the remote marine atmosphere, there remains the possibility of reaction of the OH-DMS-O_2 adduct with HO_2· or other peroxy radicals which could convert it to $DMSO_2$, particularly at low temperature, for which no information presently exists.

Although the results presented here constitute a detailed body of concentration-time product data for the ·OH radical initiated oxidation of DMS, a detailed modelling study of these results will help to a elucidate and better define the potential atmospheric importance of many of the speculative or uncertain aspects of the DMS oxidation processes.

Chapter 5

Product study of the photo-oxidation of dimethyl sulphoxide

The present work was aimed at clarifying the mechanism of the ·OH radical initiated oxidation of dimethyl sulphoxide (DMSO: $CH_3S(O)CH_3$) under different conditions. The main question was whether or not methane sulphinic acid (MSIA: $CH_3S(O)OH$) is a major product of the ·OH + DMSO reaction. Products of the gas phase oxidation of dimethyl sulphoxide by ·OH radicals, in the absence and in the presence of NO_x, have been investigated.

Long path FT-IR spectroscopy and ion chromatography were used as analytical tools in order to monitor and to quantify reactants and reaction products. Experiments were carried out at temperatures of 284, 295 and 306 ± 2 K and different initial NO_x ($NO + NO_2$) concentration: initial NO was varied between (0 - 1563) ppb and NO_2 between (0 - 145) ppb. In all the experiments 1000 mbar of synthetic air was used as the bath gas. Photolysis of H_2O_2 ($[NO]_x = 0$ ppm) or CH_3ONO (different concentration of NO_x) was used as the ·OH radical source. Infrared spectra were recorded at 1 cm^{-1} resolution and, as a rule, 10 - 15 spectra were collected over irradiation periods of 20 - 30 minutes.

In order to analyse products, such as methane sulphinic and methane sulphonic acid, ion chromatography was employed as the analytical tool. The experiments employing IC were performed at a total pressure of 1000 mbar of synthetic air and a temperature of 284 K. Initial [NO] was varied between (0 - 2046) ppb and [NO_2] was varied between (0 - 156) ppb. Photolysis of H_2O_2 in the absence of NO_x and photolysis of CH_3ONO in the presence of NO_x were used as ·OH radical sources. Collection of the sample for ion chromatographic analysis was as described in Chapter 2, Paragraph 2.2 (a total amount of 5 - 10 l air was collected). Other products were

monitored simultaneously with FT-IR. Usually IR spectra were recorded in the 700 - 4000 spectral region with 1 cm^{-1} resolution by co-adding 32 interferograms over 30 s and 5 - 6 spectra were recorded over a period of 5 - 10 minutes.

5.1 Results

The product analysis of the gas phase oxidation of dimethyl sulphoxide by ·OH radicals both in the absence and in the presence of NO_x showed the formation of dimethyl sulphone ($DMSO_2$:$CH_3S(O)_2CH_3$), sulphur dioxide (SO_2), methane sulphonic acid (MSA: $CH_3S(O)_2OH$) and methane sulphonyl peroxynitrate (MSPN: $CH_3S(O)_2OONO_2$). However, using IC methane sulphinic acid (MSIA: $CH_3S(O)OH$) was found to be the primary product of the ·OH radical initiated oxidation of DMSO. As non-sulphur-containing products methanol (CH_3OH), methyl hydroperoxide (CH_3OOH), formaldehyde (HCHO), formic acid (HCOOH), carbon monoxide (CO), carbon dioxide (CO_2) and water were identified and, with the exception of water and CO_2, quantified. The observation of methanol and methyl hydroperoxide implies formation of CH_3· radicals in the system.

5.1.1 Identification of methane sulphinic acid (MSIA) and methane sulphonic acid (MSA) by ion chromatography (IC)

The infrared spectrum of methane sulphinic acid is presently not known and, therefore, it is not possible to establish the formation of this compound in the gas phase by using long path FT-IR spectroscopy. Preliminary results concerning the direct observation of MSIA in the gas phase by using long path FT-IR spectroscopy are presented in Appendix B. A set of experiments designed to observe the direct formation of MSIA in the gas phase from DMS and DMSO oxidation has been performed in a 360 l reactor which can be temperature regulated within the range from 223 to 296 K. Experiments performed at 253 K have provided the first tentative IR spectrum of MSIA obtained by *in situ* generation (the stability of MSIA is expected to increase at low temperature).

By using ion chromatography as the analytical tool a detailed study concerning MSIA identification in the ·OH radical initiated oxidation of DMSO both in the absence and in the presence of NO_x has been performed. Simultaneously, this analytical technique gives information about the formation of MSA in the oxidative system.

Figures 5.1a-b show the chromatograms which demonstrate the detection and achieved resolution of the $CH_3S(O)O^-$ and $CH_3S(O)_2O^-$ anions from MSIA and MSA sampled from DMSO-H_2O_2 (a) and DMSO-CH_3ONO-NO_x (b) oxidation systems, respectively, at 284 K in 1000 mbar synthetic air. A third peak appearing in both chromatograms is either an impurity from DMSO or a derivative compound, or SO_4^{2-} from H_2SO_4, sampled as well from the oxidative systems, as was shown by some test experiments. Sulphate formation is certainly occurring, but no attempts at sulphate quantification have been made since the column which was used in the ion chromatographic analysis also gives a response to a possible impurity in DMSO which appears as a peak at almost the same retention time as that from SO_4^{2-}.

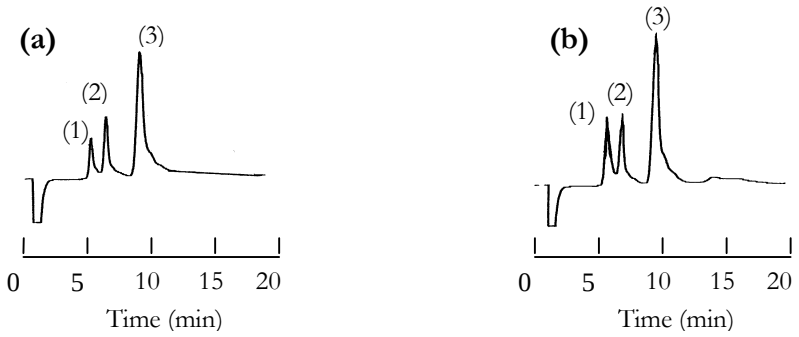

Figure 5.1: Example of chromatograms demonstrating the ion chromatographic measurements of (1) MSIA, (2) MSA, and (3) unidentified compound (an impurity from DMSO or SO_4^{2-} from H_2SO_4) from samples collected from the reactor during irradiation of DMSO/H_2O_2/synthetic air mixture (a) and DMSO/CH_3ONO/NO_x/synthetic air mixture (b) at 284 K and 1000 mbar synthetic air. Note the good resolution of the MSIA and MSA peaks.

Some tests of the ion chromatographic detection system have been performed by injection of 1) eluent (no response from the column), 2) a sample collected from pure synthetic air (no response from the column), 3) a sample from a DMSO/synthetic air mixture (appearance of a peak with t_R = *9.65* min), 4) a sample from a DMSO/H_2O_2/synthetic air mixture (appearance of a peak with t_R = *9.71* min), and also by 5) injections of standard solutions of $CH_3S(O)O^-$ (characteristic t_R = *6.23* min for the conditions employed for IC operation), $CH_3S(O)_2O^-$ (characteristic t_R = *7.05* min for the conditions employed for IC operation), SO_4^{2-} (characteristic t_R = *9.72* min for the conditions employed for IC operation) and water solution of pure DMSO (appearance of a peak with t_R = *9.69* min). These tests have been performed in order to show that the peaks attributed to the $CH_3S(O)O^-$ and $CH_3S(O)_2O^-$ anions were not affected by experimental artefacts and also to test if the column gives a response to possible impurities in DMSO (all chromatograms which have been recorded in such tests are presented in Appendix A).

During the ion chromatographic analysis some problems were encountered. A possible problem in the quantification of both MSIA and MSA acids is formation of these compounds in liquid phase reactions between hydrogen peroxide and DMSO on the surface of the sampling lines and also U-tube trap. However, investigations of the oxidation of DMSO by hydrogen peroxide in the liquid phase at temperatures between 4 and 30°C (DOMAC, 2000) let us to believe that the measurements are not affected by contributions from the liquid phase. In these studies a marked decay of DMSO in samples kept at 30°C compared with samples kept at 4°C was observed, and the decay of DMSO in the presence of hydrogen peroxide (for samples analysed for 30°C) was found to be about 1 to 2 orders of magnitude higher than that observed during the experiments performed without H_2O_2 addition.

It was also observed that dimethyl sulphoxide oxidation in aqueous solution is dependent on the H_2O_2 concentration and DMSO was found to be stable at pH = 1 (in the temperature range of 4° - 30° C) for a period up to one week (DOMAC, 2000). In the present study the two glass cryogenic U-tube traps were immersed in an ethanol-liquid nitrogen bath (-112 °C). The low temperature ensured that all compounds which passed through the trap are condensed on the walls of the tube.

Considering the observations from the work reported in DOMAC 2000, correlated with the behaviour of DMSO in aqueous phase solution, and because of the low temperature used in the sampling procedure it can be concluded that during Milli – Q water addition for dissolving and transferring sampled material only insignificant quantities of sampled DMSO undergo reaction in the liquid phase to MSIA and MSA. In order to minimise such problems, for all experiments, samples were analysed within a 4 - 5 h time frame after collection by ion chromatography.

The yields of $CH_3S(O)O^-$ and $CH_3S(O)_2O^-$ anions for all measurements performed at a temperature of 284 K using the samples collected from the DMSO/H_2O_2/synthetic air photo-irradiated mixture and DMSO/CH_3ONO/NO_x/synthetic air photo-irradiated mixture are presented in Tables 5.1 and 5.2, respectively.

Test experiments showed that when the samples were collected at the end of the irradiation period, the measured yields of both methane sulphinic and methane sulphonic acid were much lower than those obtained in experiments when the samples were collected during the irradiation. Therefore, all experiments aimed at MSIA and MSA identification and quantification by IC were performed with continuous sampling during irradiation. Since the reaction system was probed continuously, the values in Tables 5.1 and 5.2 represent integral yield values for the time period of the experiment.

The results presented in Tables 5.1 and 5.2 consists of two set of experiments: experiments where the quantification of methane sulphinic and methane sulphonic acid could be affected by DMSO photo-oxidation in the liquid phase (sampling system not protected against light) and experiments where the quantification of both acids was performed under dark conditions (*i.e.* the sampling system was protected against light; in this case all the sampling line was covered by aluminium foil to prevent possible photo-oxidative process in the sampled material).

From the results presented in Tables 5.1 and 5.2 it is clear that the measured yields of MSIA are very high in both photo-oxidative systems. The values obtained when the collection system is protected against UV light are somewhat smaller than when the system is not protected. The measured yields of MSA are much lower than the measured yields of the MSIA and are somewhat larger than the quantities measured in the gas phase using long path FT-IR spectroscopy (Paragraph 5.1.2).

Table 5.1: Ion chromatographic analysis of $CH_3S(O)O^-$ and $CH_3S(O)_2O^-$ anions from samples collected from the oxidation of DMSO in 1000 mbar synthetic air at 284 K under NO_x free conditions.

Temperature	System	Volume L	$CH_3S(O)O^-$		$CH_3S(O)_2O^-$	
			(ppm)	(% S)	(ppm)	(% S)
284 K	Not protected against $h\nu$	4.52	0.631	99.97	0.139	22.54
		4.71	0.536	98.69	0.115	22.23
		4.95	0.586	99.53	0.140	23.79
	Protected against $h\nu$	4.05	0.408	86.91	0.049	10.36
		4.81	0.457	84.51	0.076	14.15
		4.82	0.466	89.19	0.041	7.83

Table 5.2: Ion chromatographic analysis of $CH_3S(O)O^-$ and $CH_3S(O)_2O^-$ anions from samples collected from the oxidation of DMSO in 1000 mbar synthetic air at 284 K in systems containing different initial concentrations of NO_x.

Temperature	System	Volume	NO	NO_2	$CH_3S(O)O^-$		$CH_3S(O_2)O^-$	
		(L)	(ppb)	(ppb)	(ppm)	(% S)	(ppm)	(% S)
284 K	Not protected against $h\nu$	4.56	961	61	0.434	92.22	0.076	16.14
		4.82	2046	156	0.878	99.23	0.195	22.04
	Protected against $h\nu$	5.36	932	85	0.317	79.89	0.046	11.61
		4.81	1771	123	0.334	84.38	0.061	15.51

5.1.2 Identification of products formed in the gas-phase by FT-IR

5.1.2.1 Products identified in the photo-oxidation of DMSO in the absence of NO_x

Plots of the measured yield-time profiles for all the sulphur-containing products observed from the ·OH radical initiated oxidation of DMSO in a NO_x free system as a function of the different temperatures are shown in Figure 5.2a-c. The yields of the products shown in Figure 5.2a-c are not corrected for secondary loss processes such as reaction with ·OH or wall loss. The maxim of the observed yields of all the sulphur-containing products formed in the ·OH radical initiated oxidation of DMSO in the gas phase are listed in Table 5.3.

From Figure 5.2a-c and Table 5.3, it is clear that the observed yields of all the identified products increase with increasing temperature at a constant partial pressure of O_2 of 200 mbar. It is also evident that the individual product formation yields as well as the overall sulphur balance are strongly dependent on the temperature conditions employed in the experiments.

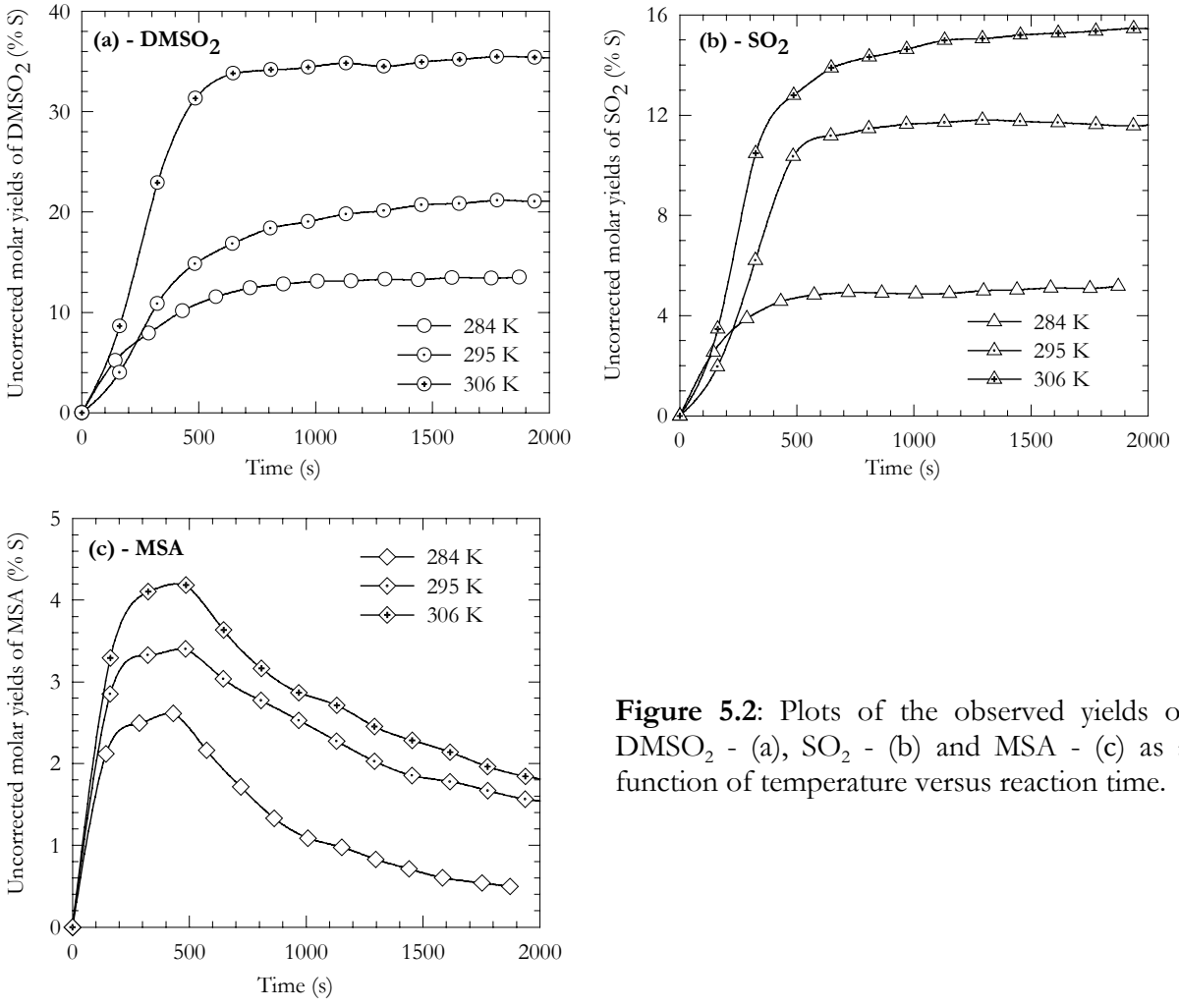

Figure 5.2: Plots of the observed yields of $DMSO_2$ - (a), SO_2 - (b) and MSA - (c) as a function of temperature versus reaction time.

Table 5.3: Observed yields of the products formed in the reaction of ·OH radicals with DMSO in 1000 mbar synthetic air as a function of temperature.

Temperature (K)	Observed yields of the products (% S)			Total (% S)
	$DMSO_2$	SO_2	MSA	
284	13.52 ± 2.26	4.82 ± 0.98	2.64 ± 0.56	20.98 ± 2.52
295	20.71 ± 3.53	11.81 ± 2.25	3.43 ± 0.71	35.95 ±4.25
306	34.53 ± 4.23	15.94 ± 2.53	4.25 ± 0.89	54.62 ± 4.99

The shape of the yield/time profiles observed in Figure 5.2a-c confirms that $DMSO_2$ and SO_2 are not main primary products of the oxidation of DMSO. The yields of $DMSO_2$ were found to be highly variable, generally, above 13 % S at 284 K and above 34 % S at 306 K (Figure 5.2a and Table 5.3). The yields of gas phase MSA were very low, between 2.5 and 4.5 % S (Figure 5.2c and Table 5.3). The highest yield value of MSA formation in the gas phase was obtained at the highest temperature but this may just reflect the higher vapour pressure of MSA at the highest temperature (as was also discussed in Chapter 3, Paragraphs 3.1.1 and 3.2.4). Formation of MSA in the oxidation of DMSO by ·OH radicals was also analysed by ion chromatography. This analysis gives information about MSA in both the gas and aerosol phase.

The response of the SO_2 yields to the variation of the temperature (as can be observed in Figure 5.2b) suggests that this compound is probably formed in secondary reactions of the primary product resulting from the gas phase oxidation of DMSO. In order to obtain the "exact" formation yields of SO_2 its measured concentration has been corrected for secondary ·OH radical reaction and also loss to the walls using the mathematical procedure outlined in Paragraph 2.3, Chapter 2. In order to calculate the rate constant k_1 for reaction of DMSO with ·OH radical, the Arrhenius expression $10^{-11.2\pm0.7}$ exp(800 ± 540/T) cm^3 $molecule^{-1}$ s^{-1} from Hynes and Wine (1996) was used. First order walls loss rates for DMSO of 5 x 10^{-5} s^{-1} at 284 K and 1 x 10^{-4} s^{-1} at 295 and 306 K, determined from experiments in the dark, were used in the calculations. The other rate constants used for the corrections, ($k_{2(SO2 + \cdot OH)}$ and $k_{3(wall\ loss)}$), are the same as those given in Chapter 2, Paragraph 2.3. Figure 5.3 shows the plots of the SO_2 concentration corrected for reaction with ·OH radicals and wall loss, versus the amount of DMSO consumed, (Δ[DMSO]), for each temperature. From the slope of the lines the true formation yields of SO_2 were determined. The formation yields of SO_2 and the estimated fractions of SO_2 oxidised by ·OH radicals to gas phase H_2SO_4 as a function of temperature are collected in Table 5.4. The errors quoted in the table are the 2σ random scatter in the data plots (Figure 5.3) and reflect the extent of the measurement errors in SO_2 and DMSO concentrations using FT-IR spectroscopy.

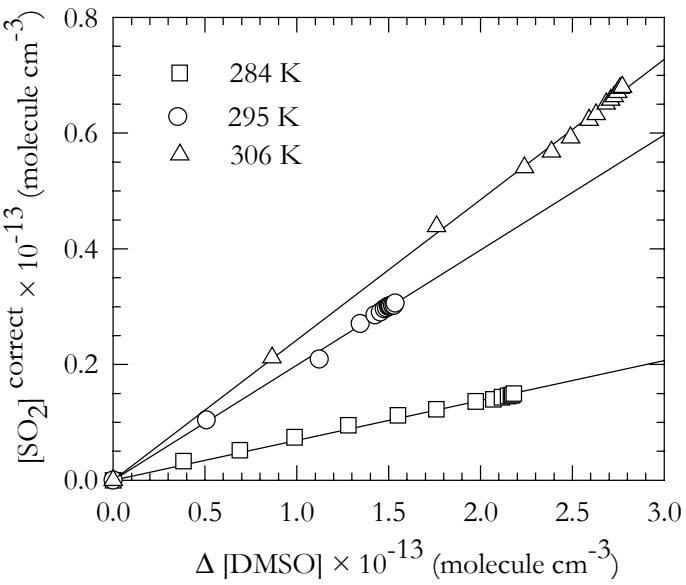

Figure 5.3: Plot of the SO_2 concentration (corrected for reaction with ·OH radicals and loss to the wall) versus the consumption of DMSO at 284, 295 and 306 K.

Table 5.4: Corrected yields of SO_2 and contribution of SO_2 to the production of H_2SO_4 in the ·OH + DMSO reaction at 1000 mbar synthetic air as a function of temperature.

Temperature (K)	Corrected SO_2 yields (% molar yield)	Estimated molar yields of H_2SO_4 (g) (% molar yield)
284	6.49 ± 1.52	1.15 ± 0.33
295	19.91 ± 3.13	2.39 ± 0.58
306	24.25 ± 3.89	3.13 ± 0.65

5.1.2.2 Products identified in the photo-oxidation of DMSO in the presence of NO_x

The plots of the measured yield-time profiles for all the sulphur-containing products observed in the gas phase oxidation of dimethyl sulphoxide by ·OH radicals at different temperatures and initial NO_x concentrations are shown in Figure 5.4a-d. The yields of the products shown in Figure 5.4a-d were not corrected for secondary loss processes such as further reaction with ·OH radicals or wall loss. The maximum observed yields of the all sulphur-containing products are listed in Table 5.5.

From Figure 5.4a-d and Table 5.5 it is clear that the observed yields of all the identified products decrease with increasing temperature at a constant partial pressure of O_2 of 200 mbar. From the results presented in Table 5.5 we see that the individual product formation yields as well as the overall sulphur balances strongly depend on both temperature and the NO_x initial concentration.

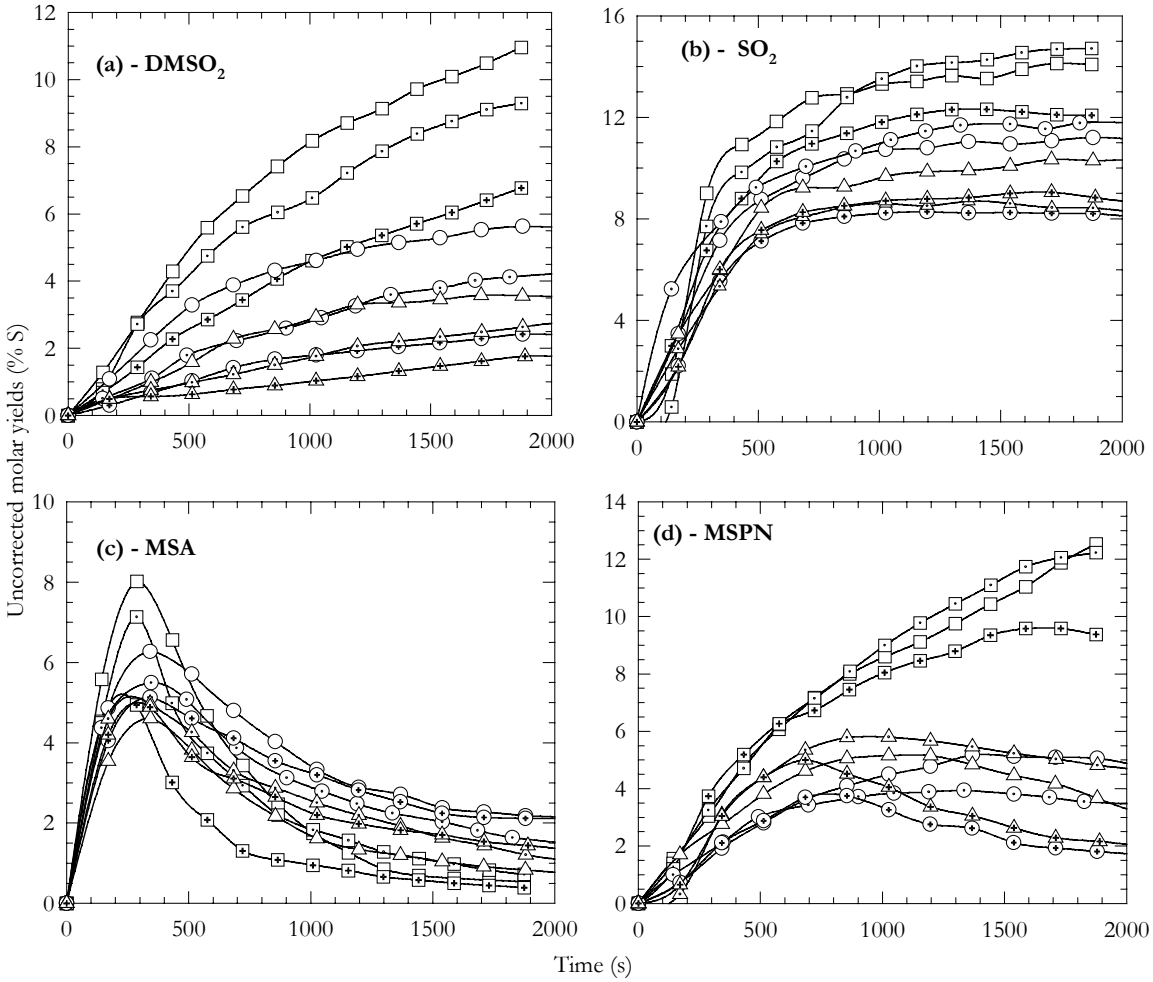

Figure 5.4: Plots of the yields of $DMSO_2$ - (a), SO_2 - (b), MSA - (c) and MSPN - (d) as a function of temperature (284, 295 and 306 K) and initial NO_x concentration versus reaction time. Variation of NO_x concentration is in the range: □ - 284 K (460 ppb NO + 54 ppb NO_2); ⊡ - 284 K (746 ppb NO + 90 ppb NO_2); ⊞ - 284 K (1471 ppb NO + 145 ppb NO_2);○ - 295 K (458 ppb NO + 65 ppb NO_2); ⊙ - 295 K (786 ppb NO + 79 ppb NO_2); ⊕ - 295 K (1563 ppb NO + 84 ppb NO_2); △ - 306 K (507 ppb NO + 18 ppb NO_2); ◬ - 306 K (964 ppb NO + 51 ppb NO_2); ⧋ - 306 K (1468 ppb NO + 86 ppb NO_2);

Table 5.5: Observed yields of the products formed in the reaction of ·OH radicals with DMSO in 1000 mbar synthetic air as a function of temperature and initial NO_x concentration.

Temperature (K)	NO (ppb)	NO_2 (ppb)	Observed yields of the products (% S)				Total
			$DMSO_2$	SO_2	MSA	MSPN	
284	460	54	10.9 ± 1.6	14.0 ± 2.2	8.1 ± 1.2	12.5 ± 1.9	45.5 ± 3.4
	746	90	9.2 ± 1.5	14.7 ± 2.4	7.1 ± 1.1	12.2 ± 1.7	43.3 ± 3.8
	1471	145	6.7 ± 1.2	12.2 ± 1.6	4.9 ± 0.95	9.5 ± 1.5	33.3 ± 2.8
295	458	65	5.5 ± 0.8	11.0 ± 1.8	6.2 ± 0.9	5.1 ± 0.7	28.0 ± 2.5
	786	79	4.1 ± 0.8	11.7 ± 1.5	5.4 ± 1.1	3.9 ± 0.5	25.3 ± 1.9
	1563	84	2.5 ± 0.5	8.2 ± 1.4	5.1 ± 0.8	3.7 ± 0.7	19.6 ± 2.0
306	507	18	3.5 ± 0.6	10.3 ± 1.2	4.6 ± 0.6	5.8 ± 0.9	24.2 ± 1.5
	964	51	2.5 ± 0.4	8.6 ± 1.3	4.8 ± 0.8	5.1 ± 0.8	21.1 ± 1.9
	1468	86	1.7 ± 0.3	8.9 ± 1.5	5.9 ± 0.8	4.5 ± 0.7	21.2 ± 1.8

The $DMSO_2$ yield was found to be highly variable from one temperature to another and also to be dependent on the initial NO_x concentration (Figure 5.4a and Table 5.5). The yields of gas phase MSA (Figure 5.4c and Table 5.5) were found to be higher compared with the yields determined in a NO_x free system and vary between 4.61 and 8.01 % S with very marginal differences between the results at 295 and 306 K. Formation of methane sulphonyl peroxy nitrate ($CH_3S(O)_2OONO_2$) was observed and its molar formation yield was found to decrease with increasing temperature.

The measured SO_2 concentration was corrected for the further reaction with ·OH radical and wall loss in order to obtain the "exact" formation yields. Figure 5.5 shows the plots of SO_2 concentration corrected for reaction with ·OH radical and wall loss, versus the amount of DMSO consumed, Δ[DMSO]. From the slope of the linear plot, the true formation yields of SO_2 have been determined. The formation yields of SO_2 and the estimated fraction of SO_2 oxidised by ·OH radicals to gas phase H_2SO_4 as a function of temperature are collected in Table 5.6.

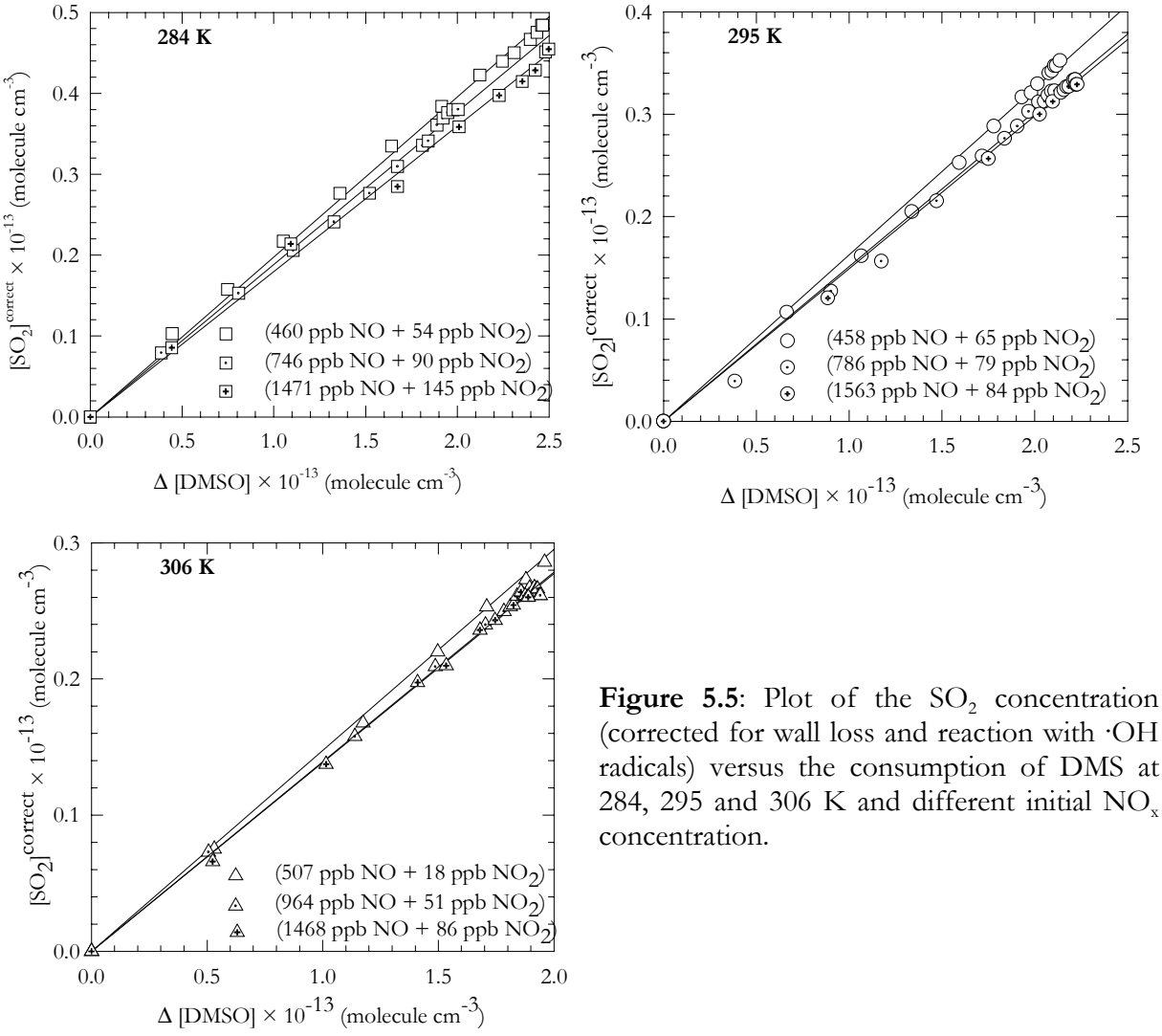

Figure 5.5: Plot of the SO_2 concentration (corrected for wall loss and reaction with ·OH radicals) versus the consumption of DMS at 284, 295 and 306 K and different initial NO_x concentration.

Table 5.6: Corrected yields of SO_2 and the estimated fraction of SO_2 oxidised by ·OH radicals to gas phase H_2SO_4 in the reaction of DMSO with ·OH radicals in 1000 mbar synthetic air as a function of temperature.

Temperature (K)	NO (ppb)	NO_2 (ppb)	Corrected SO_2 yields (% molar yield)	Estimated molar yields of H_2SO_4 (g) (% molar yield)
284	460	54	19.78 ± 2.84	3.10 ± 0.71
	746	90	18.86 ± 2.81	2.93 ± 0.64
	1471	145	17.98 ± 2.63	2.72 ± 0.53
295	458	65	16.27 ± 2.52	1.41 ± 0.31
	786	79	15.14 ± 2.11	1.26 ± 0.23
	1563	84	14.92 ± 2.34	1.28 ± 0.24
306	507	18	14.76 ± 2.14	0.65 ± 0.12
	964	51	13.88 ± 1.93	0.52 ± 0.11
	1468	86	13.93 ± 2.06	0.66 ± 0.14

5.2 Discussion

5.2.1 Formation of methane sulphinic acid (MSIA)

Yin et al. (1990a) were the first to propose that methane sulphinic acid is produced in the gas phase oxidation of DMS by ·OH radicals. According to their scheme, DMS is partially oxidised to DMSO and then further to MSIA.

In 1998, Urbanski et al. used time-resolved tunable diode laser spectroscopic detection of CH_3, CH_4 and SO_2 coupled with 248 nm laser flash photolysis of H_2O_2 in the presence of $CH_3S(O)CH_3$ to investigate the mechanism and kinetics of the ·OH + DMSO reaction at 298 K. In their study a rate coefficient $k_{(\cdot OH+DMSO)}$ = (8.7 ± 1.6) x 10^{-11} cm^3 $molecule^{-1}$ s^{-1} was reported and the CH_3· yield from the ·OH + DMSO reaction was found to be 0.98 ± 0.12 in the absence of O_2. The observed unit yield of CH_3· and nearly zero yields of CH_4 and SO_2 allowed them to conclude that the dominant ·OH + DMSO reaction channel was ·OH radical addition to $CH_3S(O)CH_3$ followed by very rapid CH_3S·$(O)(OH)CH_3$ (DMSO-OH) adduct decomposition to CH_3· and $CH_3S(O)(OH)$. They did not directly observed $CH_3S(O)(OH)$ but they assumed that $CH_3S(O)(OH)$ was the CH_3· co-product by an elimination process.

The ·OH + DMSO reaction mechanism proposed by Urbanski et al. (1998) appeared to be in contradiction with that of Sørensen et al. (1996). In the study performed by Sørensen et al. (1996) a MSIA yield of 1.5 ± 1.1 % was measured from the oxidation of DMS by ·OH, while in the ·OH initiated oxidation of DMSO they obtained a MSIA yield smaller than 0.3 %.

Urbanski et al. (1998) concluded that observation of a relatively high yield of MSIA in the oxidation of DMS in the study of Sørensen et al. (1996), but not in the oxidation of DMSO, is incompatible with their observations. Until this study, the explanation for the apparent discrepancy between the results of Urbanski et al. (1998) and Sørensen et al. (1996) has remained unclear.

In the present work high and similar yields of methane sulphinic acid have been observed in DMSO photo-oxidative systems, both with and without NO_x, showing that its formation is independent of reaction conditions. The measured MSIA yields also did not depend on whether the sampling line was protected or not. The results obtained in the present study strongly support the suggestion from the absolute study of Urbanski et al. (1998) that MSIA is a major primary product of the oxidation of DMSO by ·OH radicals through the addition channel:

$$CH_3S(O)CH_3 + \cdot OH \rightarrow CH_3S\cdot(O)(OH)CH_3 \xrightarrow{\text{thermal decomposition}} CH_3S(O)OH + CH_3\cdot \quad \text{(R 5.1)}$$

As in the study on DMS, the results do presently not allow an exact determination of the formation yield of MSIA. However, from a simple consideration of the magnitude of the measured MSIA yield, the fraction of the ·OH + DMSO reaction leading to MSIA formation must be quite considerable. This is in line with the recent absolute study of Urbanski et al. (1998) as was already mentioned.

In summary, using ion chromatography as the analytical tool for quantification of MSIA, it has been shown that this compound is the primary product of the ·OH radical initiated oxidation of DMSO. This is supported by the pronounced delays in the formation of all the other sulphur-containing products observed in the gas phase ($DMSO_2$, SO_2, MSA, MSPN) by using long-path FT-IR spectroscopy. It is concluded that formation of these products can be attributed to MSIA secondary chemistry initiated by the ·OH radicals (see also the discussion in Paragraphs 5.2.2 and 5.2.3).

5.2.2 Product formation from DMSO photo-oxidation in the absence of NO_x

The ·OH radical initiated oxidation of dimethyl sulphoxide can proceed in a manner similar to that of dimethyl sulphide, *i.e.* two reaction channels are possible, one forming a DMSO-OH adduct by addition of ·OH radicals to the sulphur atom of DMSO, and another resulting in the formation of a $CH_3S(O)CH_2\cdot$ radical by abstraction of hydrogen atom from the CH_3 group.

The study of Hynes and Wine (1996) has shown that the rate constant of the reaction between ·OH radicals and DMSO increases with decrease of temperature. This indicates that in the ·OH radical initiated oxidation of DMSO the addition reaction channel must be the major channel. The rate of the abstraction channel is expected to be close to k_{abst} from ·OH + DMS.

The idea of Yin et al. (1990a) who suggested, based on smog chamber studies, bond dissociation energy (BDE) calculations, and an analogy with liquid-phase chemistry, that the ·OH + DMSO reaction occurs mainly *via* ·OH radical addition to the sulphur atom of DMSO followed by C-S bond cleavage (in contrast to the ·OH + DMS reaction which is characterised by the reversible adduct formation) was confirmed by the study of Urbanski et al. (1998). In their study, Urbanski et *al*. (1998) found nearly unit yield of CH_3· from ·OH + DMSO in the absence of O_2 which implies a similarly high yield of the expected co-product, $CH_3S(O)(OH)$. They concluded that in the absence of oxygen the dominant ·OH + DMSO reaction channel is ·OH radical addition to DMSO, followed by the rapid decomposition of DMSO-OH adduct to CH_3· and methane sulphinic acid. However, in the presence of O_2, it is possible that reaction between molecular oxygen and the DMSO-OH adduct can compete with the decomposition of the adduct to CH_3· and MSIA. Preliminary experiments performed by the same authors and aimed at measuring the yield of CH_3OO· from the ·OH + DMSO reaction in the presence of different concentration of oxygen (3 -218 Torr) led them to the conclusion that CH_3· elimination is the dominant reaction channel even in the presence of atmospheric levels of oxygen. However, the results obtained were not considered sufficiently precise to rule out a minor but significant DMSO-OH + O_2 reaction under atmospheric conditions. New theoretical calculations as well indicate that similar to the reaction of DMS-OH adduct with O_2, the strong S-OH bond in the DMSO-OH adduct could assist the H atom abstraction by O_2 and oxidisation of DMSO to $DMSO_2$ (Wang and Zhang, 2001). Hence, a possible competition between adduct decomposition to CH_3· and MSIA and the DMSO-OH + O_2 reaction has to be taken into account when considering $DMSO_2$ production in the ·OH radical initiated oxidation of DMSO.

Formation of SO_2 and MSA in the photo-oxidation of DMSO can be explained by the further ·OH radical initiated oxidation of the primary product. On the basis of the estimated BDEs and analogy to liquid-phase chemistry, Yin et al. (1990a), have suggested that the ·OH radical can react with MSIA by the abstraction of the hydroxyl H atom, producing the $CH_3S·(O)_2$ radical. Decomposition of $CH_3S·(O)_2$ would lead to the formation of SO_2, while further reaction of this species may generate methane sulphonic acid ($CH_3S(O)_2(OH)$). Some chamber studies (Barnes et al., 1989; Sørensen et al., 1996) demonstrated that the ·OH radical initiated oxidation of DMSO produces SO_2 and room temperature LIF-mass spectrometry studies performed at

low-pressure (Ray et al., 1996; Kukui et al., 2000) demonstrated that the decomposition of $CH_3S{\cdot}(O)_2$ to SO_2 and $CH_3{\cdot}$ occurs under such conditions. These studies lend a strong support to the idea that the ·OH + DMSO reaction can lead to SO_2 production through the ·OH initiated oxidation of MSIA. Formation of gas phase MSA was observed also in the ·OH initiated oxidation of DMS in both free NO_x conditions and in the presence of NO_x (Chapters 3 and 4, Paragraphs 3.2.4, 4.2.3). The behaviour of the gas phase MSA concentrations with the change of temperature is consistent with formation of MSIA in the ·OH + DMSO reaction and the subsequent reaction of MSIA with ·OH leading, in part, to MSA production. The efficiency with which DMSO oxidation can lead to MSA and SO_2 production will depend, hence, on the rate of MSIA formation, rate of MSIA oxidation by ·OH radicals and also on the ambient aerosol surface area because MSIA is also susceptible to physical removal. Taking this into account, the results of the present study are consistent with the ·OH radical initiated oxidation of MSIA being both the source of MSA and a contributor to SO_2 production. Considering MSIA as a primary product of the ·OH radical initiated oxidation of DMSO and assuming that SO_2 and MSA are formed *via* secondary reactions involving oxidation of MSIA by ·OH radicals, the following set of reactions can be responsible for SO_2 and MSA production:

$$CH_3S(O)(OH) + {\cdot}OH \rightarrow CH_3S{\cdot}(O)_2 + H_2O \quad \text{(R 5.2)}$$

$$CH_3S{\cdot}(O)_2 \rightarrow SO_2 + CH_3{\cdot} \quad \text{(R 5.3)}$$

$$CH_3S{\cdot}(O)_2 + O_2 \rightarrow CH_3S(O)_2OO{\cdot} \quad \text{(R 5.4)}$$

$$CH_3S(O)_2OO{\cdot} + CH_3S{\cdot}(O)_{x;\,x=0\text{-}2} \rightarrow CH_3S(O)_2O{\cdot} + CH_3S{\cdot}(O)_{x;\,x=1\text{-}3} \quad \text{(R 5.5)}$$

$$CH_3S(O)_2O{\cdot} + RH \rightarrow CH_3S(O)_2(OH) + R{\cdot}. \quad \text{(R 5.6)}$$

The abstraction channel in the ·OH radical initiated oxidation of DMSO should be of minor importance since its rate constant is expected to be close to that of ·OH + DMS reaction. Hynes and Wine (1996) found experimental indications that the channel involving H-atom abstraction does not proceed at a significant rate. However, if it occurs, further reaction of the $CH_3S(O)CH_2{\cdot}$ radical, formed in the abstraction channel, with molecular oxygen can lead to SO_2.

5.2.3 Product formation from DMSO photo-oxidation in the presence of NO_x

The yield/time behaviour of $DMSO_2$, SO_2, MSA and MSPN formed in the gas phase oxidation of DMSO by ·OH radicals in the presence of NO_x clearly indicates that they are not the main primary products. Therefore, in the presence of NO_x, like in the NO_x free conditions, the adduct

formed by the ·OH radical addition to DMSO probably mainly decomposes to $CH_3S(O)(OH)$ and CH_3· radical and, hence, methane sulphinic acid is the key species whose further oxidation leads to the formation of other observed sulphur-containing products.

From the response of the $DMSO_2$ yields to the initial NO concentration at different temperatures it can be concluded that this compound is probably formed in reactions between peroxy radicals (RO_2·) and DMSO. The observed behaviour of the SO_2 yields suggests that it is also formed in secondary reactions of the primary product (probably MSIA). Formation of MSA and MSPN in the presence of NO_x can be explained by the further ·OH radical initiated oxidation of MSIA according to following scheme:

$CH_3S(O)(OH) + \cdot OH \rightarrow CH_3S\cdot(O)_2 + H_2O$ (R 5.2)

$CH_3S\cdot(O)_2 \rightarrow SO_2 + CH_3\cdot$ (R 5.3)

$CH_3S\cdot(O)_2 + O_2 + M \rightarrow CH_3S(O)_2(OO\cdot) + M$ (R 5.4)

$CH_3S(O)_2(OO\cdot) + NO_2 + M \leftrightarrow CH_3S(O)_2OONO_2 + M$ (R 5.7)

$CH_3S(O)_2(OO\cdot) + NO \rightarrow CH_3S(O)_2O\cdot + NO_2$ (R 5.8)

$CH_3S(O)_2(OO\cdot) + CH_3S(O)_{x;\,x=0\text{-}2} \rightarrow CH_3S(O)_2O\cdot + CH_3S(O)_{x;\,x=1\text{-}3}$ (R 5.5)

$CH_3S(O)_2O\cdot + RH \rightarrow CH_3S(O)_2OH + R\cdot.$ (R 5.6)

The most obvious intermediate for SO_2 formation is the $CH_3S\cdot(O)_2$ radical, which can form SO_2 directly by breaking the C-S bond. The increase of temperature favours the decomposition of the $CH_3S\cdot(O)_2$ (R 5.3), while decreases of temperature promotes formation of the adduct with O_2 (R 5.4) owing to better stabilisation. In the presence of high NO_x concentrations the further addition of NO_2 to the peroxy adducts (R 5.7) will shift the equilibrium away from $CH_3S\cdot(O)_2$, decreasing the number of decomposition events and favouring formation of the reservoir of stable species such as methane sulphonyl peroxy nitrate. The reaction between NO and the $CH_3S(O)_2(OO\cdot)$ adduct (R 5.8) is the rate limiting step in the branching between $CH_3S(O)_2O\cdot$ formation and decomposition back to $CH_3S\cdot(O)_2$. The very low observed yields of SO_2 and their behaviour with respect to the change in temperature can be explained assuming that the $CH_3S\cdot(O)_2$ radical results mainly from the oxidation of MSIA.

Anyhow, the interpretation and understanding of the obtained results was even more complicated by the observation that the total sulphur mass balance decreases with increasing the temperature and initial NO_x concentration (Table 5.5). Formation of MSIA in a very high yield was observed in the ·OH radical initiated oxidation of DMSO in the presence of NO_x at 1000 mbar synthetic air and 284 K (Chapter 5, Paragraph 5.2). Unfortunately, no experiments aimed on the identification of the acid at 295 and 306 K have been performed. Anyhow, with the

increase of temperature, a lower yield of methane sulphinic acid and, hence, a higher yields of other sulphur-containing products are expected (due to the possible faster reaction of the acid with ·OH radicals and thermal instability). The decrease of the observed yields of all products identified from the photo-oxidation of DMSO in the presence of NO_x with increase of temperature strongly differs from the behaviour of the observed yields of the products formed from the oxidation of DMSO in a NO_x free system. In the latter case an increase of the observed yields was observed with increase of temperature. The only explanation for the different behaviour is the general assumption that the presence of NO_x in the oxidative system inhibits some reaction pathways.

5.3 Summary of results and conclusions

The present study provides evidence for the formation of MSIA from the ·OH radical initiated oxidation of DMSO in a very high yield both in the absence and in the presence of NO_x. The obtained high yields of MSIA strongly support the suggestion of Urbanski et al. (1998) that this compound is formed *via* the decomposition of OH-DMSO adduct to CH_3· and $CH_3S(O)(OH)$. Therefore, in the atmosphere the gas phase oxidation of DMSO will mainly result in the production of methane sulphinic acid as the primary product; its formation will be independent of NO_x (Figure 5.6).

Based on the results obtained in the present study in combination with observations from previous studies of DMSO oxidation, a general mechanism has been constructed for the oxidation of DMSO in a NO_x free system (Figure 5.7). Figure 5.8 shows the general mechanism of DMSO oxidation corresponding to the reaction system with NO_x present.

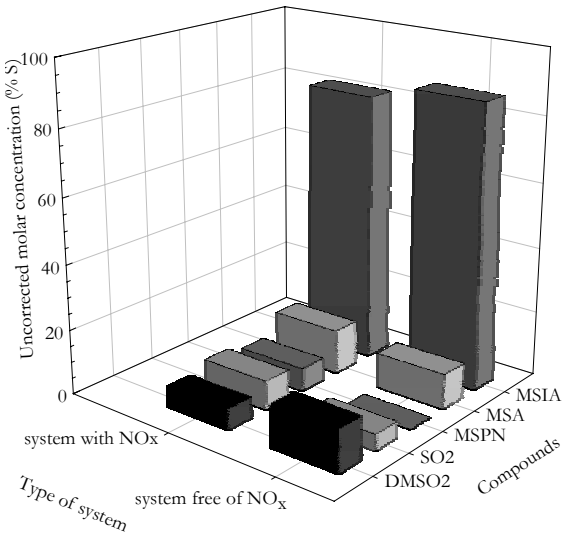

Figure 5.6: Concentration of products observed in the ·OH radical initiated oxidation of DMSO at 284 K and 1000 mbar synthetic air in the presence and absence of NO_x.

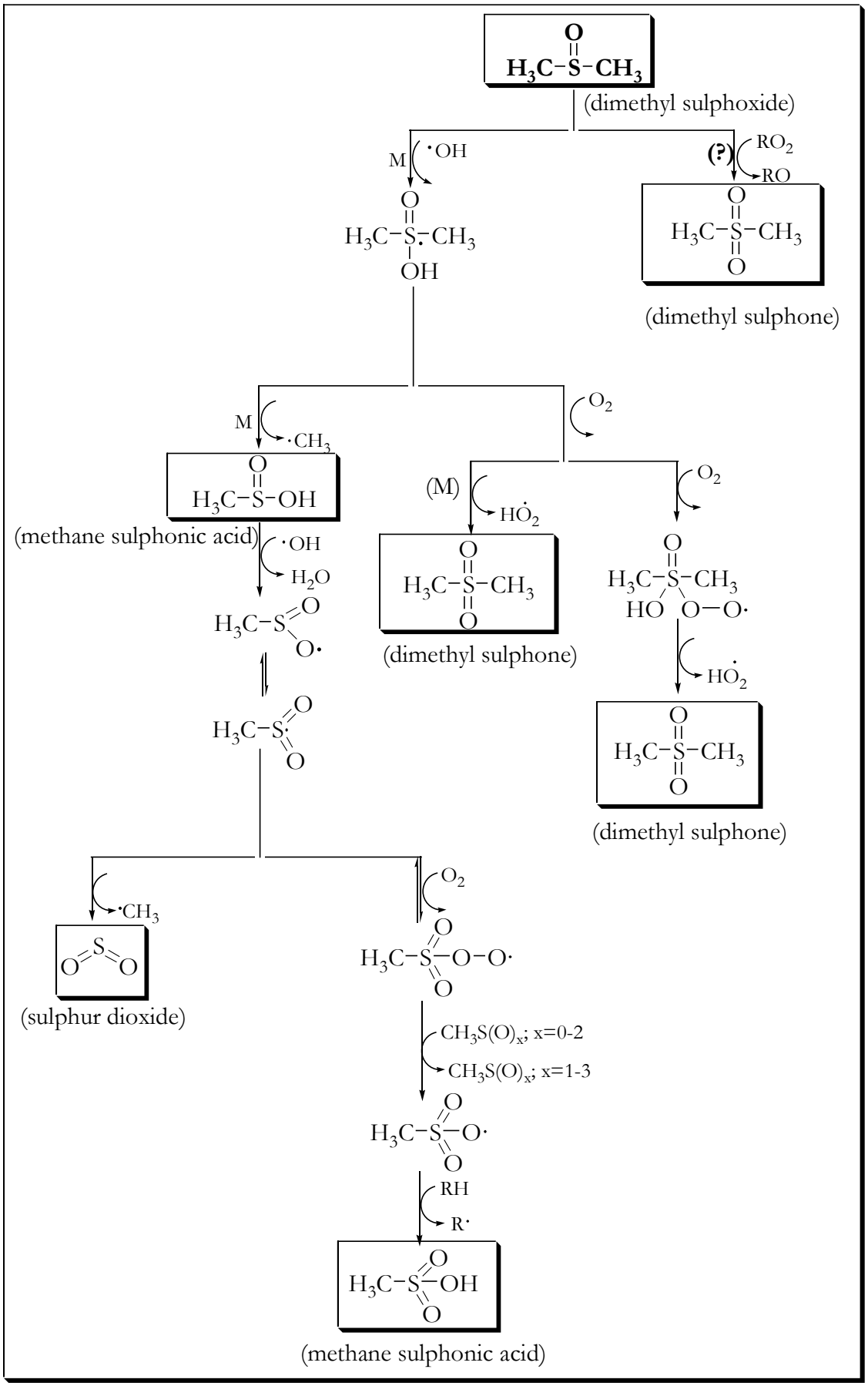

Figure 5.7: Mechanism of the oxidation of DMSO in NO_x free system.

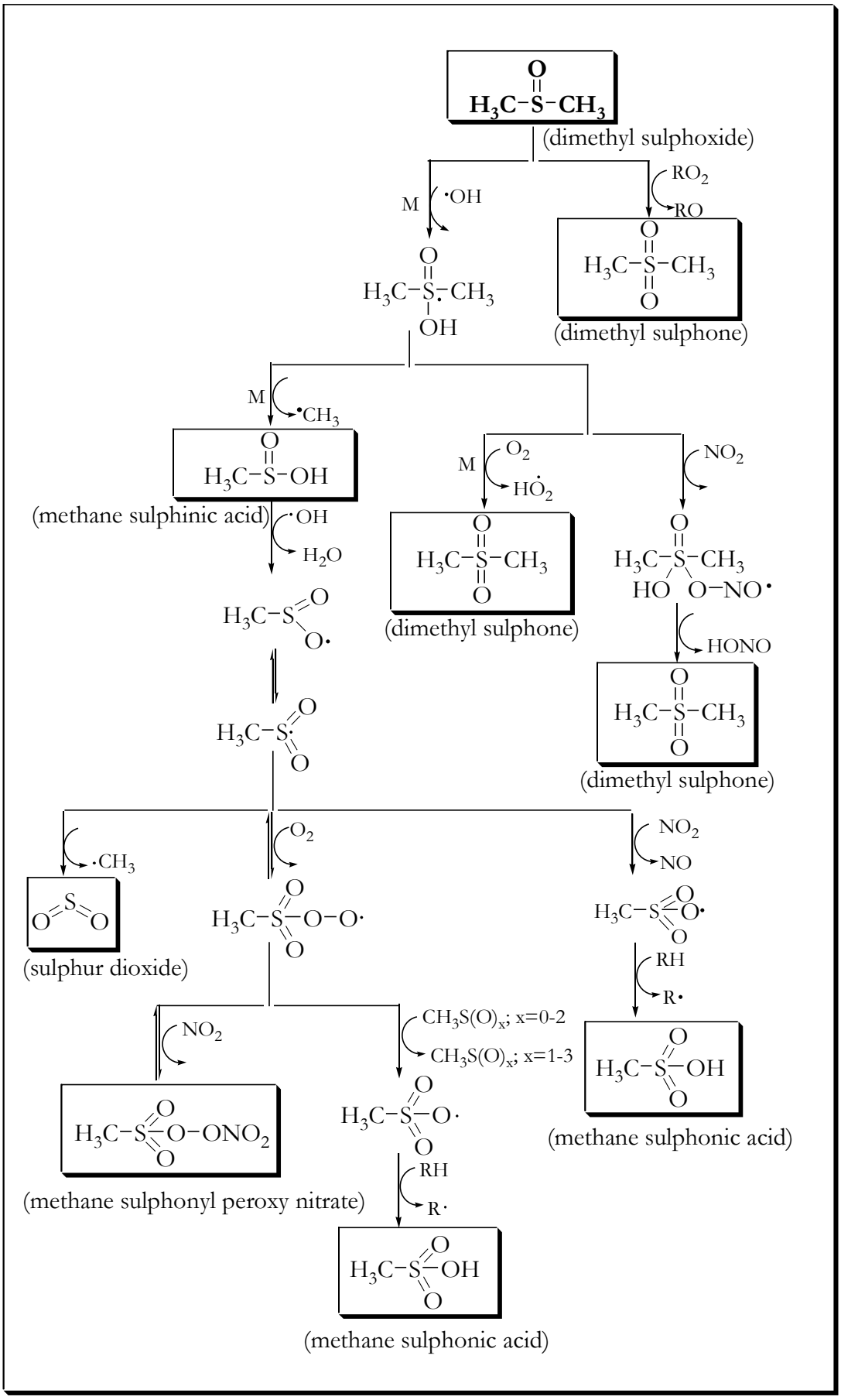

Figure 5.8: Mechanism of the oxidation of DMSO in a system containing NO_x.

The product analysis both in the absence and in the presence of NO_x also showed the formation of dimethyl sulphone ($CH_3S(O)_2CH_3$: $DMSO_2$), sulphur dioxide (SO_2), methane sulphonic acid ($CH_3S(O)_2OH$: MSA) and methane sulphonyl peroxy nitrate ($CH_3S(O)_2OONO_2$: MSPN). The formation of the above indicated sulphur-containing products in the gas phase oxidation of DMSO was found to be attributable mostly to ·OH radical initiated secondary reaction chemistry of the primary product of DMSO photo-oxidation, *i.e.* MSIA.

Methane sulphinic acid chemistry is, presently, not adequately represented in atmospheric chemical models. Possible reactions of this compound, such as oxidation by ·OH radicals to form SO_2 and MSA, formation of new particles or uptake by existing particles represent an important branch of the DMS oxidation process which must be taken into account in considerations of the chemistry of DMS and in currently assessing the contribution of DMS to CCN formation in the remote boundary layer. It is expected that the importance of the chemistry of MSIA in controlling the contribution of DMS to CCN formation will increase with the decrease of temperature, since the importance of the DMSO producing channel increases with decreasing temperature. At high latitudes where the oxygen dependent branch of the ·OH + DMS reaction dominates overall DMS reactivity and the product distribution will reflect high yields of DMSO the role of methane sulphinic acid chemistry will be also very important.

Chapter 6

General conclusions

In the present work detailed product analyses of the ·OH radical initiated oxidation of dimethyl sulphide and dimethyl sulphoxide have been performed. The studies allowed the quantification of the yields of important species produced in the oxidation of dimethyl sulphide and dimethyl sulphoxide over a wide range of conditions. Product distributions have been obtained for the first time as a function of temperature, partial pressure of oxygen and initial NO_x levels. The obtained results have led to a better knowledge of the dimethyl sulphide and dimethyl sulphoxide oxidation mechanisms, which is the basis for the understanding of the atmospheric processes controlling the contribution of dimethyl sulphide to particle formation and ultimately climate change.

It was found that dimethyl sulphoxide, sulphur dioxide and methane sulphinic acid were the major products of dimethyl sulphide oxidation. The main observations on dimethyl sulphoxide formation can be summarised as follows:

- Experiments in NO_x free systems at different temperatures and oxygen partial pressures proved that in the ·OH radical addition channel dimethyl sulphide is converted to dimethyl sulphoxide with nearly unit yield *via* reaction of a DMS-OH adduct with O_2 ($CH_3S{\cdot}(OH)CH_3 + O_2 \rightarrow CH_3S(O)CH_3 + HO_2{\cdot}$).
- The dimethyl sulphoxide yield values for 284 K (46.3 ± 5.0 % molar yield), 295 K (34.8 ± 7.6 % molar yield) and 306 K (24.4 ± 2.8 % molar yield) at 200 mbar O_2 have been found to be close to the estimated branching fractions of the addition pathway.

- The measured dimethyl sulphoxide yields shows that the importance of the channel producing dimethyl sulphoxide increases with decreasing temperature.
- Experiments at different initial NO_x concentrations showed that in the presence of NO_x the branching factor for dimethyl sulphoxide formation in the addition channel is less than unity. The branching ratio was found to decrease with increasing initial NO and to decrease with increasing temperature.
- The observed behaviour of dimethyl sulphoxide formation in systems containing NO_x supports the existence of a reaction sequence involving formation of a thermally unstable $CH_3S(OH)(OO\cdot)CH_3$ peroxy radical adduct and its subsequent reaction with NO ($CH_3S(OH)(OO\cdot)CH_3 + NO \rightarrow CH_3S(OH)(O\cdot)CH_3 + NO_2$).
- The existence of such reactions offers a plausible explanation for the difference in the dimethyl sulphoxide yields found between the systems with and without NO. Although a similar mechanism was proposed by Yin et al. (1990a), the results of the present study is the first direct experimental evidence of the importance of the reaction sequence.

Since sulphur dioxide is a precursor of sulphuric acid, its yield in the oxidation of dimethyl sulphide is a key parameter for assessing the capacity of dimethyl sulphide to produce new condensation nuclei. Some of the main observations from the present work about sulphur dioxide formation are:

- High overall molar formation yields of sulphur dioxide were obtained at a partial pressure of oxygen of 200 mbar (84.3 ± 6.5 % at 284 K; 95.0 ± 3.8 % at 295K and 99.0 ± 6.5 % at 306 K). This suggests that further oxidation of the products of both the ·OH + DMS addition and abstraction channels results in sulphur dioxide production under the NO_x free conditions employed in the present work.
- From investigations at different temperatures in the presence of NO_x it was established that the formation yield of sulphur dioxide decreases with increasing initial NO_x and this effect is most pronounced at lower temperatures. Since it is clear that sulphur dioxide is produced in a multi-step oxidation mechanism, its formation can be disturbed by NO_x at any stage involving $CH_3S\cdot(O)_x$ or $CH_3S\cdot(O)_xOO$ radicals by the formation of thermally unstable peroxy nitrate intermediates, *e.g.* $CH_3S\cdot(O)_2 + O_2 \rightarrow CH_3S(O)_2OO\cdot \overset{NO_2}{\longleftrightarrow} CH_3S(O)_2OONO_2$). A decrease in temperature and increase in NO_2 concentration, obviously, will favour formation of the peroxy nitrate.

The observation of relatively high yields of methane sulphinic acid in the oxidation of dimethyl sulphide indicated that the ·OH induced oxidation of dimethyl sulphoxide is an efficient source of the acidic species. To elucidate the role of dimethyl sulphoxide in the mechanism of dimethyl sulphide oxidation, a separate study of the ·OH radical initiated oxidation of dimethyl sulphoxide was undertaken. The main observations from the study are:

- A very high yield of methane sulphinic acid was found using a cryogenic trapping technique, which confirms the conclusion reached in a recent absolute study of Urbanski et al. (1998). In that study a near unit yield of the CH_3· radical was determined and, hence, a high yield of the co-product, methane sulphinic acid, was inferred ($CH_3S(O)CH_3 + \cdot OH \rightarrow CH_3S\cdot(O)(OH)CH_3 \xrightarrow{\text{thermaldecomposition}} CH_3S(O)OH + CH_3\cdot$).
- Formation of methane sulphinic acid in high and similar yields was observed in two different photo-oxidative systems: one free of NO_x (about 87 % S) and the other one containing NO_x (about 83 % S), indicating that its formation is independent of reaction conditions.
- The results support the conclusion that methane sulphinic acid is the main primary product of the ·OH radical initiated oxidation of dimethyl sulphoxide and that the formation of the other observed products (dimethyl sulphone, sulphur dioxide, methane sulphonic acid and methane sulphonyl peroxy nitrate) should be attributed to the secondary chemistry of methane sulphinic acid initiated either by the ·OH radicals or by peroxy compounds.

Methane sulphonic acid has been observed as a product of the ·OH radical initiated oxidation of dimethyl sulphide in photo-oxidative systems both with and without NO_x.

- Under NO_x free conditions, the determined levels of gas phase methane sulphonic acid were not very high and varied between 1 - 6 % molar yield.
- Since a part of methane sulphonic acid is taken up by aerosol, detailed information on the formation of methane sulphonic acid (gas + aerosol) in the oxidation system was obtained by using ion chromatography as an analytical tool. The methane sulphonic acid yields measured by this method were higher than the values measured in the gas phase.
- In the product study with different initial NO_x concentrations it was observed that the maximum yield of methane sulphonic acid increases with increasing initial NO concentrations and temperature. At temperatures of 284 and 295 K the maximum yield of methane sulphonic acid varied between 5 -10 %, while at 306 K it was much higher.

- The behaviour of methane sulphonic acid observed in the present study was found to be in accord with the supposition that NO and NO_2 promote formation of methane sulphonic acid via reactions involving species such as $CH_3S\cdot$, $CH_3S\cdot(O)$, $CH_3S\cdot(O)_2$.
- The direct observation of formation of methane sulphonic acid in the gas phase oxidation of dimethyl sulphoxide obtained in the present study is a clear indication that, in contrast to previous notions, this compound is formed not only in the abstraction channel, but also in the addition route of the ·OH radical initiated oxidation of dimethyl sulphide.

Another group of products, formed in smaller quantities, included dimethyl sulphone, carbonyl sulphide and methane thiol formate.

- In the NO_x free studies formation of dimethyl sulphone could be attributed either to reactions between peroxy-peroxy radicals with formation of the $CH_3S(OH)(O\cdot)CH_3$ alkoxy radical or *via* reactions of dimethyl sulphoxide. In the ·OH radical initiated oxidation of dimethyl sulphide in the presence of NO_x, direct evidence was found for the formation of dimethyl sulphone *via* the reaction of the $CH_3S(OH)(O\cdot)CH_3$ with molecular oxygen ($CH_3S(OH)(O\cdot)CH_3 + O_2 \rightarrow CH_3S(O)_2CH_3 + HO_2\cdot$).
- The yield of carbonyl sulphide at 295 K and oxygen partial pressure of 200 mbar (0.7 % molar yield) was found to be similar to that previously reported (Barnes et al., 1994; Barnes et al., 1996). In product studies in systems free of NO_x both the temperature and oxygen partial pressure trends of carbonyl sulphide and methane thiol formate have been found to be anti-correlated, which let us to conclude that photolysis of methane thiol formate is definitely not the only source of the formation of carbonyl sulphide. In the study performed in the presence of NO_x, a very strong suppression of the carbonyl sulphide formation yield with increase of the initial NO concentration was found (to ~ 0.2 % molar yield).
- Formation of methane thiol formate was observed in the NO_x free product studies, which can be due only to the abstraction channel of the primary reaction between dimethyl sulphide and ·OH radicals. The effects observed upon changing oxygen partial pressure and temperature argue against the assumption that the direct formation of this compound from the self reaction of $CH_3SCH_2OO\cdot$ radicals is the only source of methane thiol formate. The observed trends of methane thiol formate at different temperature and oxygen partial pressure correspond to its production, at least in part, in the reaction of the $CH_3SCH_2O\cdot$ radicals with oxygen. Methane thiol formate was not observed in the presence of high levels of NO_x.

The present work, which aimed to study in detail the yields of products such as dimethyl sulphoxide and sulphur dioxide obtained in the ·OH radical initiated oxidation of dimethyl sulphide and their dependence on parameters such as temperature, oxygen partial pressure and NO_x concentration, has successfully addressed these objectives.

In summary, the major scientific achievements have been:

- the establishment of a large data base on the dependence of the yields of the products from the ·OH radical initiated oxidation of dimethyl sulphide and dimethyl sulphoxide on reaction conditions;
- the variation of the yields of dimethyl sulphoxide, dimethyl sulphone and sulphur dioxide with temperature and the initial NO concentration have been quantified;
- the results prove for the first time that a mechanism involving reversible addition of oxygen to a DMS-OH adduct, formed *via* the addition channel, followed by sequential reaction with nitrogen monoxide and oxygen is operative;
- using ion chromatography evidence have been found that methane sulphinic acid is the major product of the reaction of ·OH radicals with dimethyl sulphoxide.

Based on the results of the present product studies, principal oxidation mechanisms have been constructed for the ·OH radical initiated oxidation of dimethyl sulphide and dimethyl sulphoxide. Although the present work is highlighting important mechanistic features of the oxidation process in both organic sulphur containing compounds a more probing approach of the complex mechanistic relationships is necessary by modelling analysis of the chamber runs. The modelling of the present data will give information on the branching ratios of important key reactions under atmospheric conditions.

The results obtained in this study will allow the yield of sulphur dioxide and methane sulphonic acid from the oxidation of dimethyl sulphide to be more accurately predicted for the conditions of both the remote marine boundary layer and also polluted regions characterised by very high nitrogen monoxide level.

It has been also shown that in assessing the contribution of dimethyl sulphide to cloud condensation nuclei formation in the remote boundary layer (BL), consideration of the fate of methane sulphinic acid is an important aspect of oxidation process, which needs to be taken into account.

However, the major benefit of the present work is a help in a clearer understanding of the processes involved in dimethyl sulphide oxidation leading to sulphuric acid and methane sulphonic acid, the most important components of the particulate phase in the atmosphere, and their variation with different meteorological conditions (obviously temperature) and geographical location (unpolluted and polluted atmosphere).

Appendix A

Ion chromatographic analysis

The system used for the sampling of methane sulphinic and methane sulphonic acids from the reaction chamber consisted of a short Teflon tube attached to two empty glass cryogenic U-tube traps connected in series, a flow controller and a pump, as indicated in Figure A.1. The glass cryogenic U-tubes were immersed in an ethanol-liquid nitrogen slush bath (-112^{o}C). The pump was adjusted to pass air from the reactor at a rate of 0.5 or 1 l min^{-1} through the cold trap, and from 5 to 40 l were sampled. To improve the efficiency of trapping, a glass sinter was inserted into the sampling tubes.

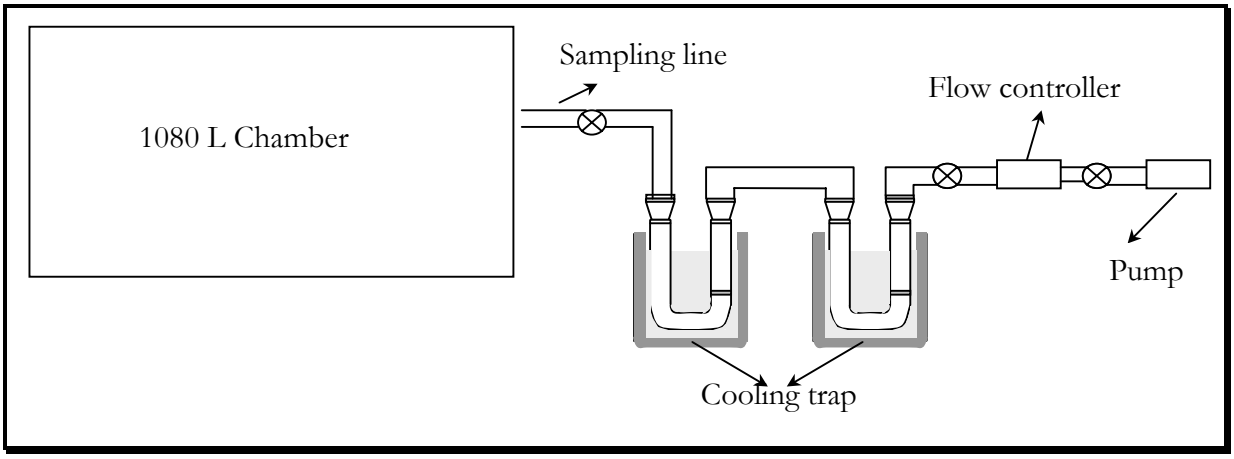

Figure A.1: Instrumental set up used for sampling MSIA, MSA and sulphate.

Calibration curves were measured weekly, and every day one or two working standards were injected for comparison. Chemical compounds were identified by comparison of the retention time, t_R, of peaks of the unknown sample with the retention times of peaks from the chromatograms of standards solutions.

Figure A.2 illustrates that the heights of the HPLC peaks corresponding to the $CH_3S(O)O^-$ $CH_3S(O)_2O^-$ and SO_4^{2-} anions were proportional to the concentration of methane sulphinate, methane sulphonate and sulphate, respectively, and in the range of 0.2 - 12 μg ml^{-1} correlation coefficients better than 0.997 (for $CH_3S(O)O^-$), 0.992 (for $CH_3S(O)_2O^-$) and 0.981 (for SO_4^{2-}) were obtained.

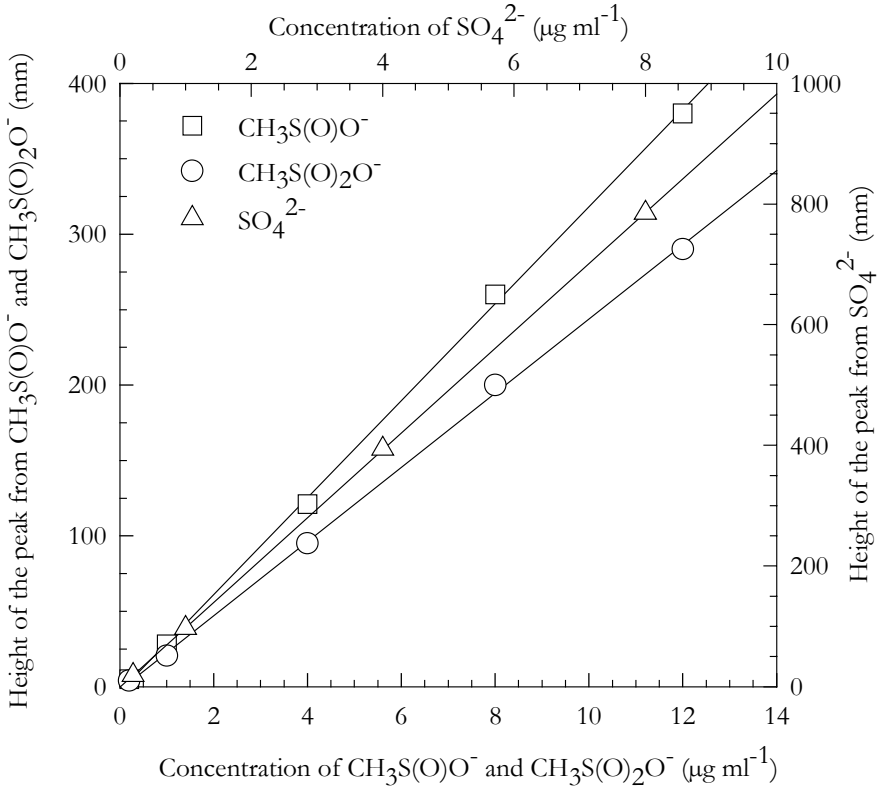

Figure A.2: Calibration curves of methane sulphinate ($CH_3S(O)O^-$), methane sulphonate ($CH_3S(O)_2O^-$) and sulphate (SO_4^{2-}).

Figure A.3 shows some test chromatograms, which were measured by injection into the ion chromatograph of a) the eluent (no response from the column), b) a sample collected from the synthetic air mixture (no response from the column), c) sample from a DMSO/synthetic air mixture (appearance of a peak with t_R = *9.65* min), d) a sample from a DMSO/H_2O_2/synthetic air mixture (appearance of a peak with t_R = *9.71* min), e) a standard solution of $CH_3S(O)O^-$ (corresponding t_R = *6.23* min), f) a standard solution of $CH_3S(O)_2O^-$ (corresponding t_R = *7.05* min), g) a standard solution of SO_4^{2-} (corresponding t_R = *9.72* min) and h) a water solution of pure DMSO (appearance of a peak with t_R = *9.69* min). These tests were performed in order to confirm the correct assignment of the peaks of the $CH_3S(O)O^-$ and $CH_3S(O)_2O^-$ anions and also to test for potential sampling artefacts.

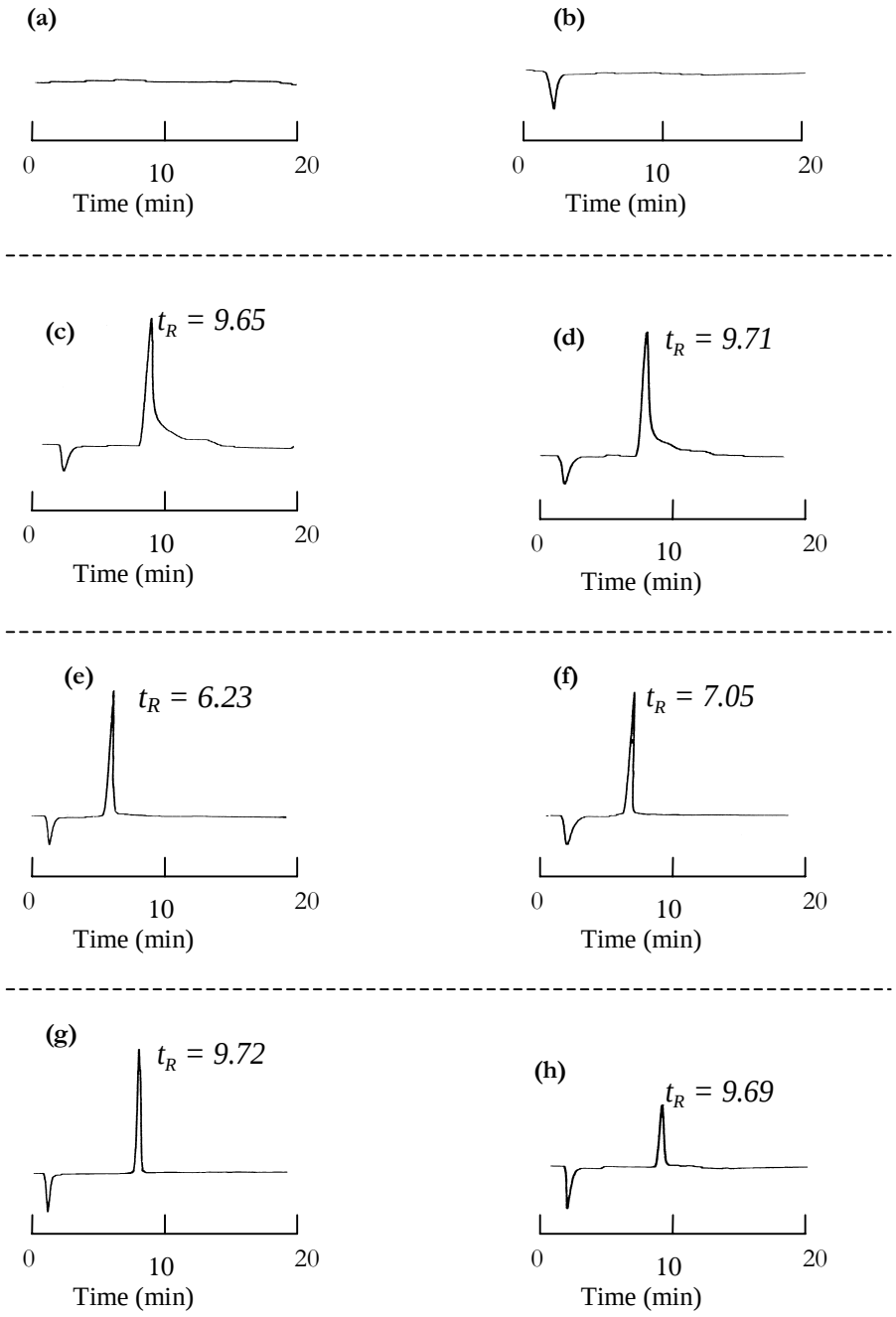

Figure A.3: Example of chromatograms obtained by injection of (a) eluent, (b) a sample collected from the synthetic air in the reaction chamber, (c) a sample collected from the DMSO/synthetic air mixture in the chamber, (d) a sample collected from DMSO/H_2O_2/synthetic air mixture in the chamber, (e) a standard solution of $CH_3S(O)O^-$, (f) a standard solution of $CH_3S(O)_2O^-$, (g) a standard solution of SO_4^{2-} and (h) a injection of solution of pure DMSO.

Appendix B

Gas phase infrared spectrum of methane sulphinic acid (tentative assignment)

Methane sulphinic acid (MSIA: $CH_3S(O)OH$) has been tentatively identified in an IR spectrum obtained from the irradiation of DMS/CH_3ONO/($NO+NO_2$) mixtures in 1000 mbar of synthetic air at a temperature of 243 K. Since it was expected that the stability of MSIA will increase with decreasing temperature the experiments were performed at the lowest possible temperature in the 360 l reactor. A very strong absorption band, with a maximum at about 1139 cm^{-1}, has been observed in spectra collected after the initiation of irradiation of the mixture (Figure B.1).

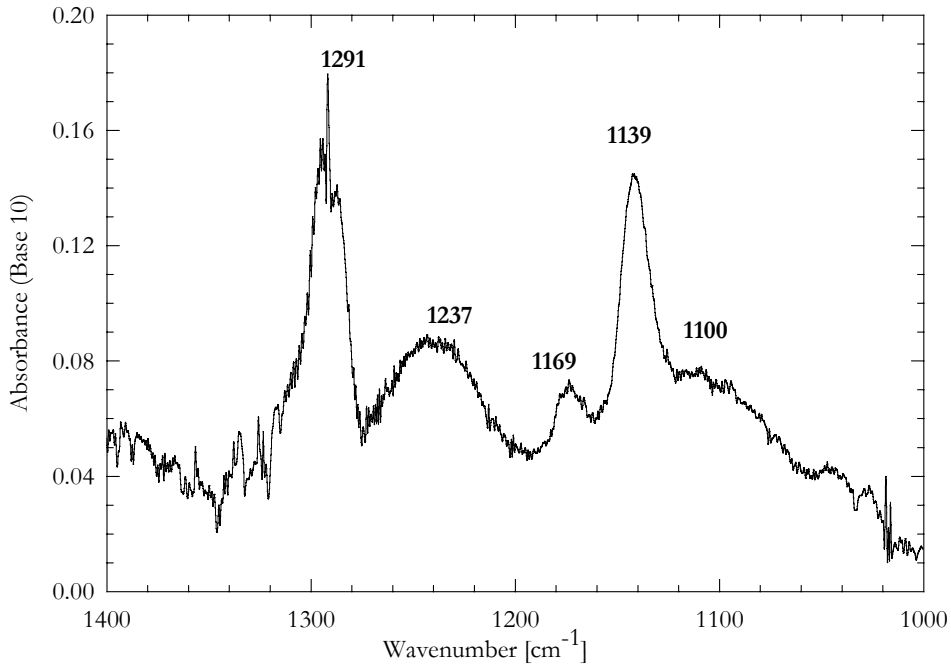

Figure B.1: Residual spectrum obtained from a spectrum recorded after 30 minutes irradiation of a DMS/CH_3ONO/($NO+NO_2$) mixture in 1000 mbar of synthetic air at a temperature of 243 K which include features of the possible IR spectrum of $CH_3S(O)OH$.

A preliminary *ab initio* calculation of the vibrational spectrum of $CH_3S(O)OH$ from the group of Ford Company (Aachen, Germany) predicts very strong absorption bands at about 1100, 1137 and 1229 cm^{-1} (Schneider, 1999). In the residual spectrum obtained after subtraction of all known compounds bands are observable which are close to those predicted by the calculations (Figure B.1). In this spectrum, the peak at 1139 cm^{-1} is very close to the value of 1137 cm^{-1} predicted by the calculations for $CH_3S(O)OH$. The peak at 1137 cm^{-1} is, therefore, tentatively assigned to methane sulphinic acid. A very distinct band with a maximum at 1291 cm^{-1} belongs to some unidentified product.

Appendix C

Gases and Chemicals

Table D1: Gases used in this work.

Gas	Origin	Purity (Vol %)
oxygen (O_2)	Messer Griesheim	99.999
nitrogen (N_2)	Messer Griesheim	99.995
synthetic air (20.5 % O_2 in N_2)	Messer Griesheim	99.995
NO	Messer Griesheim	99.5
NO_2	Messer Griesheim	98

Table D2: Chemicals used in this work.

Chemicals	Origin	Purity
dimethyl sulphide	Aldrich	99.0 %
dimethyl sulphoxide	Fluka	99.5 %
hydrogen peroxide	Peroxide Chemie	85.0 %
methane sulphinic acid sodium salt	Lancaster	97.0 %
methane sulphonic acid sodium salt	Aldrich	99.5%
sodium carbonate	Fluka	99.5 %
sodium hydrogen carbonate	Fluka	99.7 %

Appendix D

Abbreviation

BDE	Bond Dissociation Energy
BL	Boundary Layer
CCN	Condensation Cloud Nuclei
DMS	Dimethyl Sulphide
DMSO	Dimethyl Sulphoxide
$DMSO_2$	Dimethyl Sulphone
DMSPN	Dymethylsulphoniopropionate
FTIR	Fourier Transform Infrared
HPLC	High Performance Liquid Chromatography
IC	Ion Chromatography
ID	Internal Diameter
IR	Infrared
LIF	Laser Induced Fluorescence
MBL	Marine Boundary Layer
MS	Methane Sulphonate
MSA	Methane Sulphonic Acid
MSEA	Methane Sulphenic Acid
MSIA	Methane Sulphinic Acid
MSPN	Methane Sulphonyl Peroxy Nitrate
MTF	Methane Thiol Formate
NMHC	Non Methane Hydrocarbon
NO_x	$NO + NO_2$
nss-SO_4^{2-}	non sea salt sulphate
ppm	parts per million (1 ppm = 2.46×10^{13} molecules cm^{-3} at 1 bar and 298 K)
P	Pressure
T	Temperature
UV	Ultraviolet (200-400 nm)
VIS	Visible (400-700 nm)

References

Andreae, M.O. and Raemdonck, H. (1983)

Dimethyl sulphide in the surface ocean and the marine atmosphere. A global view
Science **221**, 744-747

Andreae, M.O. (1990)

Ocean-atmosphere interactions in the global biogeochemical sulphur cycle
Marine Chemistry **30**, 1-29

Andreae, M.O. and Jaeschke, W.A. (1992)

Exchange of sulphur between biosphere and atmosphere over temperate and tropical regions,
in: Sulphur Cycling on the Continents,
Howarth, R.W.; Stewart, J.W.B.; Ivanov, M.V. (eds)
Wiley&Sons, New York, pp.27-60

Andreae, T.W., Andreae, M.O., Schebescke, G. (1994)

Biogenic sulphur emissions and aerosols over the tropical South Atlantic. 1. Dimethyl sulphide in sea water and in the atmospheric boundary layer
Journal of Geophysical Research **99**, 22,819-22,829

Andreae, M.O.; Elbert, W.; De Mora, S.J. (1995)

Biogenic sulphur emissions and aerosols over the tropical South Atlantic. 3. Atmospheric dimethyl sulphide, aerosols and cloud condensation nuclei
Journal of Geophysical Research **100**, 11,335-11,356

Arsene, C.; Barnes, I.; Becker, K.H. (1999)

FT-IR product study of the photo-oxidation of dimethyl sulphide: temperature and O_2 partial pressure dependence
Physical Chemistry Chemical Physics **1**, 5463-5470

Arsene, C.; Barnes, I.; Becker, K.H.; Mocanu, R. (2000)

Product studies on the photo-oxidation of dimethyl sulphoxide (DMSO: $CH_3S(O)CH_3$)

in: Proceeding of the EC/EUROTRAC-2 Joint Workshop

EPFL Lausanne-Ecublens, Switzerland, September 11-13

Arsene, C.; Barnes, I.; Becker, K.H.; Mocanu, R. (2001)

FT-IR product study in the photo-oxidation of dimethyl sulphide in the presence of NO_x - temperature dependence

Atmospheric Environment **35**, 3769-3780

Atkinson, R.; Pitts, J.N.; Aschmann, S.M. (1984)

Tropospheric reactions of dimethyl sulphide with NO_3 and OH radicals

Journal of Physical Chemistry **88**, 1584-1587

Atkinson, R.; Baulch, D.; Cox, R.A.; Hampson, R.; Kerr, J.A.; Rossi, M.J.; Troe, J. (1997)

Evaluated kinetic and photochemical data for atmospheric chemistry. Supplement VI

Journal of Physical Chemistry. Reference Data **25**, 1329-1499

Bandy, A.R.; Thornton, D.C.; Blomquist, B.W.; Chen, S.; Wade, T.P.; Ianni, J.C.; Mitchell, G.M.; Nadler, W. (1996)

Chemistry of dimethyl sulphide in the equatorial Pacific atmosphere

Geophysical Research Letters **23**, 741-744

Barnard, W.R.; Andreae, M.O.; Watkins, W.E.; Bingemer, H.; Georgii, H.W. (1982)

The flux of dimethyl sulphide from the oceans to the atmosphere

Journal of Geophysical Research **87**, 8787-8793

Barnes, I.; Bastian, V.; Becker, K.H.; Wirtz, K. (1987a)

Atmospheric sulphur compounds. Sources and tropospheric oxidation processes,

In: Formation, Distribution and Chemical Transformation of Air Pollutants,

Zellner, R. (ed.)

DECHEMA Monographie VOL 104, VCH Verlagsgesellschaft, pp. 59-73

Barnes, I.; Bastian, V.; Becker, K.H.; Niki, H. (1987b)

FTIR spectroscopic studies of the $CH_3S + NO_2$ reaction under atmospheric conditions

Chemical Physics Letters **140**, 451-457

Barnes, I.; Bastian, V.; Becker, K.H. (1988)

Kinetics and mechanisms of the reaction of OH radicals with dimethyl sulphide

International Journal of Chemical Kinetics **20**, 415-431

Barnes, I.; Bastian, V.; Becker, K.H.; Martin, D. (1989)

Fourier Transform IR studies of the reactions of dimethyl sulphoxide with OH, NO_3, and Cl radicals,
in: Biogenic Sulphur in the Environment,
Saltzman, E.S. and Cooper, W.J., (eds.)
ACS Symposium Series 393, Washington, pp. 476-488

Barnes, I.; Bastian, V.; Becker, K.H.; Overath, R.D. (1991)

Kinetic studies of the reactions of IO, BrO, and ClO with dimethyl sulphide
International Journal of Chemical Kinetics, **23**, 579-591

Barnes, I. (1993)

Overview and atmospheric significance of the results from laboratory kinetic studies performed within the CEC project "OCEANONOX",
in: Dimethyl sulphide. Oceans, Atmosphere and Climate,
Restelli, G. and Angeletti, G., (eds.)
Kluwer Academic Publishers, Dordrecht, pp. 223-237

Barnes, I.; Becker, K.H.; Overath, R.D. (1993)

Oxidation of organic sulphur compounds,
in: The Tropospheric Chemistry of Ozone in the Polar Regions,
Niki, H. and Becker, K.H., (eds)
ASI Series, Vol. I7, Springer-Verlag Berlin, pp. 371-383

Barnes, I.; Becker, K.H.; Patroescu, I. (1994)

The tropospheric oxidation of dimethyl sulphide. A new source of carbonyl sulphide
Geophysical Research Letters **21**, 2389-2392

Barnes, I.; Becker, K.H.; Patroescu, I. (1996)

FTIR products study of the initiated oxidation of dimethyl sulphide. Observation of carbonyl sulphide and dimethyl sulphoxide
Atmospheric Environment **30**, 1805-1814

Barone, S.B.; Turnipseed, A.A.; Ravishankara, A.R. (1995)

Role of adducts in the atmospheric oxidation of dimethyl sulphide
Faraday Discussions **100**, 000-000

Barone, S.B.; Turnipseed, A.A.; Ravishankara, A.R. (1996)

Reaction of OH with dimethyl sulfide (DMS). 1. Equilibrium constant for OH + DMS reaction and the kinetics of the $OH \cdot DMS + O_2$ reaction
Journal of Physical Chemistry **100**, 14,694-14,702

Barth, M.C.; Rasch, P.J.; Kiehl, J.T.; Benkovitz, C.M.; Schwartz, S.E. (2000)
Sulphur chemistry in the National Centre for Atmospheric Research Community Climate Model: Description, evaluation, features, and sensitivity to aqueous chemistry
Journal of Geophysical Research **105**, 1387-1415

Bates, T.S.; Cline, J.D.; Gammon, R.H.; Kelly-Hansen, S.R. (1987)
Regional and seasonal variations in the flux of oceanic dimethyl sulphide to the atmosphere,
Journal of Geophysical Research **92**, 2930-2938

Bates, T.S.; Lamb., B.K.; Guenther, A.; Dignon, J.; Stoiber, R.E. (1992a)
Sulphur emissions to the atmosphere from natural sources
Journal of Atmospheric Chemistry **14**, 315-337

Bates, T.S.; Calhoun, J.A.; Quinn, P.K. (1992b)
Variations in the methane sulphonate to sulphate molar ratio in submicrometer marine aerosol particles over the south Pacific ocean
Journal of Geophysical Research **97**, 9859-9865

Bates, T.S.; Kiene, R.P.; Wolfe, G.V.; Matrai, P.A.; Chavez, F.P.; Buck, K.R.; Blomquist, B.W.; Cuhel, R.L. (1994)
The cycling of sulphur in surface water of the north east Pacific
Journal of Geophysical Research **99**, 7835-7843

Berresheim, H.; Eisele, F.L.; Tanner, D.J.; McInnes, L.M.; Ramsey-Bell, D.C.; Covert, D.S. (1993)
Atmospheric sulphur chemistry and cloud condensation nuclei (CCN) concentrations over the north eastern Pacific coast
Journal of Geophysical Research **98**, 12,701-12,711

Berresheim, H.; Wine, P.H.; Davis, D.D. (1995)
Sulphur in the atmosphere,
in: Composition, Chemistry, and Climate of the Atmosphere,
Singh, H.B. (ed.)
Van Nostrand Reinhold, New York, pp. 251-307

Berresheim, H.; Huey, J.W.; Thorn, R.P.; Eisele, F.L.; Tanner, D.J.; Jefferson, A., (1998)
Measurements of dimethyl sulphide, dimethyl sulphoxide, dimethyl sulphone, and aerosol ions at Palmer station, Antarctica
Journal of Geophysical Research **103**, 1629-1637

Beyer, H. (1998)

Diploma Thesis

Untersuchungen über die oxidation von dimethylsulphoxid unter atmosphärichen bedingungen

Bergische Universität Wuppertal, June

Brasseur, G.P.; Orlando, J.J.; Tyndall, G.S. (1999)

Trace gas exchanges and biogeochemical cycles,

in: Atmospheric Chemistry and Global Change (Topics in Environmental Chemistry), Oxford University Press, New York, pp. 181-231

Butkovskaya, N.I. and LeBras, G. (1994)

Mechanism of the NO_3 + DMS reaction by discharge flow mass spectrometry

Journal of Physical Chemistry **98**, 2582-2591

Campolongo, F.; Saltelli, A.; Jensen, N.R.; Wilson, J.; Hjorth, J. (1999)

The role of multiphase chemistry in the oxidation of dimethyl sulphide (DMS). A latitude dependent analysis

Journal of Atmospheric Chemistry **32**, 327-356

Cerqueira, M.A. and Pio, C.A. (1999)

Production and release of dimethyl sulphide from an estuary in Portugal

Atmospheric Environment **33**, 3355-3366

Charlson, R.J.; Lovelock, J.E.; Andreae, M.O.; Warren, S.G. (1987)

Oceanic phytoplankton, atmospheric sulphur, cloud albedo and climate

Nature **326**, 655-661

Chen, G; Davis, D.D.; Kasibhatala, P.; Bandy, A.R.; Thornton, D.C.; Huebert, B.J.; Clarke, A.D.; Blomquist, B.W. (2000)

A study of DMS oxidation in the tropics: comparison of Christmas island field observations of DMS, SO_2, and DMSO with model simulations

Journal of Atmospheric Chemistry **37**, 137-160

Crutzen, P.J. (1976)

The possible importance of COS for the sulphate layer of the stratosphere

Geophysical Research Letters **3**, 73-76

Dacey, J.W.H.; King, G.M.; Wakeham, S.M. (1987)

Factors controlling emission of dimethyl sulphide from salt marshes

Nature **330**, 643-645

Davis, D.; Chen, G.; Kasibhatla, P.; Jefferson, A.; Tanner, D.; Eisele, F.; Lenschow, D.; Neff, W.; Berresheim, H. (1998)

DMS oxidation in the Antarctic marine boundary layer. Comparison of model simulations and field observations for DMS, DMSO, $DMSO_2$, H_2SO_4(g), MSA(g) and, MSA(p)
Journal of Geophysical Research **103**, 1657-1678

Davis, D.; Chen, G.; Bandy, A.; Thornton, D; Eisele, F.; Mauldin, L.; Tanner, D.; Lenschow, D.; Fuelberg, H.; Huebert, D.; Heath, J.; Clarke, A.; Blake, D. (1999)

Dimethyl sulphide oxidation in the equatorial Pacific: Comparison of model simulations with field observations for DMS, SO_2, H_2SO_4(g), MSA(g), MS and, NSS
Journal of Geophysical Research **104**, 5765-5784

Davison, B.; O'Dowd, C.O.; Hewitt, C.N.; Smith, M.H.; Harrison, R.M.; Peel, D.A.; Wolf, E.; Mulvaney, R.; Schwikowski, M.; Baltensperger, U. (1996)

Dimethyl sulphide and its oxidation products in the atmosphere of the Atlantic and southern oceans
Atmospheric Environment **30**, 1895-1906

DeMoore, W.B.; Sander, S.P.; Golden, D.M., Hampson, R.F.; Kurylo, M.J.; Howard, C.J.; Ravishankara, A.R.; Kolb, C.E.; Molina, M. (1997)

Chemical kinetics and photochemical data for use in stratospheric modelling
Evaluation No.12, JPL Publications No. 97-4

DOMAC (2000)

Dimethyl Sulphide (DMS): Oxidation Mechanism in Relation to Aerosols and Climate,
DOMAC final SCA project report, European Commission Joint Research Centre, Environment Institute, EUR 19569 EN

Eisele, F.L. and Tanner, D.J. (1993)

Measurement of the gas phase concentration of H_2SO_4 and methane sulphonic acid and estimates of H_2SO_4 production and loss in the atmosphere
Journal of Geophysical Research **98**, 9001-9010

Erickson III, D.J.; Walton, J.J.; Ghan, S.J.; Penner, J.E. (1991)

Three-dimensional modelling of the global atmospheric sulphur cycle. A first step
Atmospheric Environment **25**, 2513-2520

Erickson III, D.J. (1993)

A stability dependent theory for air-sea gas exchange
Journal of Geophysical Research **98**, 8471-8488

Falbe-Hansen, H.; Sorensen, S.; Jensen, N.R.; Pedersen, T.; Hjorth, J. (2000)

Atmospheric gas phase reactions of dimethyl sulphoxide and dimethyl sulphone with OH and NO_3 radicals, Cl atoms and ozone

Atmospheric Environment **34**, 1543-1551

Frank, A.J. and Tureček, F. (1999)

Methylsulphonyl and methylsulphinil radicals and cations in the gas phase. A variable time and photo-excitation neutralisation-reionisation mass spectrometric and ab initio/RRKM study

Journal of Physical Chemistry **103**, 5348-5361

Georgii, H.W. and Warneck, P. (1999)

Chemistry of the tropospheric aerosol and of cloud. Sulphur compounds in the troposphere

in: Global Aspects of Atmospheric Chemistry, Topics in Physical Chemistry Vol. 6,
Zellner, R.; Baumgärtel, H.; Grünbein, W.; Hensel, F., (eds.)
Steinkopff Darmstadt, Springer, Heidelberg, New York, pp. 111-179

Ginzburg, B.; Chalifa, I.; Gun, J.; Dor, I.; Hadas, O.; Lev, O. (1998)

DMS formation by dimethylsulfoniopropionate route in freshwater

Environmental Science and Technology **32**, 2130-2136

Grosjean, D. (1984)

Photo-oxidation of methyl sulphide, ethyl sulphide, and methanethiol

Environmental Science and Technology **18**, 460-468

Hansen, T.A.; Quist, P.; Van der Maarel, M.J.E.C.; Dijkhuizen, L. (1993)

Isolation of marine dimethyl sulphide oxidising bacteria,

in: Dimethyl sulphide: Oceans, Atmosphere and Climate,
Restelli, G. and Angeletti, G., (eds.)
Kluwer Academic Publishers, Dordrecht, pp. 37-41

Hatakeyama, S. and Akimoto, H. (1983)

Reactions of OH radicals with methanethiol, dimethyl sulphide, and dimethyl disulphide in air

Journal of Physical Chemistry **87**, 2387-2395

Hatakeyama, S.; Izumi, K., Akimoto, H. (1985)

Yield of SO_2 and formation of aerosol in the photo-oxidation of DMS under atmospheric conditions

Atmospheric Environment **19**, 135-141

Hertel, O.; Christensen, J.; Hov, Ø. (1994)

Modelling of the end products of the chemical decomposition of DMS in the marine boundary layer

Atmospheric Environment **28**, 2431-2449

Hynes, A.J.; Wine, P.H.; Semmes, D.H. (1986)
Kinetics and mechanism of OH reactions with organic sulphides
Journal of Physical Chemistry **90**, 4148-4156

Hynes, A.J.; Stickel, R.E.; Pounds, A.J.; Zhao, Z.; McKay, T., Bradshaw, J.D.; Wine, P.H. (1993)
Mechanistic studies of the OH-initiated oxidation of dimethyl sulphide,
in: Dimethyl sulphide: Oceans, Atmosphere and Climate,
Restelli, G. and Angeletti, G., (eds.)
Kluwer Academic, Publishers, Dordrecht, pp. 211-221

Hynes, A.J. and Wine, P.H. (1996)
The atmospheric chemistry of dimethyl suphoxide (DMSO). Kinetics and mechanism of the OH + DMSO reaction
Journal of Atmospheric Chemistry **24**, 23-37

Ingham, T.; Bauer, D.; Sander, R.; Crutzen, P.J.; Crowley, J.N. (1999)
Kinetics and products of the reactions BrO + DMS and Br + DMS at 298 K
Journal of Physical Chemistry **103**, 7199-7209

Jefferson, A.; Tanner, D.J.; Eisele, F.L.; Berresheim, H. (1998)
Sources and sinks of H_2SO_4 in the remote Antarctic marine boundary layer
Journal of Geophysical Research **103**, 1639-1645

Jensen, N.R.; Hjorth, J.; Lohse, C.; Skov, H.; Restelli, G. (1991)
Products and mechanism of the reaction between NO_3 and dimethyl sulphide in air
Atmospheric Environment **25**, 1897-1904

Jensen, N.R.; Hjorth, J.; Lohse, C.; Skov, H.; Restelli, G. (1992)
Products and mechanisms of the gas phase reactions of NO_3 with CH_3SCH_3, CD_3SCD_3, CH_3SH and CH_3SSCH_3
Journal of Atmospheric Chemistry **14**, 95-108

Kettle, A.J. and Andreae, M.O. (2000)
Flux of dimethyl sulphide from the oceans. A comparison of updated data sets and flux models
Journal of Geophysical Research **105**, 26793-26808

Kettle, A.J.; Rhee, T.S.; von Hobe, M.; Poulton, A.; Aiken, J.; Andreae, M.O. (2001)
Assesing the flux of different volatile sulphur gases from the ocean to the atmosphere
Journal of Geophysical Research **106**, 12193-12209

Kieber, D.J.; Jiao, J.; Kiene, R.P.; Bates, T.S. (1996)

Impact of dimethyl sulphide photochemistry on methyl sulphur cycling in the equatorial Pacific ocean
Journal of Geophysical Research **101**, 3715-3722

Koga, S. and Tanaka, H. (1993)

Numerical study of the oxidation process of dimethyl sulphide in the marine atmosphere
Journal of Atmospheric Chemistry **17**, 201-228

Koga, S. and Tanaka, H. (1999)

Modelling the methane sulphonate to non-sea-salt sulphate molar ratio and dimethyl sulphide oxidation in the atmosphere
Journal of Geophysical Research **104**, 13,735-13,747

Kukui, A.; Bossoutrot, V.; Leverdet, G.; Le Bras, G. (2000)

Mechanism of the reaction of CH_3SO with NO_2 in relation to atmospheric oxidation of dimethyl sulphide. Experimental and theoretical study
Journal of Physical Chemistry, **104**, 935-946

Li, Y.F.; Zhang, Y.J.; Cao, G.L.; Liu, J.H.; Barrie, L.A. (1999)

Distribution of seasonal SO_2 emissions from fuel combustion and industrial activities in Shanxi province, China, with $1/6^o \times 1/4^o$ longitude/latitude resolution
Atmospheric Environment **33**, 257-265

Malm, W.C.; Trijonis, J.; Sisler, J.; Pitchford, M.; Dennis, R.L. (1994)

Assessing the effect of SO_2 emission changes on visibility
Atmospheric Environment **28**, 1023-1034

Mauldin III, R.L.; Tanner, D.J.; Heath, J.A.; Huebert, B.J.; Eisele, F.L. (1999)

Observations of H_2SO_4 and MSA during PEM-Tropics-A
Journal of Geophysical Research **104**, 5801-5816

Maurer, T.; Barnes, I.; Becker, K.H. (1999)

FT-IR kinetic and product study of the Br-initiated oxidation of dimethyl sulphide
International Journal of Chemical Kinetics **31**, 883-893

McKee, M.L. (1993a)

Computational study of addition and abstraction reactions between OH radical and dimethyl sulphide. A difficult case
Journal of Physical Chemistry **97**, 10,971-10,976

McKee, M.L. (1993b)

Theoretical study of the CH_3SOO radical
Chemical Physics Letters **211**, 643-648

McKee, M.L. (1994)

Theoretical study of the CH_3SCH_2OO and CH_3SCH_2O radicals

Chemical Physics Letters 231, 257-262

Mellouki, A. and Ravishankara, A.R. (1994)

Does the HO_2 radical react with H_2S, CH_3SH, and CH_3SCH_3?

International Journal of Chemical Kinetics **26**, 355-365

Mihalopoulos, N.; Nguyen, B.G.; Boissard, C.; Campin, J.M.; Putaud, J.P.; Belviso, S.; Barnes, I.; Becker, K.H. (1992a)

Field study of dimethyl sulphide oxidation in the boundary layer. Variations of dimethyl sulphide, methane sulphonic acid, sulphur dioxide, non-sea-salt-sulphate and Aitken nuclei at a coastal side

Journal of Atmospheric Chemistry **14**, 459-477

Mihalopoulos, N.; Barnes, I.; Becker, K.H. (1992b)

Infrared absorption spectra and integrated band intensities for gaseous methane sulphonic acid (MSA)

Atmospheric Environment **26**, 807-812

Mihalopoulos, N.; Putaud, J.P.; Nguyen, B.C. (1993)

Seasonal variation of methane sulphonic acid in precipitation at Amsterdam island in the southern Indian ocean

Atmospheric Environment **27**, 2069-2073

Mukai, H.; Yokouchi, Y.; Suzuki, M. (1995)

Seasonal variation of methane sulphonic acid in the atmosphere over the Oki islands in the sea of Japan

Atmospheric Environment **29**, 1637-1648

Nagao, I.; Matsumoto, K.; Tanaka, H. (1999)

Characteristics of dimethyl sulphide, ozone, aerosols, and cloud condensation nuclei in air masses over the north-western Pacific ocean

Journal of Geophysical Research **104**, 11,675-11,693

Nguyen, B.C.; Bonsang, B.; Gaudry, A. (1983)

The role of the ocean in the global atmospheric sulphur cycle

Journal of Geophysical Research **88**, 10,903-10,914

Nguyen, B.C.; Mihalopoulos, N.; Belviso, S. (1990)

Seasonal variations of atmospheric dimethyl sulphide at Amsterdam island in the southern Indian ocean

Journal of Atmospheric Chemistry **11**, 123-141

Nguyen, B.C.; Mihalopoulos, N.; Putaud, J.P.; Gaudry, A.; Gallet, L.; Keene, W.C.; Galloway, J.N. (1992)

Covariations in oceanic dimethyl sulphide, its oxidation products and rain acidity at Amsterdam island in the southern Indian ocean,

Journal of Atmospheric Chemistry **15**, 39-53

Niki, H.; Maker, P.D.; Savage, C.M.; Breitenbach, L.P. (1983)

An FTIR study of the mechanism for the reaction HO + CH_3SCH_3

International Journal of Chemical Kinetics **15**, 647-654

Patroescu, I.V.; Barnes, I.; Becker, K.H. (1996)

FTIR kinetic and mechanistic study of the atmospheric chemistry of methyl thiolformate

Journal of Physical Chemistry **100**, 17,207-17,217

Patroescu, I.V. (1996)

Doctoral Thesis: Reaktionen von organischen schwefelverbindungen in der atmosphäre

Bericht Nr. 35, pp. 121-124

Patroescu, I.V.; Barnes, I.; Becker, K.H.; Mihalopoulos, N. (1999)

FT-IR product study of the OH-initiated oxidation of DMS in the presence of NO_x

Atmospheric Environment **33**, 25-35

Pham, M.; Müller, J.F.; Brasseur, G.P.; Granier, C.; Megie, G. (1995)

A three-dimensional study of the tropospheric sulphur cycle

Journal of Geophysical Research **100**, 26,061-26,092

Putaud, J. and Nguyen, B.C. (1996)

Assessment of dimethyl sulphide sea-air exchange rate

Journal of Geophysical Research **101**, 4403-4411

Putaud, J.; Davison, B.; Watts, S.F.; Mihalopoulos, N.; Nguyen, B.C.; Hewitt, C.N. (1999)

Dimethyl sulphide and its oxidation products at two sites in Brittany (France)

Atmospheric Environment **33**, 647-659

Ravishankara, A.R.; Rudich, Y.; Talukdar, R.; Barone, S.B. (1997)

Oxidation of atmospheric reduced sulphur compounds. Perspective from laboratory studies

Phil. Trans. R. Soc. Lond. **332**, 171-182

Ray, A.; Vassalli, I.; Laverdet, G.; Le Bras, G. (1996)

Kinetics of the thermal decomposition of the CH_3SO_2 radical and its reaction with NO_2 at 1 Torr and 298 K

Journal of Physical Chemistry **100**, 8895-8900

Resende, S.M. and De Almeida, W.B. (1999)

Mechanism of the atmospheric reaction between the radical CH_3SCH_2 and O_2

Journal of Physical Chemistry **103**, 4191-4195

Restad, K.; Isaksen, I.S.A.; Berntsen, T.K. (1998)

Global distribution of sulphate in the troposphere. A three-dimensional model study

Atmospheric Environment **32**, 3593-3609

Saltelli, A. and Hjorth, J. (1995)

Uncertainty and sensitivity analyses of OH-initiated dimethyl sulphide (DMS) oxidation kinetics

Journal of Atmospheric Chemistry **21**, 187-221

Schneider, W. F. (1999)

IR spectrum for $CH_3S(O)OH$

private communication

Seinfeld, J.H. and Pandis, S.N. (1998)

Cloud Physics,

in: Atmospheric Chemistry and Physics

Wiley, New York, pp. 777-841

Sekušak, S.; Piecuch, P.; Bartlett, R.J.; Cory, M.G. (2000)

A general reaction path dual-level direct dynamics calculation of the reaction of hydroxyl radical with dimethyl sulphide

Journal of Physical Chemistry **104**, 8779-8786

Sharma, S.; Barrie, L.A.; Hastie, D.R.; Kelly, C. (1999)

Dimethyl sulphide emissions to the atmosphere from lakes of the Canadian boreal region

Journal of Geophysical Research **104**, 11,585-11,592

Shon, Z.H.; Davis, D.; Chen, G.; Grodzinsky, G.; Bandy, A.; Thornton, D.; Sandholm, S.; Bradshaw, J.; Stickel, R.; Chameides, W.; Kok, G.; Russel, L.; Mauldin, L.; Tanner, D.; Eisele, F., (2001)

Evaluation of the DMS flux and its conversion to SO_2 over the southern ocean

Atmospheric Environment **35**, 159-172

Spiro, P.A.; Jacob, D.J.; Logan, J.A. (1992)

Global inventory of sulphur emissions with $1^o \times 1^o$ resolution

Journal of Geophysical Research **97**, 6023-6036

Staubes, R. and Georgii, H.W. (1993)

Measurements of atmospheric and sea water DMS concentrations in the Atlantic, the Arctic and Antarctic regions,

in: Dimethyl sulphide: Oceans, Atmosphere and Climate,

Restelli, G. and Angeletti, G., (eds.)

Kluwer Academic Publishers, Dordrecht, pp. 95-102

Stein, A.F. and Lamb, D. (2000)

The sensitivity of sulphur wet deposition to atmospheric oxidants

Atmospheric Environment **34**, 1681-1690

Sørensen, S; Falbe-Hansen, H.; Mangoni, M; Hjorth, J.; Jensen, N.R. (1996)

Observation of DMSO and $CH_3S(O)OH$ from the gas phase reaction between DMS and OH

Journal of Atmospheric Chemistry **24**, 299-315

Thornton, D.C.; Bandy, A.R.; Blomquist, B.W.; Driedger, A.R.; Wade, T.P. (1999)

Sulphur dioxide distribution over the Pacific ocean 1991-1996

Journal of Geophysical Research **104**, 5845-5854

Tuazon, E.C.; Mac Leod, H.; Atkinson, R.; Carter, W.P.L. (1986)

α- dicarbonyl yields from the NO_x - air photo-oxidation of a series of aromatic hydrocarbons in air

Environmental Science and Technology **20**, 383-387

Tureček, F. (1994)

The dimethyl sulphide-hydroxyl radical reaction. an ab initio study

Journal of Physical Chemistry **98**, 3701-3706

Turnipseed, A.A. and Ravishankara, A.R. (1992)

Observation of CH_3S addition to O_2 in the gas phase

Journal of Physical Chemistry **96**, 7502-7505

Turnipseed, A.A. and Ravishankara, A.R. (1993)

The atmospheric oxidation of dimethyl sulphide. Elementary steps in a complex mechanisms,

in: Dimethyl sulphide. Oceans, Atmosphere and Climate,

Restelli, G. and Angeletti, G., (eds.)

Kluwer Academic Publishers, Dordrecht, pp. 185-195

Turnipseed, A.A.; Barone, S.B.; Ravishankara, A.R. (1996)

Reaction of OH with dimethyl sulphide. 2. Products and mechanisms

Journal of Physical Chemistry **100**, 14,703-14,713

Tyndall, G.S. and Ravishankara, A.R. (1989)

Kinetics and mechanism of the reactions of CH_3S with O_2 and NO_2 at 298 K

Journal of Physical Chemistry **93**, 2426-2435

Tyndall, G.S. and Ravishankara, A.R. (1991)

Atmospheric oxidation of reduced sulphur species

International Journal of Chemical Kinetics **23**, 483-527

Urbanski, S.P.; Stickel, R.E.; Zhao, Z.; Wine, P.H. (1997)

Mechanistic and kinetic study of formaldehyde production in the atmospheric oxidation of dimethyl sulphide

Journal of the Chemical Society, Faraday Transactions **93**, 2813-2819

Urbanski, S.P.; Stickel, R.E.; Wine, P.H. (1998)

Mechanistic and kinetic study of the gas-phase reaction of hydroxyl radical with dimethyl sulphoxide

Journal of Physical Chemistry **102**, 10,522-10,529

Urbanski, S.P. and Wine, P.H. (1999)

Spectroscopic and kinetic study of the $Cl\text{-}S(CH_3)_2$ adduct

Journal of Physical Chemistry **103**, 10,935-10,944

Van Dingenen, R.; Jensen, N.R.; Hjorth, J; Raes, F. (1994)

Peroxy nitrate formation during the night-time oxidation of dimethyl sulphide. Its role as a reservoir species for aerosol formation

Journal of Atmospheric Chemistry **18**, 211-237

Waggoner, A.P.; Weiss, R.E.; Ahlquist, N.C.; Covert, D.S.; Will, S.; Charlson, R.J. (1981)

Optical characteristics of atmospheric aerosol

Atmospheric Environment **15**, 1891-1909

Wallington, T.J.; Hurley, M.D.; Ball, J.C.; Jenkin, M.E. (1993a)

FTIR product study of the reaction $CH_3OCH_2O_2 + HO_2$

Chemical Physics Letters **211**, 41-47

Wallington, T.J.; Ellermann, T.; Nielsen, O.J. (1993b)

Atmospheric chemistry of dimethyl sulphide: UV spectra and self reaction kinetics of CH_3SCH_2 and $CH_3SCH_2O_2$ radicals and kinetics of the reactions $CH_3SCH_2 + O_2$ - $CH_3SCH_2O_2$ and $CH_3SCH_2O_2 + NO$ - $CH_3SCH_2O + NO_2$

Journal of Physical Chemistry **97**, 8442-8449

Wang, L. and Zhang, J. (2001)

Addition complexes of dimethyl sulphide (DMS) and OH radical and their reactions with O_2 by ab initio and density functional theory

Journal of Molecular Stucture **543**,167-175

Warneck, P. (1999)

Fundamentals,

in: Global Aspects of Atmospheric Chemistry, Topics in Physical Chemistry Vol. 6,

Zellner, R.; Baumgärtel, H; Grünbein, W.; Hensel, F., (eds.)

Steinkopff Darmstadt, Springer, Heidelberg, New York, pp. 1-20

Whitby, K.T. (1978)

The physical characteristics of sulphur aerosols

Atmospheric Environment **12**, 135-159

Wilson, J.C. and McMurry, P.H. (1981)

Studies of aerosol formation in power plant plumes: II. Secondary aerosol formation in the Navajo generating station plume

Atmospheric Environment **15**, 2329-2339

Winer, A.M.; Atkinson, R.; Pitts, J.N. (1984)

Gaseous nitrate radical: possible night-time atmospheric sink for biogenic organic compounds

Science **224**, 156-159

Wuebbles, D.J. (1995)

Air Pollution and Climate Change,

in: Composition, Chemistry, and Climate of the Atmosphere,

Singh, H.B. (ed.)

Van Nostrand Reinhold, New York, pp. 480-518

Xu, Y. and Carmichael, G.R. (1999)

An assessment of sulphur deposition pathways in Asia

Atmospheric Environment **33**, 3473-3486

Yin, F.; Grosjean, D.; Seinfeld, J.H. (1990a)

Photo-oxidation of dimethyl sulphide and dimethyl disulphide. I. Mechanism development

Journal of Atmospheric Chemistry **11**, 309-364

Yin, F.; Grosjean, D.; Flagan, R.C.; Seinfeld, J.H. (1990b)

Photo-oxidation of dimethyl sulphide and dimethyl disulphide. II. Mechanism evaluation

Journal of Atmospheric Chemistry **11**, 365-399